ALMA MATER STUDIORUM
UNIVERSITÁ DI BOLOGNA

SCUOLA DI INGEGNERIA E ARCHITETTURA
Sede di Forlí

Corso di Laurea Magistrale in
INGEGNERIA MECCANICA
Classe LM-33

TESI DI LAUREA IN
Meccanica e Dinamica delle Macchine LM

DESIGN OF A FLUID INERTER FOR THE CONTROL OF ROTOR VIBRATIONS

CANDIDATO:
Igli Matija

RELATORE:
Prof. Ing. Alessandro Rivola

CORRELATORE:
Prof. Ing. Roberto Lot
Prof. Ing. Emiliano Rustighi

Anno Accademico 2015/2016

Abstract

Nel 2008, due articoli della rivista sportiva Autosport rilevarano dettagli di una nuova sospensione meccanica nota con il nome di "J-damper" che era entrata in Formula Uno e che aveva offerto in termini di prestazioni significativi aumenti di maneggevolezza e aderenza. Si trattava di un "inerter", la cui origine sta nel lavoro accademico su circuiti meccanici ed elettrici realizzati dal prof. Malcolm C. Smith del Department of Engineering presso University of Cambridge UK. Gli Inerter sono particolari dispositivi meccanici con la proprietá che la forza applicata ai punti fissi, detti terminali, é direttamente proporzionale all'accelerazione. Tale dispositivo ha offerto nuove possibilitá per il controllo meccanico passivo in una varietá di applicazioni ed é tuttora impiegato in F1 e in altre parti del settore automotive ma potenzialmente potrebbe avere molte altre applicazioni.

Nel caso dei rotori (es. turbine, motori elettrici, la girante di un propulsore etc.) non vi sono al momento applicazioni per cui risulta molto interessante capirne le potenzialitá. Pertanto l'obiettivo di questa tesi, in parte svolta all'estero presso l'Institute Of Sound Vibration Research (ISVR) dell'Universitá di Southampton é stato quello di studiare le performance e la stabilitá, tramite modelli matematici e simulazioni numeriche, di un sistema con diverse configurazioni di inerter.

In particolare, nella prima parte di questa tesi, sono state sviluppate le equazioni della dinamica dei rotori utilizzando il linguaggio Maple. Nella seconda parte della tesi, dopo aver introdotto l'inerter, si é studiato la stabilitá di un sistema molla, smorzatore e inerter collegati fra loro in parallelo, di un sistema molla, smorzatore e inerter collegati fra loro in serie e di altre combinazioni possibili. Sono stati analizzati sistemi a diversi gradi di libertá (1GdL, 2GdL, 4GdL, 5GdL e 6GdL) e ricavate le frequenze naturali in

funzione dell'inertanza. Infine, nell'ultima parte della tesi, per comprendere meglio il concetto dell'inerter si é costruito presso i laboratori dell'University of Southampton un fluid inerter e si é realizzato un banco prova per testare l'inerter.

In questa tesi si é dimostrato la validitá delle equazioni della dinamica dei rotori ricavate nella prima parte del lavoro; si é inoltre dimostrato che anche nel caso dei rotori l'inerter abbassa le frequenze naturali del sistema. Infine i risultati sperimentali del Fluid Inerter, ottenuti a diversi valori di ampiezza e frequenza, hanno dimostrato che l'oggetto costruito si comporta effettivamente come un inerter.

In qualitá di relatore autorizzo la redazione della tesi in lingua inglese e mi faccio garante della qualitá linguistica dell'elaborato.

Prof. Ing. Alessandro Rivola

Contents

List of Figures

Chapter 1

Introduction

1.1 Work Introduction

In 2008, two articles in Autosport revealed details of a new mechanical suspension component with the name "J-Damper" which had entered Formula One Racing and which was delivering significant performance gains in handling and grip. The autosport articles revealed that the J-Damper was in fact an "inerter" and that its origin lay academic work on mechanical and electrical circuits at Cambridge University [1]. McLaren was interesed to try out the idea and signed an agreement with the University for exclusive rights in Formula One for a limited period. The inerter was raced for the first time by Kimi Raikkonen at the 2005 Spanish Grand Prix, who achieved a victory for the McLaren F1 team [1].

An inerter is a two-terminal mechanical device which applies force between its terminals proportional to the relative acceleration between them [1], similar to a spring and damper which apply forces proportional to the relative displacement for the spring and velocity for the damper between their terminals. A new word inerter was coined to describe such device. The constant of proportional is called the inertance and has the units of kilograms (i.e, dimensions of mass) Inerters have become a hot topic in recent years especially in veihicle [2], train [3], building suspension system [4] etc. but in the case of the rotors (i.e turbines, electric motors) doesn't exist any applications at the moment. Hence, it is very interesting to investigate the potential for the application of an inerter on rotordynamic systems.

1

Therefore the aim of this thesis is to study perfomance and stability of a Rigid Rotor on flexible supports, through mathematical and numerical simulations, with different configurations of inerter. The thesis was partly carried out at Institute of Sound Vibration Research (ISVR) at the University of Southampton.

In this thesis takes into consideration the process of creating adequate models of simple rotor system in order to examine their lateral vibration both in the absence of any applied forces and in presence of external excitation forces. The equation of motion for the rotor system are obtained and manipulated using the software Maple while the free and forced lateral response are numerically evaluated using Matlab. The configuration of the studied system is such that the rotor shaft is supported at its extremities by two bearings called bearing 1 and bearing 2. Both supports are given horizontal and vertical stiffness (or damping or inerter). The numerical value was chosen accordingly with the book Dynamics of Rotating Machines [5] and two different cases are considered. Case A is suitable to model the behaviour of a rigid Rotor on Isotropic Flexible supports while case B simulates a rigid Rotor on Anisotropic Flexible supports.

The first objective of this thesis is to develop the correct set of analytical equations to model the dynamics of a rotor with an inerter. A validation for the analytical modelling is provided in Appendix D. The second objective of this thesis is to study fundamental influence of inerter on the natural frequencies of vibrations system. The fact that inerter can reduce the natural frequencies of vibration system is theoretically demostrated in Chapter 6. Moreover the effectiveness of using the inerter to reduce the natural frequencies is also addressed. Finally, the ultimate aim of the thesis was to assemble an inerter. A fluid inerter was built at the Dynamics Laboratory of ISVR at the University of Southampton. It has been shown theoretically that the object built actually behaves as a inerter.

The thesis is structured as following: in Chapter 2 and 3 the dynamics of a rigid rotor on flexible support are studied. The analytical equations of the motion for the 4 Degrees of Freedom rotor system are found for both the Isotropic and Anisotropic supports configurations. The effect of viscous damping in the bearing is then introduced and illustrated by means the Campbell Diagram through some numerical examples. Furthermore, in the first part of this thesis it is examined how the rotor-bearing systems responds

to external forces. In particular, the response to a mass eccentricity is investigated for Isotropic and Anisotropic Supports.

In the second part of this thesis (Chapter 4, 5 and 6) the Inerter is introduced. The inertance of a Passive Mechanical Inerter, the inertance of Hydraulic Inerter and the inertance of Fluid Inerter are examined and studied. Chapter 5 highlights the reported Performance Benets of employing Inerters which can be found in literature [2], [9], [11], [15] and [16]. In the Chapter 6, the Dynamics of Rotating Machines with Inerter are studied starting with a simple single degree of freedom System and then raising the complexity to a final 6 DoFs System with Inerter.

Finally, in the third and last part of this thesis (Chapter 7) is presented the mechanical design of a fluid inerter and investigated its modelling and experimental behaviour. The fluid inerter it is built in the Dynamics Laboratory of ISVR and it is realized as test bench for some experiments. In Chapter 7 the tests on the fluid inerter under different loads, amplitudes and frequencies are presented.

Chapter 2

Free Lateral Response

2.1 Rigid Rotor on Flexible Support

A uniform rigid rotor, that is considered in this thesis for our study, is shown in Figure(2.1). The rotor has a length of 0.5m and a diameter of 0.2m and is made from steel with a density of 7810 . It is supported at the ends by two bearings: bearing 1 and bearing 2 as indicated in Figure(2.1). The rotor is to be considered symmetric because the bearings are arranged at the same distance from the center of rotor. For all cases considered the distance of the bearings from the center of rotor was $0.5\,m$. In this study only symmetric rotor is analysed.

The mass of rotor is:

$$m = \rho \pi D^2 \frac{L}{4} = 7810 \cdot \pi \cdot 0.2^2 \cdot \frac{0.5}{4} = 122.68 kg \qquad (2.1)$$

and the polar and diametral inertias are:

$$I_P = \frac{mD^2}{8} = \frac{122.68 \cdot 0.2^2}{8} = 0.6134 kg \cdot m^2 \qquad (2.2)$$

$$I_d = \frac{I_P}{2} + \frac{mL^2}{12} = 2.8625 kg \cdot m^2 \qquad (2.3)$$

This value of mass of the rotor and these values of polar and diametral inertias will be used in all study models in this thesis.
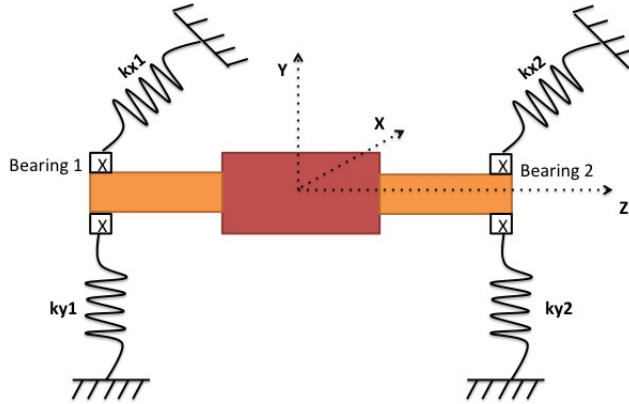
Figure 2.1: Rigid Rotor on Elastic Support

2.2 Dynamic of a Rigid Rotor on Flexible Support

To develop the equations of the motion for this system, it is possible to use an energy method (e.g Lagranges equations) or, alternatively, directly, apply Newtons second law of motion.
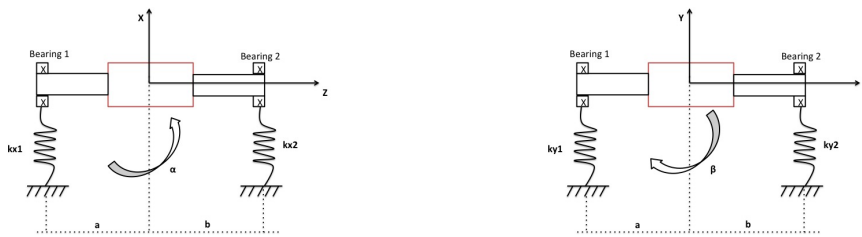
Figure 2.2: Rigid Rotor on elestic support

This Rotor has four degrees of freedom because it can translate in the directions Ox and Oy and it also can rotate about these axes. Practitioners

often term the translation and rotation as bounce and tilt motion, respectively. It is chosen to describe the movement of the rotor in terms of the displacements of its center of mass in the directions Ox and Oy, x and y, respectively, and the clockwise rotations about Ox and Oy, β and α, respectively.

The equations of motion for a Rigid Rotor on Flexible Supports are obtained using the software Maple 2015; The partial code of Maple that it is used for develop the equations of motion is reported in following script:

```
 1 >restart: with(MBSymba_r6):
 2 >with(LinearAlgebra):
 3
 4 %First define the body frame:
 5 >linear_modeling({x(t),y(t),alpha(t), beta(t)}); ...
      %rotations due to bearings elasticicy
 6 >Omega; %constant spin velocity
 7 >BF := translate(x(t),y(t),0) * rotate('X',alpha(t)) * ...
      rotate ('Y',beta(t))  *
 8 rotate('Z',Omega*t);# * translate(r,0,0);
 9
10 %definition of rotor mass properties
11 >rotor := ..................... show(rotor);
12
13 %Center of gravity:
14 >G := make_POINT(BF, 0, 0, 0); show(G);
15
16 %Right Bearing
17 >R := make_POINT(BF,0,0, b): show(R):
18 >FxR := -kX2*comp_X(R,ground):
19 >FyR := -kY2*comp_Y(R,ground):
20 >bearing_R := make_FORCE( .................): show(bearing_R);
21
22 %Left Bearing
23 >L := make_POINT(BF,0,0,-a): show(L):
24 >FxL := -kX1*comp_X(L,ground):
25 >FyL := -kY1*comp_Y(L,ground):
26 >bearing_L := make_FORCE( .................): show(bearing_L);
27
28 %Newton Equation
29 >eqnsN := newton_equations(.................): show(%);
30
31 %Euler Equation
32 >eqnsE := euler_equations(...................,CoM(rotor)):
```

```
33
34  >project(eqnsE,BF): show(%):
35  >q := [x(t),y(t), alpha(t), beta(t)]; nq:=nops(q); ...
       generalized coordinates
36  >qdot    := map(diff,q,t):
37  >qdotdot := map(diff,qdot,t):
38
39  %Equation of Motion
40  >qeqns := [comp_X(eqnsN), comp_Y(eqnsN), comp_X(eqnsE), ...
       comp_Y(eqnsE)]: <%>;
41  ..........
42  text
43  ..........
```

The equations of motion for a rigid rotor on flexible support obtained by using Maple 2015 are:

$$
\begin{cases}
m\ddot{x} + (k_{x1} + k_{x2})x + (-ak_{x1} + bk_{x2})\alpha = 0 \\
m\ddot{y} + (k_{y1} + k_{y2})y + (ak_{y1} - bk_{y2})\beta = 0 \\
I_d\ddot{\alpha} - I_p\Omega\dot{\beta} - (ak_{x1} + bk_{x2})y + (a^2k_{x1} + b^2k_{x2})\alpha = 0 \\
I_d\ddot{\beta} + I_p\Omega\dot{\alpha} + (ak_{y1} - bk_{y2})y + (a^2k_{y1} + b^2k_{y2})\beta = 0
\end{cases}
\tag{2.4}
$$

Letting:

$$
\begin{cases}
k_{xT} = k_{x1} + k_{x2} \\
k_{yT} = k_{y1} + k_{y2} \\
k_{xC} = -ak_{x1} + bk_{x2} \\
k_{yC} = -ak_{y1} + bk_{y2} \\
k_{xR} = a^2k_{x1} + b^2k_{x2} \\
k_{yR} = a^2k_{y1} + b^2k_{y2}
\end{cases}
$$

where the subscripts T,C and R have been chosen to indicate translational, coupling between displacement and rotation and rotational stiffness cofficients. Then, the equation of the motion can be written more concisely as:

$$
\begin{cases}
m\ddot{x} + k_{xT}x + k_{xC}\alpha = 0 \\
m\ddot{y} + k_{yT}y - k_{yC}\beta = 0 \\
I_d\ddot{\alpha} - I_p\Omega\dot{\beta} + k_{xC}x + k_{xR}\alpha = 0 \\
I_d\ddot{\beta} + I_p\Omega\dot{\alpha} - k_{yC}y + k_{yR}\beta = 0
\end{cases}
\tag{2.5}
$$

The last system with the equations of the motion shows that there is elastic coupling between the first and third equations as well as the second and fourth equations. Futhermore, gyroscopic couples introduce a coupling between the 3th and 4th equations. Thus, we conclude that all these are coupled.

2.3 Isotropic Flexible Support

Let us assume that the flexibility of the bearing support is the same in both of the transverse directions; that is, the bearing supports are isotropic. Letting:

$$\begin{cases} k_{xT} = k_{yT} = k_T \\ k_{xC} = k_{yC} = k_C \\ k_{xR} = k_{yR} = k_R \end{cases}$$

It is possible to simplify the Equation[2.4] using these simplifying relationships:

$$\begin{cases} m\ddot{x} + k_T x + k_C \alpha = 0 \\ m\ddot{y} + k_T y - k_C \beta = 0 \\ I_d\ddot{\alpha} - I_p\Omega\dot{\beta} + k_C x + k_R \alpha = 0 \\ I_d\ddot{\beta} + I_p\Omega\dot{\alpha} - k_C y + k_R \beta = 0 \end{cases} \tag{2.6}$$

if $k_C = 0$ which implies that $k_{xC} = 0$ and $k_{yC} = 0$ the relationships become:

$$\begin{cases} m\ddot{x} + k_T x = 0 \\ m\ddot{y} + k_T y = 0 \\ I_d\ddot{\alpha} - I_p\Omega\dot{\beta} + k_R \alpha = 0 \\ I_d\ddot{\beta} + I_p\Omega\dot{\alpha} + k_R \beta = 0 \end{cases} \tag{2.7}$$

The first two equations uncoupled give:

$$\omega_1 = \omega_2 = \sqrt{\frac{k_T}{m}} \tag{2.8}$$

The second pair of equations is coupled; letting:

$$\alpha(t) = \alpha_0 e^{\omega t} \tag{2.9}$$

and

$$\beta(t) = \beta_0 e^{\omega t} \tag{2.10}$$

The last two natural frequencies are:

$$\omega_3 = -\frac{I_p \Omega}{2I_d} + \sqrt{\left(\frac{I_p \Omega}{2I_d}\right)^2 + \frac{k_R}{I_d}} \tag{2.11}$$

and

$$\omega_4 = \frac{I_p \Omega}{2I_d} + \sqrt{\left(\frac{I_p \Omega}{2I_d}\right)^2 + \frac{k_R}{I_d}} \tag{2.12}$$

These natural frequencies are dependent on the speed of rotation. As this speed tends to zero, the natural frequencies become identical to the second pair of roots of Equations [2.7]:

For example, if $\Omega = 0$ the natural frequencies are:

$$\omega_3 = \omega_4 = \sqrt{\frac{k_R}{I_d}} \tag{2.13}$$

2.4   Anisotropic Flexible Support

For general flexible supports, the task is to solve Equation[2.6], repeated here for convenience:

$$\begin{cases} m\ddot{x} + k_{xT}x + k_{xC}\alpha = 0 \\ m\ddot{y} + k_{yT}y - k_{yC}\beta = 0 \\ I_d\ddot{\alpha} - I_p\Omega\dot{\beta} + k_{xC}x + k_{xR}\alpha = 0 \\ I_d\ddot{\beta} + I_p\Omega\dot{\alpha} - k_{yC}y + k_{yR}\beta = 0 \end{cases} \tag{2.14}$$

These are the equations of motion for a flexibly supported with differing stiffness proprieties in the x and y directions.

It is helpful to express these equations in the matrix form as:

$$M\ddot{q} + \Omega G\dot{q} + Kq = 0 \tag{2.15}$$

where:

$$M = \begin{bmatrix} m & 0 & 0 & 0 \\ 0 & m & 0 & 0 \\ 0 & 0 & I_d & 0 \\ 0 & 0 & 0 & I_d \end{bmatrix} \tag{2.16}$$

$$G = \begin{bmatrix} 0 & 0 & 0 & 0 \\ 0 & 0 & 0 & 0 \\ 0 & 0 & 0 & I_p \\ 0 & 0 & -I_p & 0 \end{bmatrix} \tag{2.17}$$

$$K = \begin{bmatrix} k_{xT} & 0 & 0 & k_C \\ 0 & k_{yT} & -k_{yC} & 0 \\ 0 & -k_{yC} & k_{yR} & 0 \\ k_{xC} & 0 & 0 & k_{xR} \end{bmatrix} \tag{2.18}$$

and

$$q = \begin{bmatrix} x & y & \beta & \alpha \end{bmatrix}^T \tag{2.19}$$

The mass and stiffness matrices, M and K, respectively, are symmetric, positive definite matrices. In contrast, the gyroscopic matrix G is skew-symmetric. To determine the roots of Equations[2.14], the equations must be rearranged in the following form:

$$\begin{bmatrix} \Omega G & M \\ M & 0 \end{bmatrix} \frac{d}{dt} \begin{Bmatrix} q \\ \dot{q} \end{Bmatrix} + \begin{bmatrix} K & 0 \\ 0 & -M \end{bmatrix} \frac{d}{dt} \begin{Bmatrix} q \\ \dot{q} \end{Bmatrix} = \begin{Bmatrix} 0 \\ 0 \end{Bmatrix} \tag{2.20}$$

This equation can be written as:

$$A\dot{x} + Bx = 0 \tag{2.21}$$

where:

$$x = \begin{Bmatrix} q \\ \dot{q} \end{Bmatrix} \tag{2.22}$$

$$\dot{x} = \frac{d}{dt} \begin{Bmatrix} q \\ \dot{q} \end{Bmatrix} \tag{2.23}$$

$$A = \begin{bmatrix} \Omega G & M \\ M & 0 \end{bmatrix} \tag{2.24}$$

$$B = \begin{bmatrix} K & 0 \\ 0 & -M \end{bmatrix} \qquad (2.25)$$

Looking for solutions of the form $x(t) = x_0 e^{st}$, then $\dot{x} = s x_0 e^{st}$; Thus, the Equation[2.21] become:

$$s A x_0 = -B x_0 \qquad (2.26)$$

This is an $8x8$ eigenvalue problem and it must be solved numerically. In our cases the partial Matlab code shown below is used to risolve this problem; If the system is described by n coordinates (4 in this case, but in the next chapter were used 5 and 6 coordinates), then there are $2n$ roots in the form of n complex conjugates pairs. Each pair of complex conjugate rapresents one natural frequency. Thus, for Rigid Rotor:

$$\begin{cases} s_1 = +j\omega_1 \\ s_2 = +j\omega_2 \\ s_3 = +j\omega_3 \\ s_4 = +j\omega_4 \\ s_5 = -j\omega_5 \\ s_6 = -j\omega_6 \\ s_7 = -j\omega_7 \\ s_8 = -j\omega_8 \end{cases} \qquad (2.27)$$

where s_i and s_{4+i} form complex conjugate pair for each i. Corrisponding to these roots are n complex conjugate pairs of eigenvectors. For each pair of eigenvectors, the first n elements correspond to a mode of system.

This script is shows the Matlab code that I use to resolve Eigenvalue problem.

```matlab
1  % Rigid rotor on two flexible isotropic support.
2  %dimensions of rotor
3  L = 0.5; a = L/2;   b = L/2;
4  D=0.2;
5  rho=7810;
6  m = rho*pi*D^2*(L/4);
7  Ip = (m*D^2)/8;
8  Id = Ip/2 + (m*L^2)/12;
```

```
 9  kT = 2*10^6;
10  kR = 125*10^3;
11  kC = 0;
12
13  omega=[0:100:4000]*2*pi/60;
14  omega_n=zeros(4,length(omega));
15
16  for i=1:length(omega)
17          M = diag([m m Id Id]);
18          G = [0 0 0 0;0 0 0 0;0 0 0 Ip;0 0 -Ip 0];
19          Z = zeros(4,4);
20          A = .................
21  .................
22  end
```

2.5   The Effect of Damping
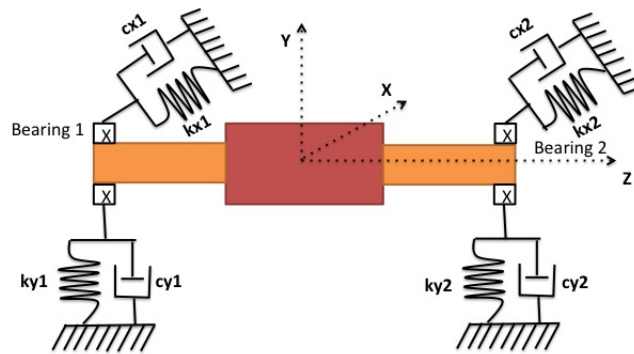
Figure 2.3: Rigid Rotor with Damping

Now the effect of viscous damping in the bearings is considered in comparison with the previous case where it had only stiffness as shown in Figure[2.1]. Assuming that a viscous damper is placed in parallel with each spring element supporting the bearing.

If c is the viscous damping coefficient and is defined as the force required to produce a unit velocity accross the damping element, let:

$$
\begin{cases}
c_{xT} = c_{x1} + c_{x2} \\
c_{yT} = c_{y1} + c_{y2} \\
c_{xC} = -ac_{x1} + bc_{x2} \\
c_{yC} = -ac_{y1} + bc_{y2} \\
c_{xR} = a^2 c_{x1} + b^2 c_{x2} \\
c_{yR} = a^2 c_{y1} + b^2 c_{y2}
\end{cases}
\tag{2.28}
$$

Using these definitions, susbstituting Equation[2.28] into Equation[2.14] and rearranging these equations the result is:

$$
\begin{cases}
m\ddot{x} + c_{xT}\dot{x} + c_{xC}\dot{\alpha} + k_{xT}x + k_{xC}\alpha = 0 \\
m\ddot{y} + c_{yT}\dot{y} - c_{yC}\dot{\beta} + k_{yT}y - k_{yC}\beta = 0 \\
I_d\ddot{\alpha} - I_p\Omega\dot{\beta} + c_{xC}\dot{x} + c_{xR}\dot{\alpha} + k_{xC}x + k_{xR}\alpha = 0 \\
I_d\ddot{\beta} + I_p\Omega\dot{\alpha} - c_{yC}\dot{y} + c_{yR}\dot{\beta} - k_{yC}y + k_{yR}\beta = 0
\end{cases}
\tag{2.29}
$$

The following script reports the limited Maple Code used to obtain the Equations [2.29].

```
1  >restart: with(MBSymba_r6):
2  >with(LinearAlgebra):
3
4  %First define the body frame:
5  >linear_modeling({x(t),y(t),alpha(t), beta(t)}); ...
       %rotations due to bearings elasticicy
6  >Omega; %constant spin velocity
7  >BF := translate(......................);# * ...
       translate(r,0,0);
8
9  %definition of rotor mass properties
10 >rotor := make_BODY(...................); show(rotor);
11
12 %Center of gravity:
13 >G := make_POINT(BF, 0, 0, 0); show(G);
14
15 %Right Bearing
16 >R := make_POINT(...................): show(R):
17 >FxR := -kX2*comp_X(R,ground)-cX2*diff(comp_X(R,ground),t):
```

```
18  >FyR := -kY2*comp_Y(R,ground)-cY2*diff(comp_Y(R,ground),t):
19  >bearing_R := make_FORCE( .......................): ...
       show(bearing_R);
20  ...............
21  %text
22  ...............
23  %Newton Equation
24  >eqnsN := newton_equations(........................): show(%);
25
26  %Euler Equation
27  >eqnsE := ...
       euler_equations(..........................,CoM(rotor)):
28
29  >project(eqnsE,BF): show(%):
30  >q := [x(t),y(t), alpha(t), beta(t)]; nq:=nops(q); ...
       generalized coordinates
31  >qdot    := map(diff,q,t):
32  >qdotdot := map(diff,qdot,t):
33
34  %Equation of Motion
35  >qeqns := [.................................]: <%>;
36  ...............
37  %text
38  ...............
39  end
```

2.6   Natural Frequencies - Campbell Diagram

Due to Gyroscopic effects, the roots of the characteristic equation (i.e., the eigenvalues) vary with rotational spees. This is not the only reason why the eigenvalues vary with rotational speed. For example, hydrodynamic bearing have stiffness and damping properties that vary with rotational speed; these, in turn, effect the eigenvalues.

It is convenient to illustrate graphically the way in which the roots change with rotational speed. Graps can be plotted that show these changes in various ways. Typically, the rational speed is plotted on the x-axis and the imaginary part of the roots, or the natural frequencies are plotted on the y-axis.

Campbell Diagram can also illustrate the relationship between resonances and parameters as well as rotational speed. In this way, the effect of varying a bearing stiffness or rotor-inertia propriety may be examined.
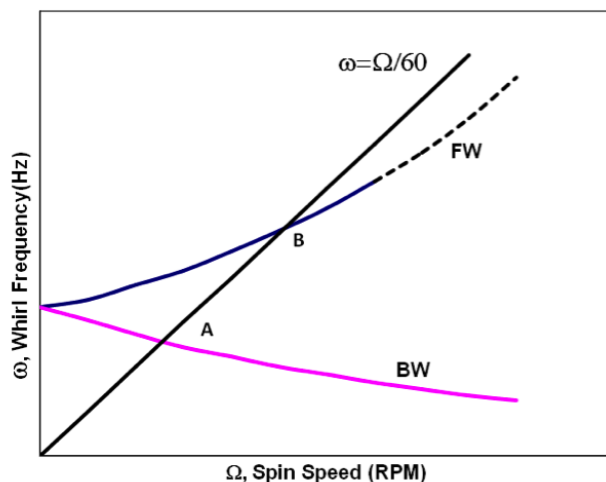
Figure 2.4: Campbell Diagram

2.6.1   Example Campbell Diagram

In this Example [Ref. [5]-Ex. 3.7.1] the natural frequencies maps are plotted of rotor spin speed up to 2000 rev/min for the rigid rotor described in Chapter [2], supported by the following bearing stiffnesses:

- A) : $k_{x1} = 1.0MN/m$, $k_{y1} = 1.0MN/m$, $k_{x2} = 1.0MN/m$, $k_{y2} = 1.0MN/m$.

- B) : $k_{x1} = 1.0MN/m$, $k_{y1} = 1.0MN/m$, $k_{x2} = 1.3MN/m$, $k_{y2} = 1.3MN/m$.

- C) : $k_{x1} = 1.0MN/m$, $k_{y1} = 1.5MN/m$, $k_{x2} = 1.0MN/m$, $k_{y2} = 1.5MN/m$.

- D) : $k_{x1} = 1.0MN/m$, $k_{y1} = 1.5MN/m$, $k_{x2} = 1.3MN/m$, $k_{y2} = 2.0MN/m$.

Case A

The natural frequency map for this system is shown in Figure(2.5). In this case therefore the first and the second equations of Equation[2.6] are uncoupled from the rest of system and are independent of rotational speed.
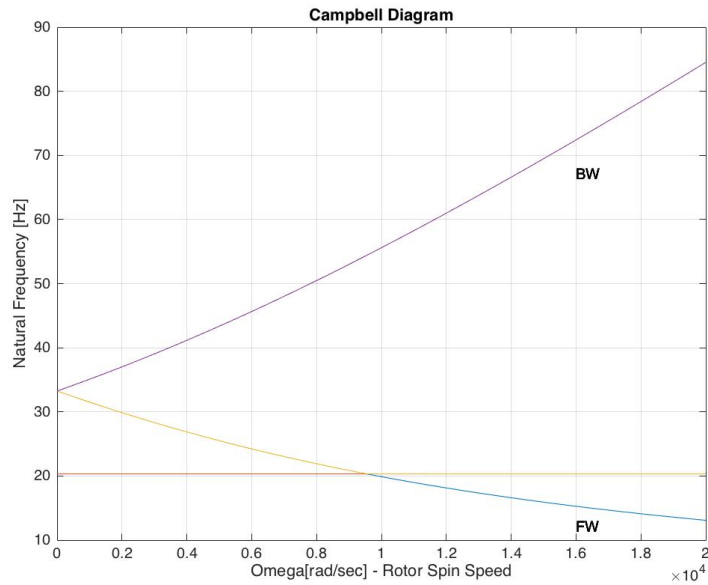
Figure 2.5: Campbell Diagram: case A

The stiffnesses in the x and y direction are identical; therefore, the two natural frequencies that are derived from these two equations are identical and are equal to approximately 20Hz. At zero rotational speed, the third and fourth equations are uncoupled; hence, the two natural frequencies that are derived from these equations also are identical. Once the rotor begins to spin, the third and fourth equations become coupled due to gyroscopic effects and the two natural frequencies separate.

Case B

The natural map for this system is shown in Figure(2.6). In this case $k_C \neq 0$ and all of the equation are coupled, expet when $\Omega = 0$.

All natural frequencies are influenced by gyroscopic effects. Two frequencies decrease with rotational speed; the other two frequencies increase, although the increase from approximately 20Hz is barely perceptible. In this case, all of the equations are coupled and frequency line do not intersect.
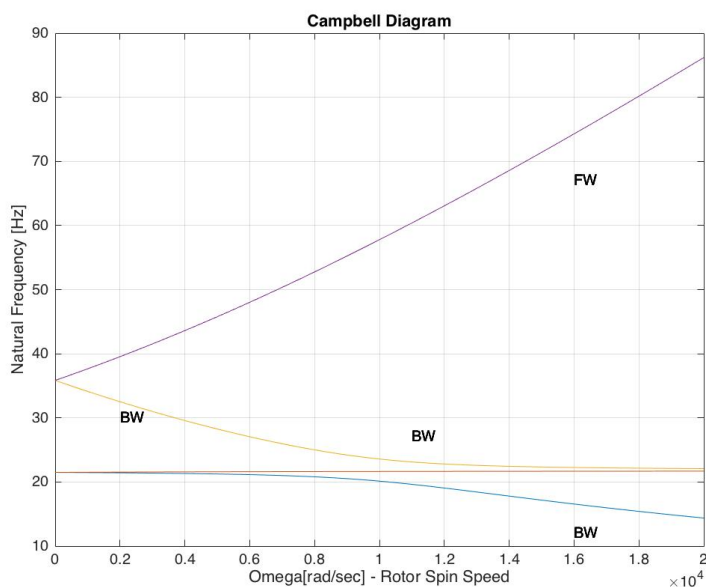
Figure 2.6: Campbell Diagram: case B

Case C

The natural frequency map for this system is shown in firgure (2.7). In this example $k_{xC} = k_{yC} = 0$. The first and the second equations are uncoupled from the rest of the system and they are independent of rotational speed. At zero rotational speed, the third and fourth equations are also uncoupled and the two natural frequencies derived from them are also distinct. When rotor begins to spin, the map shows that one of these natural frequencies increases and the other decreases, due to gyroscopic effects.

Case D

The natural frequency map for this system system is shown in Figure(2.8). In this case, $k_{xC} \neq 0$ and $k_{yC} \neq 0$ so that all of the equations are coupled, except when $\Omega = 0$. From the natural frequency map, we see that all of the frequencies are influenced by gyroscopic couples and frequency lines do not intersect.
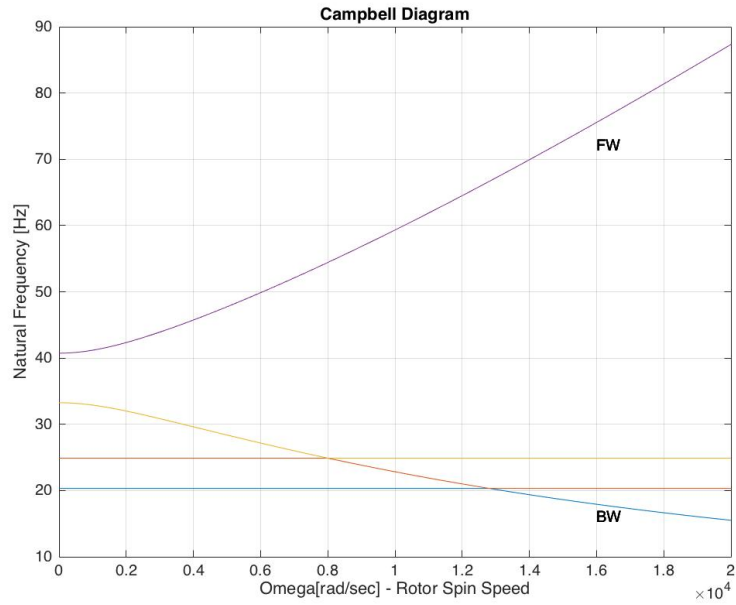
Figure 2.7: Campbell Diagram: case C
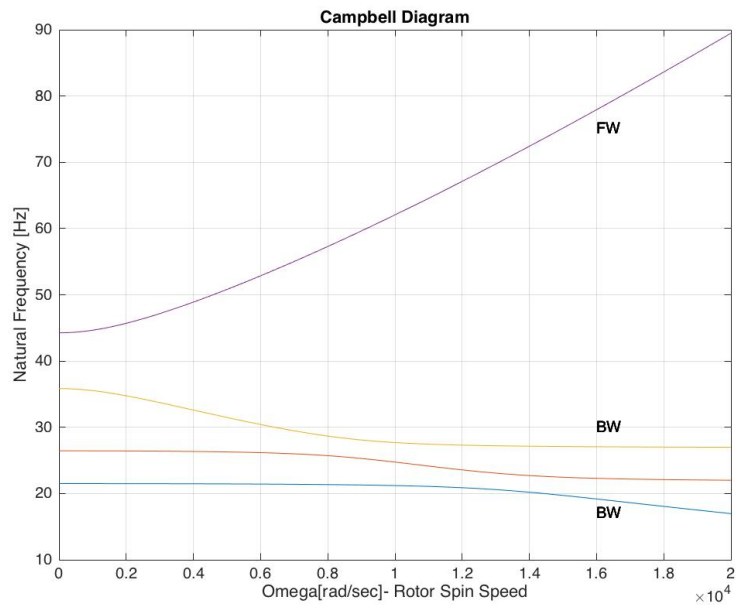
Figure 2.8: Campbell Diagram: case D

2.6.2 Example Campbell Diagram with Damping

The rigid rotor of Chapter[2] is supported by bearings with the following dynamics proprieties:

$$
\begin{cases}
k_{x1} = 1.0\,MN/m \\
k_{y1} = 1.0\,MN/m \\
k_{x2} = 1.0\,MN/m \\
k_{y2} = 1.0\,MN/m \\
c_{x1} = 1.0\,kNs/m \\
c_{y1} = 1.0\,kNs/m \\
c_{x2} = 1.2\,kNs/m \\
c_{y2} = 1.2\,kNs/m
\end{cases}
\tag{2.30}
$$

The aim of this example is to plot the variation of the damping factors, ξ, and the natural frequencies with rotational speed in the range 0 to 500 rev/min. The eigenvalue problem is solved for various rotor speeds to determine the roots s_i. Now, because $\{s_i, s_{i+4}\} = -\xi_i \omega_i \pm j\omega_{di}$, it is possible to deduce ξ.

Figure (2.10) shows that the damping factors of the two higher modes become identical at 194.60 rev/min. The natural frequencies of the two higher modes are identical below 194.60 rev/min and the bifurcate.

In the Figure (2.10) the modal damping ratios and natural frequencies against rotor spin speed are plotted:
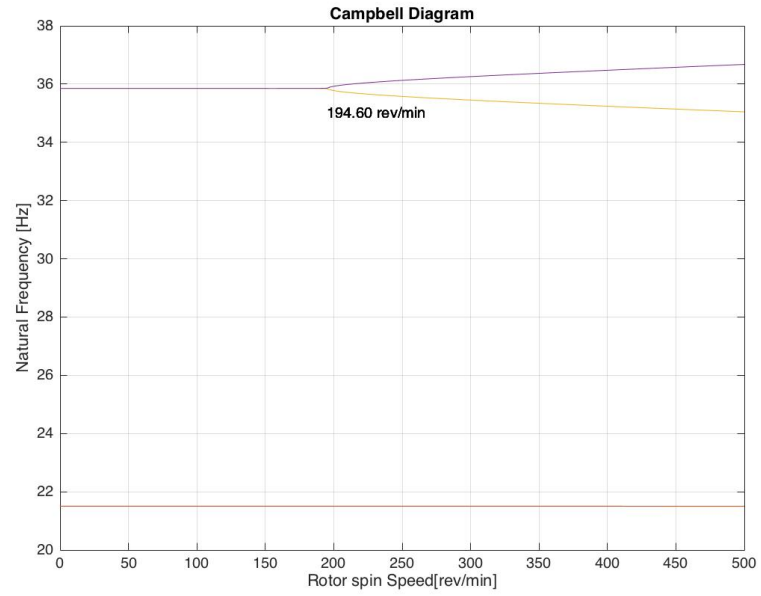
Figure 2.9: Campbell Diagram
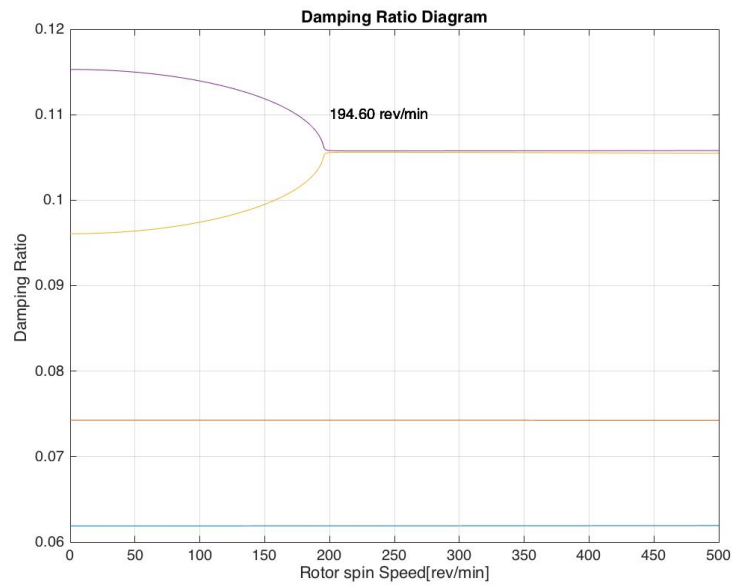
Figure 2.10: Damping Ratio

Chapter 3

Forced Lateral Response

3.1 Introduction

In Chapter 2 methods are presented to determine the dynamic characteristics of a rotor-bearing system, such as the natural frequencies and damping factors. In this chapter, it is examined how rotor-bearing systems respond to force. The most common forces acting in rotating machines are lateral forces and moments whose frequency is identical to rotor speed or multiples of rotor speed. A force whose frequency is identical to rotor speed is said to be a synchronous force. The most significant lateral forces and moments are usually caused by an imperfect distribution of mass in the rotor. As the rotor spins about its equilibrium position, forces and moments are generated that are called out-of balance forces and moments. The direction of these forces and moments is fixed relative to the rotor; therefore, their direction rotates with the rotor. Thus, the excitation frequency in any plane, lateral to the axis of the rotor, is locked to the speed of rotation; for this reason, they are synchronous forces and moments. Due to manufacturing tolerances and other factors, it is not possible to ensure that rotor are perfectly balanced.

3.2 Modeling Out-of-Balance Forces

To begin with it is necessary to examine the synchronous response of a rotor to out of balance forces. The analysis is developed in terms of a rigid rotor but extends readily to flexible rotor. To determine the effect of out of balance mass on the rigid circular rotor shown in Figure(2.1), it is initially assumed

that the center of mass of the rotor is displacement a distance from the shaft centerline at equilibrium. Considering the displacement of the rotor center of mass along axes O_x and O_y, Figure (3.1) shows the equilibrium position, O ; the instantaneous position of the disturbed roto centerline, S; and the position of the mass center of the rotor, G. Note that $|SG| = \varepsilon$.
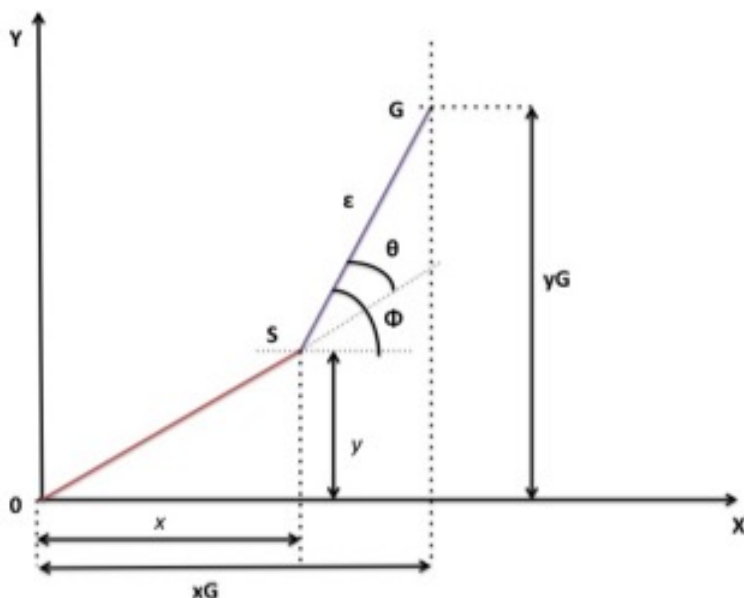
Figure 3.1: Displacement of the rotor

The instantaneous angle between the line SG(which represents a line on the rotor) and the O_x axis is Φ, and the istantaneous angle between the line OS and the O_x axis is then $\Phi - \Theta$. The distance $|OS|$, which is calculated during the analysis, is the amplitude of the whirl of the rotor. The center of mass of the rotor moves x_G and y_G in the X and Y directions, respectively, whereas the centerline of the rotor deflects x and y in the corresponding directions at the flexible bearings. Now, from Figure (3.1), it is shown that:

$$x_G = x + \epsilon cos\Phi \tag{3.1}$$

$$y_G = y + \epsilon sin\Phi \tag{3.2}$$

Differentiating these equations twice with respect to time and noting that ϵ is constant gives:

$$\ddot{x}_G = \ddot{x} + \epsilon(-\ddot{\Phi}cos\Phi - \dot{\Phi}^2 sin\Phi) \tag{3.3}$$

$$\ddot{y}_G = \ddot{y} + \epsilon(-\ddot{\Phi}sin\Phi - \dot{\Phi}^2 cos\Phi) \tag{3.4}$$

In deriving the previous equation, the analysis can not be restricted to the case of a rotor spinning with a constant angular velocity. Now if this semplification is introduced , then at constant speed of rotation Ω, $\dot{\Phi} = \Omega$ and $\ddot{\Phi} = 0$. Thus,

$$\ddot{x}_G = \ddot{x} - \epsilon\Omega^2 cos\Omega t \tag{3.5}$$

$$\ddot{y}_G = \ddot{y} - \epsilon\Omega^2 sin\Omega t \tag{3.6}$$

The equations of the motion for the free vibration of this rotor, including damping at the supports and gyroscopics effects, are given in Equation[2.29] and are repeated here for convenience:

$$\begin{cases} m\ddot{x} + c_{xT}\dot{x} + c_{xC}\dot{\alpha} + k_{xT}x + k_{xC}\alpha = 0 \\ m\ddot{y} + c_{yT}\dot{y} - c_{yC}\dot{\beta} + k_{yT}y - k_{yC}\beta = 0 \\ I_d\ddot{\alpha} - I_p\Omega\dot{\beta} + c_{xC}\dot{x} + c_{xR}\dot{\alpha} + k_{xC}x + k_{xR}\alpha = 0 \\ I_d\ddot{\beta} + I_p\Omega\dot{\alpha} - c_{yC}\dot{y} + c_{yR}\dot{\beta} - k_{yC}y + k_{yR}\beta = 0 \end{cases} \tag{3.7}$$

For the rotor being considered, the center of mass is offset from the shaft centerline at equilibrium by a small quantity ϵ, and the displacement of the center of mass is given by x_G and y_G. However, the displacement of the springs and dampers (at the bearings) are still in terms of x and y.

Thus, replacing $\ddot{x}$ by $\ddot{x}_G$ and $\ddot{y}$ by $\ddot{y}_G$ in Equation [3.7], the Equation [3.7] becomes:

$$\begin{cases} m\ddot{x}_G + c_{xT}\dot{x} + c_{xC}\dot{\alpha} + k_{xT}x + k_{xC}\alpha = m\epsilon\Omega^2 cos\Omega t \\ m\ddot{y}_G + c_{yT}\dot{y} - c_{yC}\dot{\beta} + k_{yT}y - k_{yC}\beta = m\epsilon\Omega^2 sin\Omega t \\ I_d\ddot{\alpha} - I_p\Omega\dot{\beta} + c_{xC}\dot{x} + c_{xR}\dot{\alpha} + k_{xC}x + k_{xR}\alpha = 0 \\ I_d\ddot{\beta} + I_p\Omega\dot{\alpha} - c_{yC}\dot{y} + c_{yR}\dot{\beta} - k_{yC}y + k_{yR}\beta = 0 \end{cases} \tag{3.8}$$

Substituting for and from Equations [3.8] and rearranging gives:

$$\begin{cases} m\ddot{x} + c_{xT}\dot{x} + c_{xC}\dot{\alpha} + k_{xT}x + k_{xC}\alpha = 0 \\ m\ddot{y} + c_{yT}\dot{y} - c_{yC}\dot{\beta} + k_{yT}y - k_{yC}\beta = 0 \\ I_d\ddot{\alpha} - I_p\Omega\dot{\beta} + c_{xC}\dot{x} + c_{xR}\dot{\alpha} + k_{xC}x + k_{xR}\alpha = 0 \\ I_d\ddot{\beta} + I_p\Omega\dot{\alpha} - c_{yC}\dot{y} + c_{yR}\dot{\beta} - k_{yC}y + k_{yR}\beta = 0 \end{cases} \quad (3.9)$$

Equations [3.9] shows that the lateral offset of the mass center from the equilibrium position causes out of balance forces to act the system. Thus, it can develop the equations of the motion for a system with a disk or rotor with an offset either by modifying the position of the center of mass or more directly by adding forces on the right-hand side of the Equations [3.9], whichever is more convenient.

3.3 Response for Isotropic Supports

Example Response to a Mass eccentricity for Isotropic Supports

In this example it is found the response to a mass eccentricity of 0.1mm and it is plotted the Campbell Diagram. It is referred at esercise 6.2.1 of the book [5]. It is considered the rotor in the Chapter[1]. The stiffness coefficients are:

- k_T=1000+1300=2300 kN/m

- k_R=$0.25^2 \cdot 1000 + 0.25^2 \cdot 1300 = 143.75 kN/m$

- k_C=$-0.25 \cdot 1000 + 0.25 \cdot 1300 = 75 kN$

Similary,

- c_T=23 Ns/m

- c_R=1.4375 Nms

- c_C=0.75 kN

Firstly, using the Equations [2.6] for Isotropic bearings, it is considered the free lateral vibrations to calcolate the natural frequencies and to obtained the Campbell Diagram:

$$\begin{cases} m\ddot{x}_G + c_{xT}\dot{x} + c_{xC}\dot{\alpha} + k_{xT}x + k_{xC}\alpha = 0 \\ m\ddot{y}_G + c_{yT}\dot{y} - c_{yC}\dot{\beta} + k_{yT}y - k_{yC}\beta = 0 \\ I_d\ddot{\alpha} - I_p\Omega\dot{\beta} + c_{xC}\dot{x} + c_{xR}\dot{\alpha} + k_{xC}x + k_{xR}\alpha = 0 \\ I_d\ddot{\beta} + I_p\Omega\dot{\alpha} - c_{yC}\dot{y} + c_{yR}\dot{\beta} - k_{yC}y + k_{yR}\beta = 0 \end{cases} \tag{3.10}$$

It is helpful to express these equations in the matrix form as:

$$M\ddot{q} + (\Omega G + C)\,\dot{q} + Kq = 0 \tag{3.11}$$

where:

$$M = \begin{bmatrix} m & 0 & 0 & 0 \\ 0 & m & 0 & 0 \\ 0 & 0 & I_d & 0 \\ 0 & 0 & 0 & I_d \end{bmatrix} \tag{3.12}$$

$$K = \begin{bmatrix} k_T & 0 & 0 & k_C \\ 0 & k_T & -k_C & 0 \\ 0 & -k_C & k_R & 0 \\ k_C & 0 & 0 & k_R \end{bmatrix} \tag{3.13}$$

$$C = \begin{bmatrix} c_T & 0 & 0 & c_C \\ 0 & c_T & -c_C & 0 \\ 0 & -c_C & c_{cR} & 0 \\ c_C & 0 & 0 & c_R \end{bmatrix} \tag{3.14}$$

$$G = \begin{bmatrix} 0 & 0 & 0 & 0 \\ 0 & 0 & 0 & 0 \\ 0 & 0 & 0 & I_p \\ 0 & 0 & -I_p & 0 \end{bmatrix} \tag{3.15}$$

and,

$$q = \begin{bmatrix} x & y & \beta & \alpha \end{bmatrix}^T \tag{3.16}$$

The mass and the stiffness matrices, M and K, respectively, are symmetric, positive definite matrices. In contrast, the gyroscopic matrix G is

skew-symmetric. To determine the roots of the Equations [3.10], it is neces-
sary to rearrange the equation in the following form:

$$\begin{bmatrix} C + \Omega G & M \\ M & 0 \end{bmatrix} \frac{d}{dt} \begin{Bmatrix} q \\ \dot{q} \end{Bmatrix} + \begin{bmatrix} K & 0 \\ 0 & -M \end{bmatrix} \begin{Bmatrix} q \\ \dot{q} \end{Bmatrix} = \begin{Bmatrix} 0 \\ 0 \end{Bmatrix} \qquad (3.17)$$

This is an $8x8$ eigenvalue problem and it must be solved numerically.
Forming and solving Eigenvalue problem using Matlab it is possible to obtain
the following mass, stiffness and gyroscopic matrices:

$$M = \begin{bmatrix} 122.68 & 0 & 0 & 0 \\ 0 & 122.68 & 0 & 0 \\ 0 & 0 & 2.86 & 0 \\ 0 & 0 & 0 & 2.86 \end{bmatrix} \qquad (3.18)$$

$$K = \begin{bmatrix} 2.3 \cdot 10^6 & 0 & 0 & 75 \cdot 10^3 \\ 0 & 2.3 \cdot 10^6 & -75 \cdot 10^3 & 0 \\ 0 & -75 \cdot 10^3 & 1.44 \cdot 10^5 & 0 \\ 75 \cdot 10^3 & 0 & 0 & 1.44 \cdot 10^5 \end{bmatrix} \qquad (3.19)$$

$$C = \begin{bmatrix} 23.00 & 0 & 0 & 0.75 \\ 0 & 23.00 & -0.75 & 0 \\ 0 & -0.75 & 1.44 & 0 \\ 0.75 & 0 & 0 & 1.44 \end{bmatrix} \qquad (3.20)$$

$$G = \begin{bmatrix} 0 & 0 & 0 & 0 \\ 0 & 0 & 0 & 0 \\ 0 & 0 & 0 & 0.61 \\ 0 & 0 & -0.61 & 0 \end{bmatrix} \qquad (3.21)$$

The natural frequency map for this system is shown in Figure (3.2).

In this case it has only one unbalance and it is possible to calculate the
response relative to that unbalance. In Matrix notation, Equation [3.8] can
be written as:

$$M\ddot{q} + (\Omega G + C)\dot{q} + Kq = F \qquad (3.22)$$

where:

$$F = \begin{Bmatrix} m\epsilon\Omega^2 cos\Omega t \\ m\epsilon\Omega^2 sin\Omega t \\ 0 \\ 0 \end{Bmatrix} = \Re \begin{Bmatrix} m\epsilon \\ -jm\epsilon \\ 0 \\ 0 \end{Bmatrix} \Omega^2 e^{j\Omega t} \qquad (3.23)$$
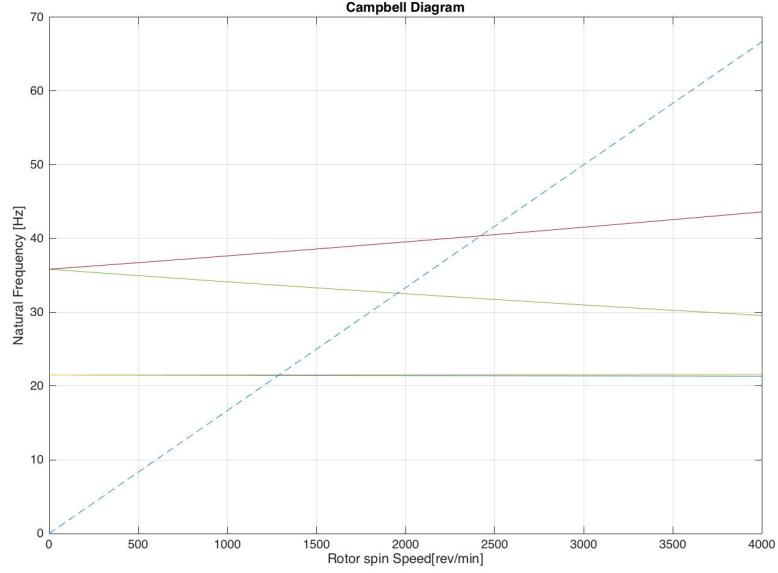
Figure 3.2: Campbell Diagram for response to a mass eccentricity

The steady-state solution is found by assuming a response of the form $q(t) = \Re(q_0 e^{j\Omega t})$. Thus,

$$\left[-\Omega^2\left[M\right] + j\Omega\left(\Omega\left[G\right] + \left[C\right]\right) + \left[K\right]\right] q_0 e^{j\Omega t} = \Omega^2 b_0 e^{j\Omega t} \tag{3.24}$$

where,

$$b_0 = \left\{ \begin{array}{c} m\epsilon \\ -jm\epsilon \\ 0 \\ 0 \end{array} \right\} \tag{3.25}$$

and, hence:

$$q_0 = \left[-\Omega^2\left[M\right] + j\Omega\left(\Omega\left[G\right] + \left[C\right]\right) + \left[K\right]\right]^{-1} \Omega^2 b_0 \tag{3.26}$$

where:

$$FRF = \frac{1}{\left[-\Omega^2\left[M\right] + j\Omega\left(\Omega\left[G\right] + \left[C\right]\right) + \left[K\right]\right]} \tag{3.27}$$

FRF is defined Frequency Response Function. The Response can be obtained as a function of rotational speed which is shown in Figure (3.3).

The figure shows that there are two peaks in the response; the speeds of rotation at which these peaks occur are called critical speeds. They occur when the frequency of the out of balance force is close to the natural frequency of the rotor-bearing system.
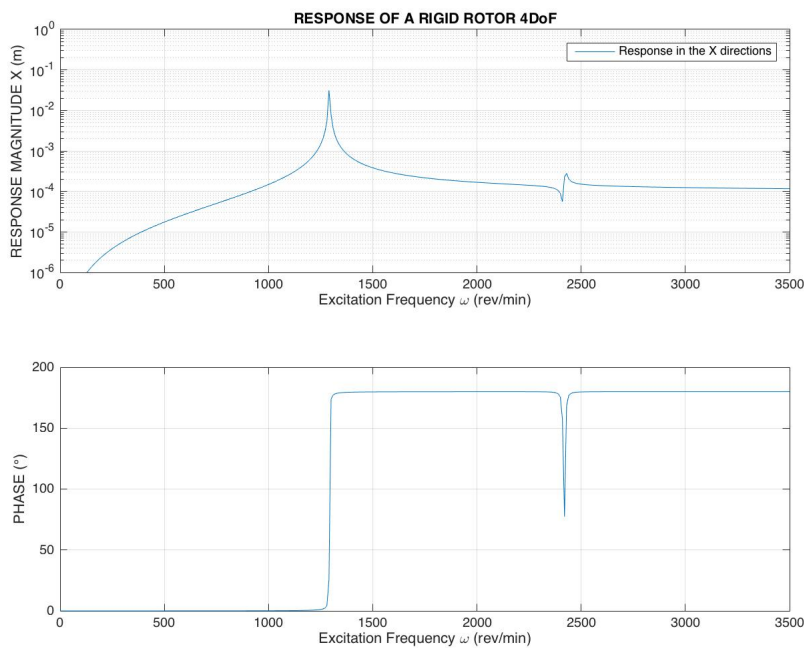

Figure 3.3: Response of a Rigid Rotor

To find the Response of the rigid rotor the following partial Matlab Code is used:

```
1  %TRANSFER FUNCTION
2  omega=[0:10:4000]*2*pi/60;
3  epsilon=0.1*10^-3; %eccentricity
4
5  %FRF%
6  for i=1:length(omega)
```

```matlab
7  H(:,:,i)=.........................;
8  end
9
10 %X e Y Displacements%
11 H11(1,:)=H(1,1,:);
12 H22(2,:)=H(2,1,:);
13 X=abs(H11);
14 Y=abs(H22);
15
16 figure(2);
17 subplot(2,1,1);
18 semilogy(omega*60/(2*pi),X);
19 grid;
20 hold on
21 semilogy(omega*60/(2*pi),Y,'--');
22 legend('Response in the x directions (solid)','Response in ...
      the y directions (dashed)');
23 xlabel('Excitation Frequency \omega (rev/min)');
24 ylabel('RESPONSE MAGNITUDE (m)');
25 axis([0 3500 10^-6 10^0])
26 title('RESPONSE OF A RIGID ROTOR 4DoF');
27
28 subplot(2,1,2);
29 plot(omega*60/(2*pi),(-angle(H11))*180/pi);
30 grid;
31 hold on
32 plot(omega*60/(2*pi),(-angle(H22))*180/pi,'--');
33 axis([0 3500 0 200])
34 xlabel('Excitation Frequency \omega (rev/min)');
35 ylabel('PHASE (\circ)');
36 end
```

3.4 Response for Anisotropic Supports

Example Response to a Mass eccentricity for Anisotropic Supports

This example aims at determining the unbalance response over the speed range 0 to $4000 rev/min$. The dimensions of the rotor are the same of the last example but in this case it has different value of damping in bearing 1 and bearing 2.

The horizontal and vertical support stiffnesses are:

- k_{x1}=1.0 MN/m

- k_{y1}=1.5 MN/m

- k_{x2}=1.3 MN/m

- k_{y2}=1.8 MN

respectively at bearing 1 and bearing 2. The damping value in the horizontal and vertical supports at both bearings are proportional to the stiffnesses and are:

- c_{x1}=20 Ns/m

- c_{y1}=30 Ns/m

- c_{x2}=26 Ns/m

- c_{y2}=36 Ns/m

respectively at bearing 1 and bearing 2. To solve this problem the equations of motion is wiritten in the matrix form:

$$M\ddot{q} + (\Omega G + C)\,\dot{q} + Kq = F \qquad (3.28)$$

where:

$$M = \begin{bmatrix} 122.68 & 0 & 0 & 0 \\ 0 & 122.68 & 0 & 0 \\ 0 & 0 & 2.86 & 0 \\ 0 & 0 & 0 & 2.86 \end{bmatrix} \qquad (3.29)$$

$$K = \begin{bmatrix} 2.3 \cdot 10^6 & 0 & 0 & 75 \cdot 10^3 \\ 0 & 3.3 \cdot 10^6 & -75 \cdot 10^3 & 0 \\ 0 & -75 \cdot 10^3 & 175 \cdot 10^3 & 0 \\ 75 \cdot 10^3 & 0 & 0 & 1.44 \cdot 10^5 \end{bmatrix} \qquad (3.30)$$

$$C = \begin{bmatrix} 46 & 0 & 0 & 1.5 \\ 0 & 66 & -1.5 & 0 \\ 0 & -1.5 & 3.5 & 0 \\ 1.5 & 0 & 0 & 2.88 \end{bmatrix} \qquad (3.31)$$

$$G = \begin{bmatrix} 0 & 0 & 0 & 0 \\ 0 & 0 & 0 & 0 \\ 0 & 0 & 0 & 0.61 \\ 0 & 0 & -0.61 & 0 \end{bmatrix} \quad (3.32)$$

and,

$$q = \begin{bmatrix} x & y & \beta & \alpha \end{bmatrix}^T \quad (3.33)$$

$$F = \begin{Bmatrix} m\epsilon\Omega^2 cos\Omega t \\ m\epsilon\Omega^2 sin\Omega t \\ 0 \\ 0 \end{Bmatrix} = \Re \begin{Bmatrix} m\epsilon \\ -jm\epsilon \\ 0 \\ 0 \end{Bmatrix} \Omega^2 e^{j\Omega t} \quad (3.34)$$

Firstly, the free solution response is solved to determine the natural frequencies and the Campbell Diagram. Forming and solving Eigenvalue problem using Matlab it has the following natural frequency Maps and Damping Ratios Diagram:
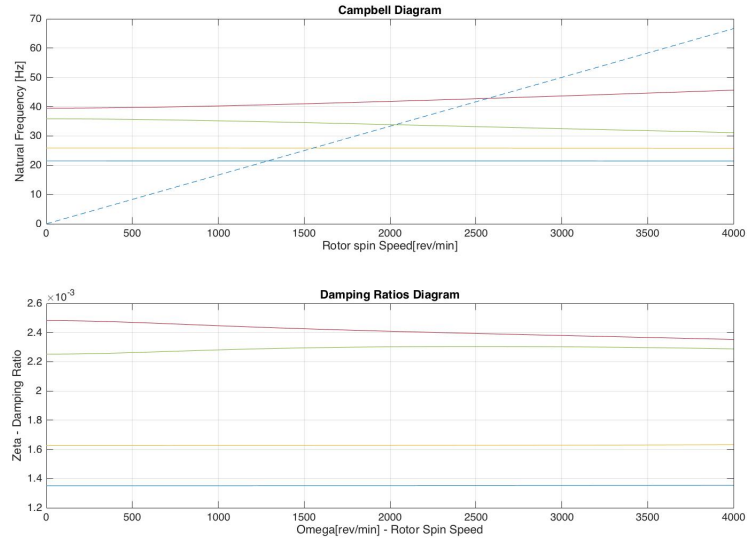

Figure 3.4: Campbell Diagram for Response to a mass eccentricity

It is clear from the Campbell Diagram, shown in Figure (3.4), that when a rotor resonance frequency is coincident with the rotational speed, a maximum response to out-of-balance is occured. These maximum responses are the system critical speed; thus, there are four critical speeds in this four degrees of freedom model of a system.

Figure [3.5] shows the response in the X and Y directions. It shows that the maximum response in the X and Y directions occurs at different frequencies because the stiffnesses in the two directions are different from one another.
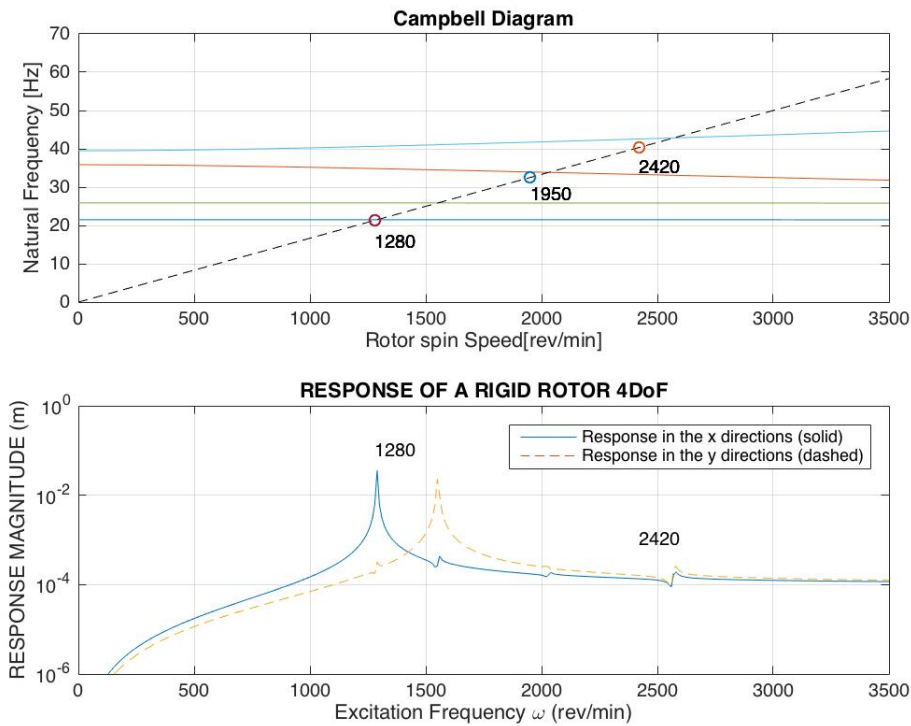

Figure 3.5: Response of a Rigid Rotor for Anisotropic case

Chapter 4

Inerter

4.1 Introduce to Inerter

In 2008, two articles in Autosport revealed details of a new mechanical suspension component with the name J-Damper which had entered Formula One racing and which was delivering significant performance gains in handling and grip. The Autosport articles revealed that the J-Damper was in fact an inerter and that its origin lay in academic work on mechanical and eletrical circuits at Cambridge University. An inerter is a two-terminal mechanical device which applies force between its terminals proportional to the relative acceleration between them [1], similar to a spring and damper which apply forces proportional to the relative displacement for the spring and velocity for the damper between their terminals. Inerter was first introduced by Malcom C. Smith in his paper [1] and patened [2]. The idea originated from the extension of force-current analogy[2] for mechanical and elettrical circuits where an inductor is analogous to a spring, a resistor is to a damper and capacitor is to inertia as shown in Figure (4.1) and Figure (4.2). It is known that the correspondence is perfect in the case of the spring and damper. A fact which is also known, but frequently glossed over, is that there is a restriction in the case of the mass. All the above elements except the mass have two terminal (for a mechanical element the terminals are the attachment points which should be freely and independently movable in space). In contrast, the mass element has only one such terminal-the center of mass. This implies that a mass is equivalent to a grounded capacitor, but there is no mechanical analogue for a general capacitor whose one terminal

is not necessarily grounded. This poses a restriction if it is needed to derive an equivalent mechanical circuit from given elettrical one. To bypass this restriction a new mechanical modelling element was proposed by Smith[1]. The elements has two terminals, and has the proprety that the applied force at the terminals is proprotional to the relative acceleration between them. A new word inerter was coined to describe such device. The constant of proportional is called the inertance and has the units of kilograms (i.e, dimensions of mass)

4.2 Background on the Inerter

The are two well-known analogies between mechanical and eletrical system, namley the Force-Voltage Analogy and Force-Current Analogy. In the force-current analogy, the spring, damper and mass of mechanical systems are analogues of the inductor, resistor and capacitor of eletrical systems, as shown in Figure (4.1). Furthermore, the mass is one terminal element for which the displacement, velocity and the acceleration are measured relative to the ground. Therefore, eletrical systems with ungrounded capacitors do not have a direct analogy to mechanical systems composed of springs, dampers and masses. As a result, the achievable performance of a passive mechanical system is restricted.

To remedy the situation a network called the inerter was proposed as an ideal mechinacal two terminal element with following dynamic equation:

The ideal inerter is a two-terminal mechanical device with the proprety that the equal and apposite force F applied at the terminals is proportional to the relative acceleration between the nodes:

$$F = b\left(\dot{v}_2 - \dot{v}_1\right) = b\left(\ddot{x}_2 - \ddot{x}_1\right) \tag{4.1}$$

where F rappresents the applied force between two mechanical terminals and b is the constant of proportianality called *inertance* which ha units of kilograms, while v_1 and v_2 are the velocity of two terminals. The storeg energy in the inerter is equal to $\frac{1}{2}b\left(v_2 - v_1\right)^2$. With the invention of the inerters, the new force-current analogy can be shown as Figure (4.2), such that all passive network impedances can be mechanically realized by inerter, dampers and springs.

The first inerter device was a rack and pinion inerter [9], in which the mechanical power was transferred by gears. Next, ball-screw inerters were

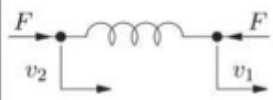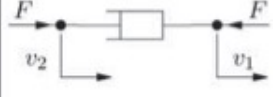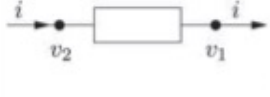Figure 4.1: Force-Current Analogy
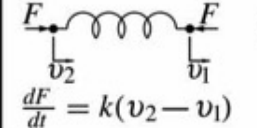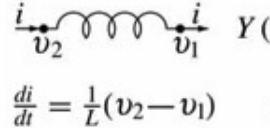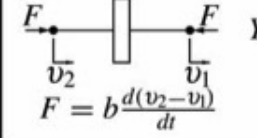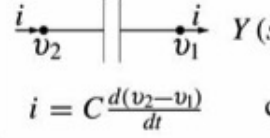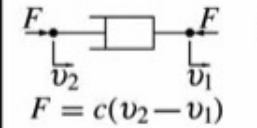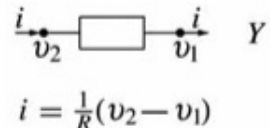
Figure 4.2: Passive network impedences

proposed in refernces[1] to [20] that had slightly different working principles. To demostrate their perfomance benefits for mechanical systems inerters have been applied to car suspensions[2], motorcycle steering [3], train suspensions [4] and building vibration control system [5]. The performance of these systems has been shown to be significantly improved by inerters.
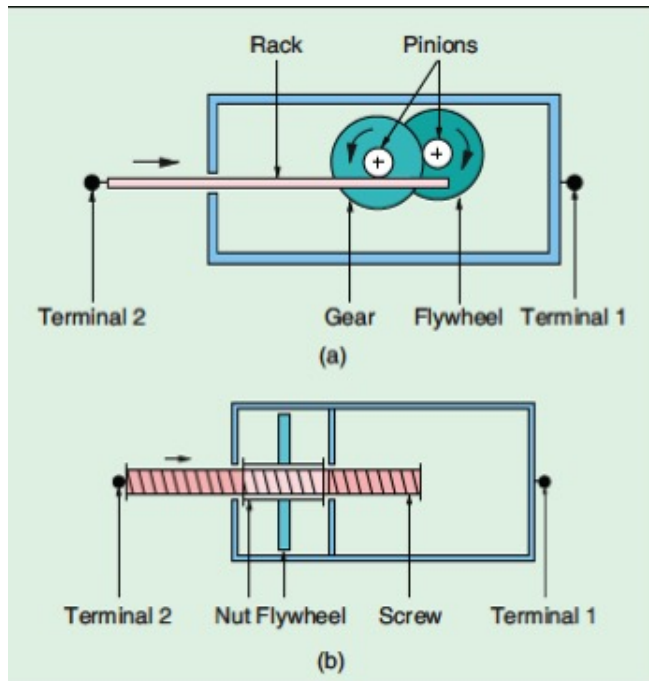
Figure 4.3: Rack and Pinions Inerter

4.3   Inertance of Inerter

Any device wich satisfies this mathematical property of Equation [4.2] can be termed as an *inerter* where with b is indicated the costant of proportionality called "inertance".Inertance ha units of kilograms (i.e dimensions of mass) and is obtained for three different Inerter.

$$F = b\left(\dot{v}_2 - \dot{v}_1\right) = b\left(\ddot{x}_2 - \ddot{x}_1\right) \tag{4.2}$$
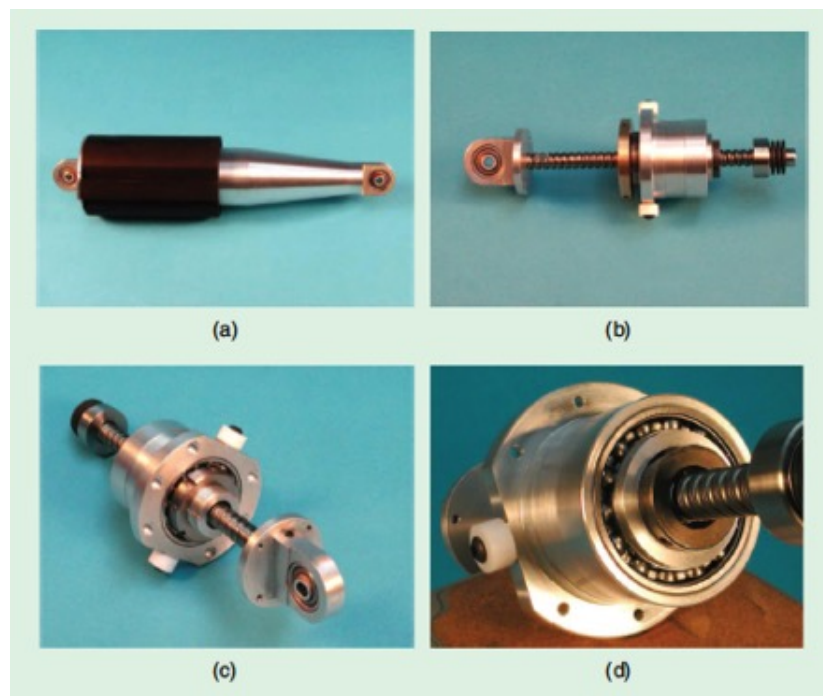
Figure 4.4: Ballscrew inerter made at Cambridge University

4.3.1   Inertance of Passive Mechanical Inerter

The inerter is the device that satisfies the Equation [4.2], but to used in suspension system, should have small mass, finite linear travel no attachament with the phisical ground and should be compact. One simple method to achieve that as in [] is to convert the relative linear motion between the two terminals into the rotary motion of flywheel by using rack and pinion or a ball screw.
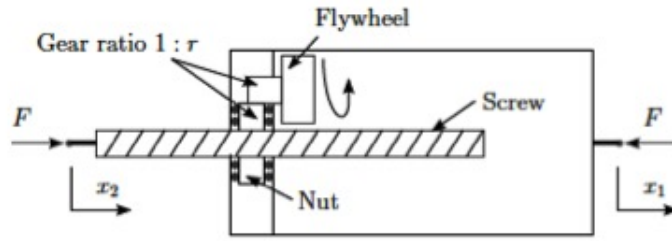
Figure 4.5: Passive Mechanical Inerter

The mechanism is considered that has a flywheel with rotational inertia J (in the unit of $kg \cdot m^2$), a ball srew with lead $l[m/rev]$, a gear ratio of 1 r between the nut (or pinion) and the flywheel. Assuming tha the rotational inertia of the screw and other gears is negligible compared to that of the flywheel, angular acceleration and angular velocity of the flywheel is given by:

$$\alpha = \frac{2\pi}{l} \cdot r \cdot (\ddot{x}_2 - \ddot{x}_1) \tag{4.3}$$

$$\omega = \frac{2\pi}{l} \cdot r \cdot (\dot{x}_2 - \dot{x}_1) \tag{4.4}$$

By conservation of energy, the power input through linear motion should be equal to the power output through rotational motion, therefore:

$$F(\dot{x}_2 - \dot{x}_1) = T\omega \tag{4.5}$$

$$F(\dot{x}_2 - \dot{x}_1) = J\frac{2\pi}{l} \cdot r \cdot (\ddot{x}_2 - \ddot{x}_1) \cdot \frac{2\pi}{l} \cdot r \cdot (\dot{x}_2 - \dot{x}_1) \tag{4.6}$$

$$F = \left(\frac{2\pi}{l}r\right)^2 \cdot J \cdot (\ddot{x}_2 - \ddot{x}_1) \tag{4.7}$$

and comparing the Equation [4.7] with the Equation [4.2] we can calculated the inertance from this type of inerter:

$$F = \left(\frac{2\pi}{l}r\right)^2 \cdot J \cdot (\ddot{x}_2 - \ddot{x}_1) = b\,(\ddot{x}_2 - \ddot{x}_1) \tag{4.8}$$

$$b = \left(\frac{2\pi}{l}r\right)^2 J \tag{4.9}$$

thus, the constant b is the inertance measured in $[kg]$.

4.3.2 Inertance of Hydraulic Inerter

The proposed hydraulic inerter is a closed hydraulic system that consists of a hydraulic motor, a hydraulic cylinder and a connection pipe, as shown in Figure (4.6).
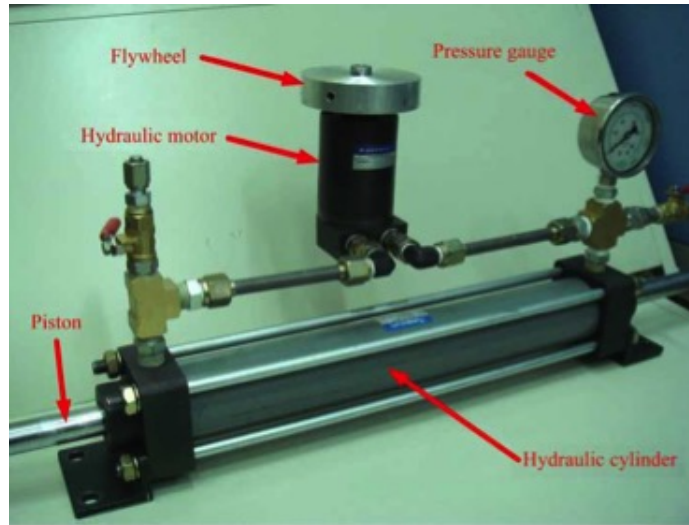
Figure 4.6: Hydraulic Inerter

The working principle of the hydraulic inerter is similar to a hydropower generator, as shown in figure (4.7). Two terminals of the hydraulic inerter

are the hydraulic cylinder (terminal 1) and the piston (terminal 2). F is the
applied force, and x is the relative displacement of the two terminals. When
F is positive, the piston moves rightwards relative to the cylinder and the
pressure P2 (P3) is higher than the pressure P1 (P4). The hydraulic motor
is operated by the pressure difference between P3 and P4, and the fluid flows
through the pipes. Similarly, when the apllied force F is negative, the piston
and the hydraulic motor move in the reverse direction.
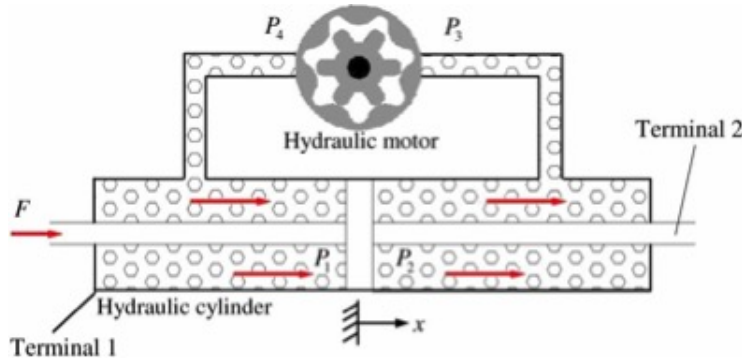
Figure 4.7: Dynamics of Cylinder - Hydraulic Cylinder
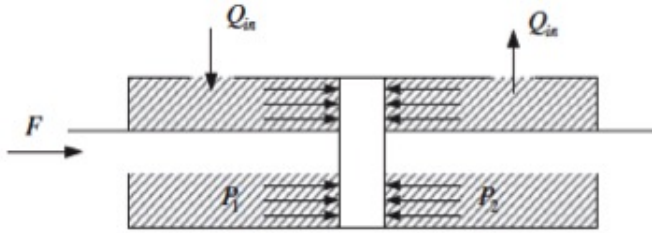
Figure 4.8: Dynamics of Cylinder - Hydraulic Cylinder

To construct the hydraulic inerter, a double-rod cylinder is used, such
that the volume of the cylinder remains costant. As illustrated in Figure
(4.8), the dynamics of the cylinder is as follows:

$$(F - f) = A\,(P_2 - P_1) + m\ddot{x} \qquad (4.10)$$

where f is the friction force, A the area of the piston, m the mass of
the piston and rod and $\ddot{x}$ the acceleration of the piston. For the inerter
applications, the mass of the componenet is normally much less than the

inertance and can be neglected. Suppose the friction is small, the Equation [4.10] can be semplified as:

$$F = A(P_2 - P_1) \tag{4.11}$$

The input flowrate Q_{in} of the hydraulic cylinder is defined as:

$$Q_{in} = Au_2 = A\dot{x} \tag{4.12}$$

where $\dot{x}$ is the velocity of the piston. On the other hand, the input flow drives the motor, and the amount is proprotional to the angular velocity of the motor, as in the following:

$$Q_{in} = D\dot{\theta} \tag{4.13}$$

where D is the units of m^3 and $\dot{\theta}$ is the angular velocity of the motor. Combining Equations [4.12] and [4.13] gives:

$$A\dot{x} = D\dot{\theta} \tag{4.14}$$

Taking the derivate of the Equation [4.14] results in:

$$\ddot{\theta} = \frac{A}{D}\ddot{x} \tag{4.15}$$

In the ideal case, there is no energy loss in the power trasmission, i.e. the input power is equal to the output power of the mechanism, as in the following:

$$F\dot{x} = T\dot{\theta} \tag{4.16}$$

where $T = I\ddot{\theta}$ is the output torque of the motor, in which I is the moment of inertia of the motor and the flywheel. Thefore, substituting Equation [4.14] and [4.15] into Equation [4.16] gives:

$$F = T\frac{\theta}{x} = I\ddot{\theta}\frac{\theta}{x} = I\left(\frac{A}{D}\right)^2\ddot{x} = b\ddot{x} \tag{4.17}$$

i.e the ideal system inertance of the hydraulic device is:

$$b = I\left(\frac{A}{D}\right)^2 \tag{4.18}$$

which can be modified by tuning the flywheel I, the hydraulic cylinder A and the hydraulic motor D.

4.3.3   Inertance of Fluid Inerter

A Schematic diagram of the new implementation is shown in Figure (4.9) and (4.10). The cylinder body and the piston rod are the two device terminals, their relative motion driving fluid through the helical channel.
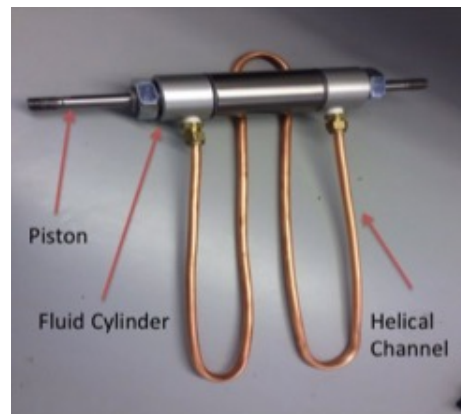
Figure 4.9: Fluid Inerter

The channel fluid velocity is scaled up from the piston velocity by the ratio of the areas of the channel and the piston. Thus, the device inertance can be increasing by reducing the area of the channel or increasing the area of the piston, both of which increase the fluid velocity for given rate of strut movement.

Consider a Piston and cylinder driving fluid through a helical tube surroinding the cylinder, as shown in Figure (4.10).

Let:

$A1=$ annular area of the main cylinder

$A2=$ channel cross sectional area

$l =$ channel length

$\rho =$ fluid density

Let F be the equal and opposite force applied to the terminals and x be the relative displacement between them. An ideal inerter is described by the following equation:
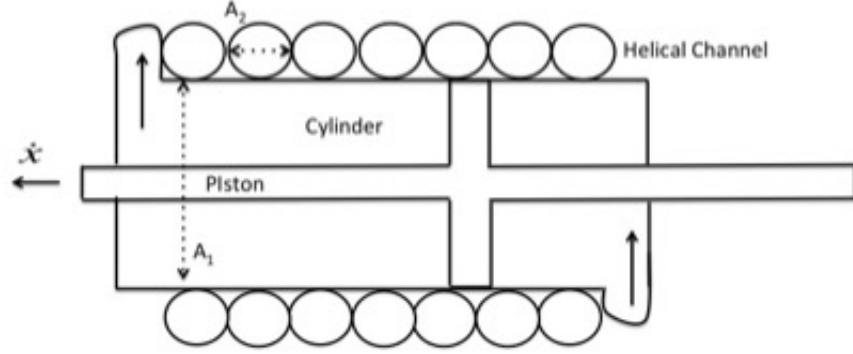
Figure 4.10: Schematic of external-helix fluid inerter

$$F = b\ddot{x} \tag{4.19}$$

where b is the *inertance* (costant of proportionality) in the unit of kg. We first neglect any dissipative effect due to fluid viscosity and density and consider the fluid as incompressible. If u is the mean velocity of the fluid in the helical path, we have:

$$\dot{x}A_1 = uA_2 \tag{4.20}$$

by conservation of volume. The stored energy of the fluid in the helical path given by:

$$stored\,energy = \frac{1}{2}\rho A_2 l u^2 \tag{4.21}$$

and the stored energy in an ideal inerter is:

$$stored\,energy\,(ideal\,inerter) = \frac{1}{2}b\dot{x}^2 \tag{4.22}$$

which suggests the following approximate value for the device inertance:

$$\frac{1}{2}\rho A_2 l u^2 = \frac{1}{2}b\dot{x}^2 \tag{4.23}$$

$$b = \rho A_2 l \frac{u^2}{\dot{x}^2} \tag{4.24}$$

From Equation [4.20] we have:

$$\dot{x} = u\frac{A_2}{A_1} \tag{4.25}$$

substituiting the value of $\dot{x}$ in the Equation [4.24] we have:

$$b = \rho A_2 l\frac{u^2}{\left(u\frac{A_2}{A_1}\right)^2} = \rho l\frac{A_1^2}{A_2} \tag{4.26}$$

Thus, the *inertance* of ideal inerter for a fluid inerter device is:

$$b = \rho l\frac{A_1^2}{A_2} \tag{4.27}$$

This calculation only considers the inertia of the fluid flowing in the channel and neglects the inertia of the fluid in the piston chamber and the inertia of the piston itself. Large inertance values are possible increasing the length of helix-channel or using fluid with high density. This prototypes of Inerter have been constructed for this thesis in Dynamics Laboratory at University of Southampton and It will be described in Chapter 7.
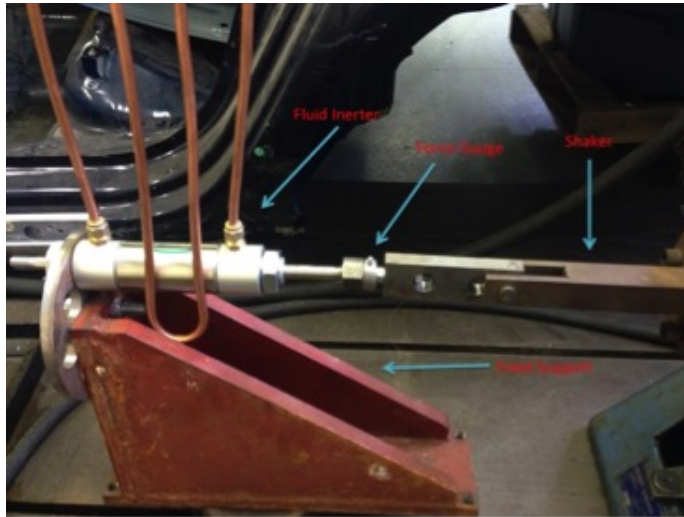
Figure 4.11: Prototype of fluid inerter

Chapter 5

Performance Benefits Employing Inerters

What we know of the inerter

Inerters have become a hot topic in recent years especially in vehicle, train, building suspesion system, etc. The first use of inerter is reported in [1]. This Chapter reported results of different suspension designs with different configuration of the element like *spring*, *damper* and *inerter* for simple passive mechanical struts. Automotive suspensions are design to provide many functions such a vibration isolation of the passenger compartment from road inputs and control vertical tire loads to optimize braking, acceleration and handling. This interest in improved and optimized suspension has become great interest in the academic community and auto manufactures.

5.1 Suspension Struts

In this chapter it is introduced a few simple networks as candidates for a suspension strut each of which contains at most one damper and one inerter.Figure (5.1a) shows the conventional parallel spring-damper arragement. In figure (5.1b) there is the relaxation spring k_b in series with damper. Figures (5.1c), (5.1d) shown a parallel spring-damper augmented by an inerter in parallel or in series with the damper. In figure (5.1e) is proposed with a pair of springs of stiffness k_1, which we call centring springs. Figure(5.1f) is similar but allows for unequal springs k_1 and k_2. Figure (5.1g), (5.1h) differ

from (5.1e), (5.1f) by having an additional relaxation spring k_b.

(a) layout S1   (b) layout S2   (c) layout S3   (d) layout S4

(e) layout S5   (f) layout S6   (g) layout S7   (h) layout S8

Figure 5.1: The eight suspension layout

The mechanical admittance $Y(s)$ for two of these layouts (layout S3 and S7) is now given for illustration:

$$Y_3(s) = \frac{k}{s} + c + bs \tag{5.1}$$

and

$$Y_7(s) = \frac{k}{s} + \frac{1}{\frac{s}{k_b} + \frac{s}{cs+k_1} + \frac{s}{bs^2+k1}} \tag{5.2}$$

where b is the value of *inertance*.

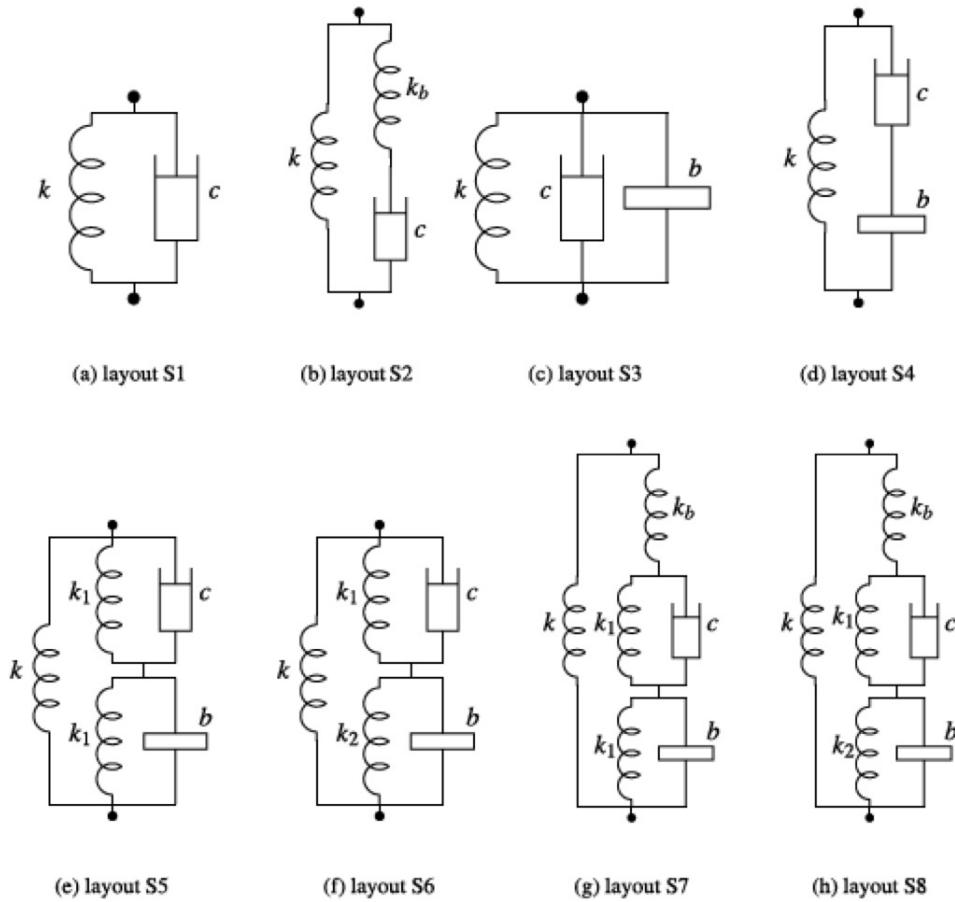## 5.2 Vehicle Suspension-The quarter-car model

In general, a good suspension should provide a comfortable ride and good handling for a reasonable range of suspension deflections.The specific criteria used depend on the purpose of the vehicle. In the [12] to evaluate ride comfort and handling have used the frequency response function H_{sprung} and H_{tire} for a Quarter-car model. Quarter-car is a simplified model focusing on one wheel and one equivalent sprung mass to study only the vertical dynamics of a vehicle assuming that all the four wheels are decoupled as Figure (5.2).

The component of the quarter-car are:

- sprung mass m_s is usually one-fourth of the vehicle's chassis mass.

- m_{us} is unsprung mass, includes the mass of the wheel and parts of suspensions not resting on the spring.

- k_s is the passive stiffness in the suspension.

- c_s is the passive damping in the suspension.

- z_s and z_{us} are the vertical displacement of the sprung mass and un-sprung mass respectively from the equilibrum position.

- z_r rappresents the displacement due to road surface irregularities.

In order to analyze such systema and obtain their frequency response functions, it would be easier to consider a quarter car model with a general admittance $Y(s)$ as shown in Figure (5.3).

The admittance of common components is given in Table.

	Component	Admittance Y(s)
Spring	k_p	$\frac{k_p}{s}$
Damper	d_p	d_p
Inerter	b	bs

The equation of the motion in the Laplace transformed domain are:

$$m_s s^2 \hat{z}_s = \hat{F}_s - sY(s)(\hat{z}_s - \hat{z}_u) \tag{5.3}$$
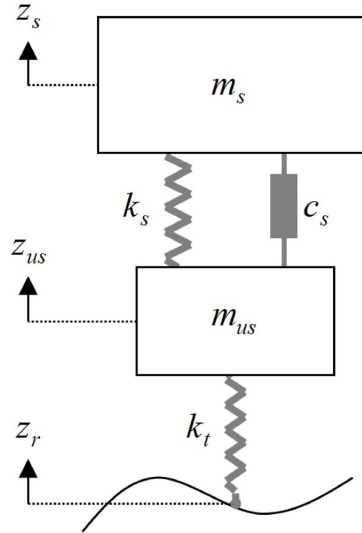
Figure 5.2: Quarter-car model for behicle suspension

and

$$m_u s^2 \hat{z}_u = sY(s)(\hat{z}_s - \hat{z}_u) + k_t(\hat{z}_r - \hat{z}_u) \tag{5.4}$$

In the [15] will fix the parameters of the quarter-car model as follow: $m_s = 250\,kg$, $m_u = 35\,kg$, $k_t = 150\,kN/m$. In the following section we report the perfomance measures the reported in [].

5.3 Perfomance measures

There are a number of pratical design requirements for a suspension system such as passenger comfort, handling, tyre normal loads, limits on suspension travel etc. which require careful optimisation. In the simplified quarter-car model these can be translated approximately into the specifications on the disturbance response from F_s and z_r to z_s and z_u.

We now consider in according with [] this several basic measures:

- parameter J_1 is the body vertical acceleration (RIDE COMFORT).
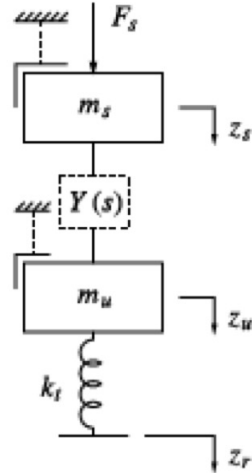
Figure 5.3: Quarter-car model with a general admittance

- parameter J_3 is the dynamic tyre road.

Optimisation of J_1

The results of optimation are shown in figure (5.4). It was found the the relaxation spring k_b did not improve helpful to reduce J_1. This left five of the eight struts in Figure (5.1) to be considered. Optimisation for layouts $S1$, $S3$, and $S4$ appears to be convex in the free parameters. Both the parallel ($S3$) and series ($S4$) arrangements gave improvements over the conventional strut ($S1$) for the full range of static stiffness with $S4$ giving the biggest improvement for stiff suspensions. It should be noted that the parallel arrangement gives lower values of inertance than the series arrangement. For example, at the midrange value of $k = 60 \, kN/m$ we have $b = 31.27 \, kg$ and $b = 333.3 \, kg$, respectively.

For layouts $S5$ and $S6$, the optimisation problem appears no longer to be convex in the parameters. The NelderMead simplex method was used for various starting points. Solutions were found which gave a clear improvement on the series arrangement $S4$ particularly for softer suspensions. For the arrangement $S6$ the improvement was at least 10% across the whole stiffness range. For much of the range, k_1 and k_2 were about $\frac{1}{3}$ and $\frac{1}{12}$ of the static

stiffness, respectively.

(a) optimal J_1

(b) Percentage improvement in J_1

(c) optimal damper setting

(d) optimal inerter setting

Figure 5.4: The optimisation of J_1 on: layout $S1$ (bold), layout $S3$ (dashed), layout $S4$ (dot-dashet), layout $S5$ (dotted) and layout $S6$ (solid)

Optimisation of J_3

The results of optimisation are shown in Figure (5.6). Here it was found that the relaxation spring k_b helped to reduce J_3 for lower values of static stiffness. Indeed, the conventional strut $S2$ is a noticeable improvement on $S1$ for softer suspensions. Again optimisation for layouts $S1$, $S2$, $S3$, and $S4$ appears to be convex in the free parameters. The results show an improvement in J_3 with parallel ($S3$) and series ($S4$) arrangements if the static stiffness is large enough, with the series arrangement again giving the biggest improvement.

For layouts $S5$ and $S6$, the optimisation problem appears no longer to be convex in the parameters. The NelderMead simplex method was again used for various starting points. As before, the use of centring springs in layouts
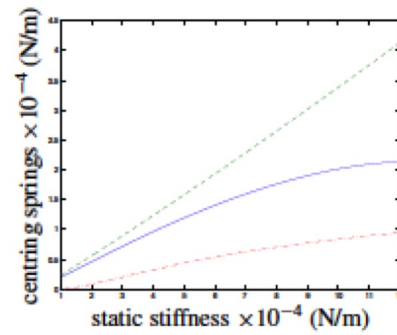
Figure 5.5: The optimisation of J_1 on: k_1 in layout $S5$ (solid), k_1 in layout $S6$ (dashed), k_2 in layout $S6$ (dot-dashed),

$S5$ and $S6$ gave further improvements over the ordinary series arrangements $S4$. The use of a relaxation spring k_b in $S7$ was needed to extend the benefits to softer suspensions.

(a) optimal J_3

(b) Percentage improvement in J_3

(c) optimal damper setting

(d) optimal inerter setting
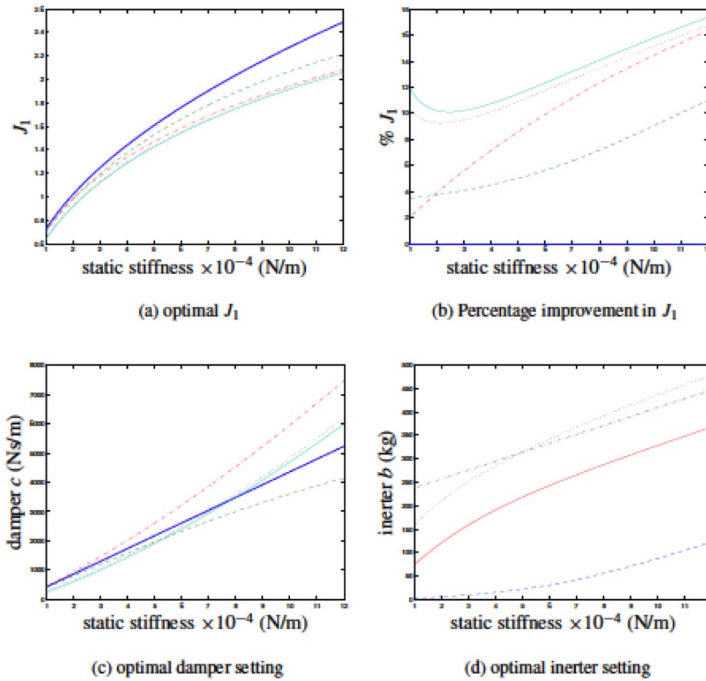
(e) centring spring

(f) spring buffer
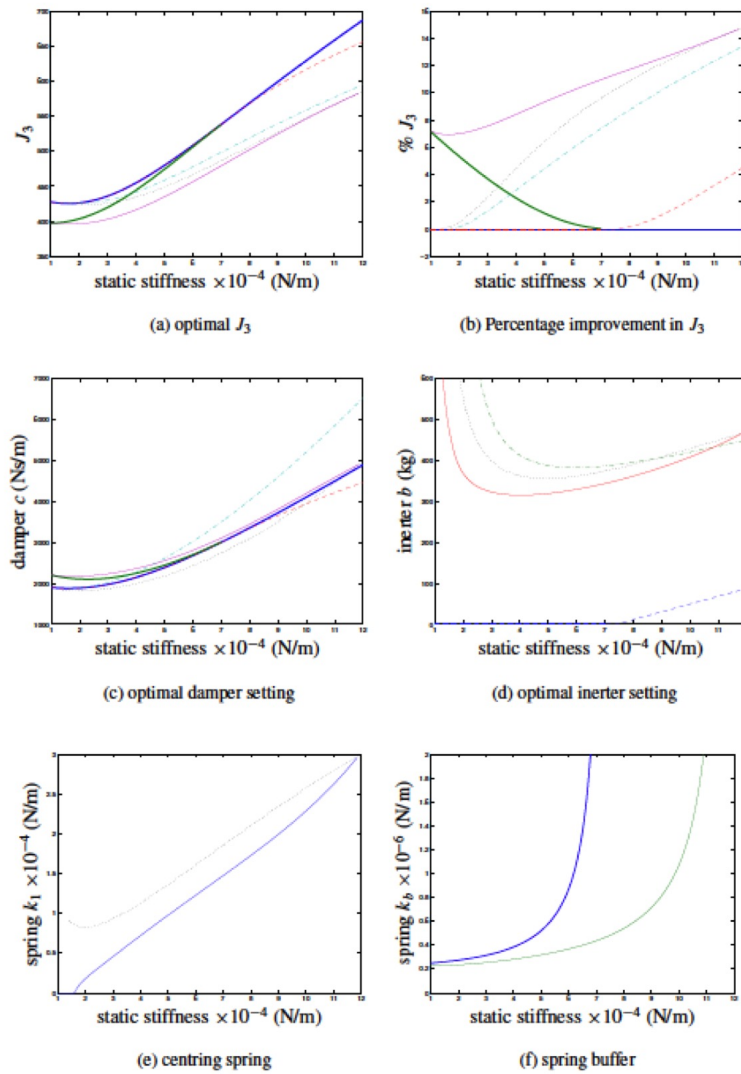
Figure 5.6: The optimisation of J_3 on: layout $S1$ and $S2$ (bold), layout $S3$ (dashed), layout $S4$ (dot-dashet), layout $S5$ (dotted) and layout $S7$ (solid)

Chapter 6

Dynamics of Rotating Machines with Inerter

6.1 Introduction

In the previous chapter the dynamics of a rigid rotor rotating with four degree of freedom was introduced and the use of the new application called Inerter was described. The objective of this chapter is to study the fundamental influence of the inerter on the natural frequencies of vibrations system. The fact that inerter can reduce the natural frequencies of vibration system is theoretically demostrated in this chapter and the question of how to efficiently use inerter to reduce the natural frequencies is also adressed. The traditional methods to reduce the natural frequencies of an elastic system are either deacreasing the elastic stiffness or increasing the mass of vibration of the system. It will be shown below that a parallel-connected inerter can also effectively reduce the natural frequencies.

6.2 SDoF Rotor System with Inerter

A SDoF Rotor System with inerter is shown in Figure (6.1). The equation of motion of free vibration system of this system is:

$$(m + v_{x1} + v_{x2})\ddot{x} + kx = 0 \tag{6.1}$$

or
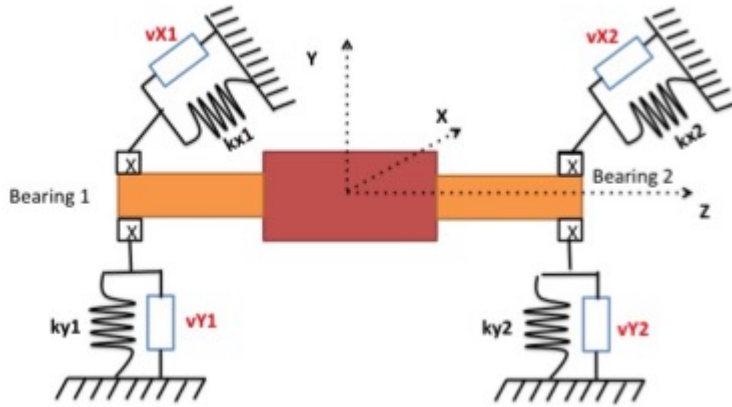
Figure 6.1: Single dregree of freedom

$$(m + v_{y1} + v_{y2})\ddot{x} + ky = 0 \tag{6.2}$$

Transformation of the above equation into the standard form for vibration analysis yields to:

$$\ddot{x} + \omega_n^2 x = 0 \tag{6.3}$$

or

$$\ddot{y} + \omega_n^2 y = 0 \tag{6.4}$$

where:

$$\omega_n = \sqrt{\frac{k}{m + v_{x1} + v_{x2}}} \tag{6.5}$$

or

$$\omega_n = \sqrt{\frac{k}{m + v_{y1} + v_{y2}}} \tag{6.6}$$

is called the natural frequency of the undamped system.

Preposition 1:
The natural frequency ω_n of an SDoF Rotor System is deacreasing function of the inertance v. Thus, inerter can reduce the natural frequency of an SDoF Rotor System.

6.3 TDoF Rotor System with Inerter
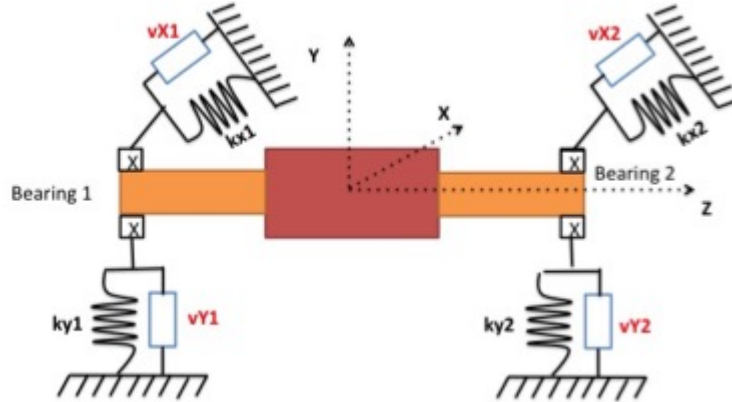
Figure 6.2: Single dregree of freedom

In this section is considered the rotor system shown in Figure (6.2) and it is investigated the general influence of the inerter on the natural frequencies of a vibration system.

The equation of motion for free vibration of this system are:

$$\begin{cases} (m + v_{x1} + v_{x2})\,\ddot{x} + (k_{x1} + k_{x2})\,x = 0 \\ (m + v_{y1} + v_{y2})\,\ddot{y} + (k_{y1} + k_{y2})\,y = 0 \end{cases} \tag{6.7}$$

or in a compact form:

$$M\ddot{x} + Kx = 0 \tag{6.8}$$

where M is called the inertia Matrix and K the stiffness matrix:

$$M = \begin{bmatrix} m + v_{x1} + v_{x2} & 0 \\ 0 & m + v_{y1} + v_{y2} \end{bmatrix} \tag{6.9}$$

$$K = \begin{bmatrix} k_{x1} + k_{x2} & 0 \\ 0 & k_{y1} + k_{y2} \end{bmatrix} \tag{6.10}$$

The two natural frequencies can be obtained by solving the characteristic equation:

$$\Delta(\omega) = \left| K - M\omega^2 \right| \tag{6.11}$$

$$\Delta(\omega) = (m + v_{x1} + v_{x2})(m + v_{x1} + v_{x2})\omega^4 - (k_{y1} + k_{y2})(m + v_{x1} + v_{x2})\omega^2 +$$
$$+ (k_{y1} + k_{y2})(m + v_{x1} + v_{x2})\omega^2 + (k_{x1} + k_{x2})(k_{y1} + k_{y2}) = 0$$

in compact form:

$$\alpha\omega^4 + \beta\omega^2 + \gamma = 0 \tag{6.12}$$

where:

$$\alpha = (m + v_{x1} + v_{x2})(m + v_{x1} + v_{x2}) \tag{6.13}$$

$$\beta = (k_{x1} + k_{x2})(m + v_{y1} + v_{y2}) + (k_{y1} + k_{y2})(m + v_{x1} + v_{x2}) \tag{6.14}$$

$$\gamma = (k_{x1} + k_{x2})(k_{y1} + k_{y2}) \tag{6.15}$$

Thus, the two natural frequencies are:

$$\begin{cases} \omega_{n1} = \sqrt{\frac{-\beta + \sqrt{\beta^2 - 4\alpha\gamma}}{2\alpha}} \\ \omega_{n1} = \sqrt{\frac{-\beta - \sqrt{\beta^2 - 4\alpha\gamma}}{2\alpha}} \end{cases} \tag{6.16}$$

For rigid rotor descripted in Section [2.1] and for the following value of stiffness we have the inertance diagram for 2DoF Rotor System reported in Figure (6.3):

$$\begin{cases} k_{x1} = 1 \cdot 10^6 \ N/m \\ k_{y1} = 1 \cdot 10^6 \ N/m \\ k_{x2} = 1.3 \cdot 10^6 \ N/m \\ k_{y2} = 1.3 \cdot 10^6 \ N/m \end{cases}$$

Using the following partial Matlab Code:

```matlab
1  %Characteristics of the rotor
2  L = 0.5; a = L/2;   b = L/2;
3  D=0.2;
4  rho=7810;
5  m = rho*pi*D^2*(L/4);
6  Ip = (m*D^2)/8;
7  Id = Ip/2 + (m*L^2)/12;
8
9  %Stiffness
10 kX1=1.0*10^6;
11 kY1=1.0*10^6;
12 kY11=1.0*10^6;
13 kX2=1.3*10^6;
14 kY2=1.3*10^6;
15
16 kxT=kX1+kX2;
17 kxC=-a*kX1+b*kX2;
18 kxR=a^2*kX1+b^2*kX2;
19 kyT=kY1+kY2;
20 kyC=-a*kY1+b*kY2;
21 kyR=a^2*kY1+b^2*kX2;
22
23 %inertance%
24 v=0:10:500;
25
26 alpha=(m+2*v(j))*(m+2*v(j));
27 beta=-(kX1+kX2)*(m+2*v(j))-(kY1+kY2)*(m+2*v(j));
28 gamma=(kX1+kX2)*(kY1+kY2);
29
30 omeg_1=s...........................;
31 omega_n=...........................;
32 freq_1(j)=real(omega_n/(2*pi));
33 omeg_2=...........................;
34 omega_n=s...........................;
35 freq_2(j)=real(omega_n/(2*pi));
36
37 disp(['Natural Freq 1= ' num2str(freq_1(j)) ' Hz '])
38 disp(['Natural Freq 2= ' num2str(freq_2(j)) ' Hz '])
39 end
40
41 % Inertance diagram %
42 figure(1);
43 plot(v,freq_1(:));
44 hold on
45 plot(v,freq_2(:),'--');
```

```
46  hold on
47
48  legend('Mode 1','Mode 2');
49  title('Inertance Diagram at 4000 rpm - 2DoF')
50  xlabel ('v=inertance [kg]')
51  ylabel ('Natural Frequency [Hz]')
52  grid on
53  %end
```

The inertance diagram of an TDoF Rotor System is reported in the following Figure.
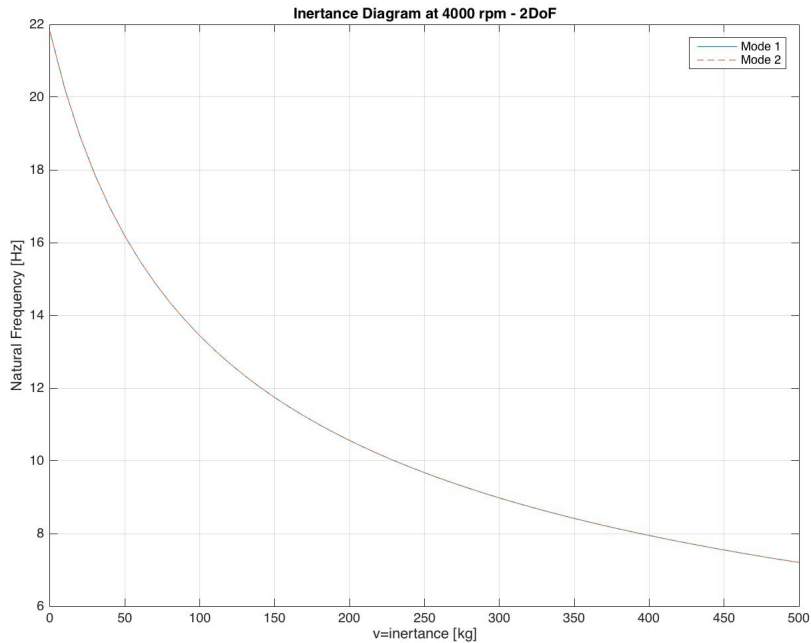

Figure 6.3: Inertance Diagram - 2DoF

Preposition 2:

The natural frequency ω_n of an TDoF Rotor System with two inerter are deacreasing function of the inertance v_{x1} and v_{x2}. Thus, inerter can reduce the natural frequency of an TDoF Rotor System like dimostred in the Figure (6.3).

6.4   System of 4DoF with Inerter

This Rotor has four degrees of freedom as it can translate in the directions O_x and O_y and it also can rotate about these axes. Practitioners often term the translation respectively and rotation as bounce and tilt motion. It is chosen to describe the movement of the rotor in terms of the displacements of its center of mass in the directions O_x and O_y, x and y, respectively, and the clockwise rotations about Ox and Oy, β and α, respectively.
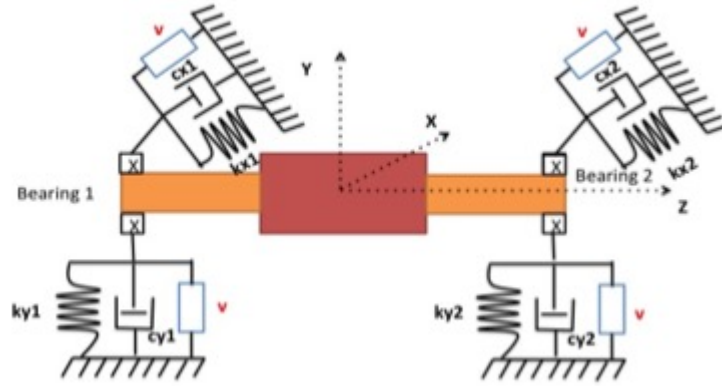

Figure 6.4: Rotor System with Inerter - 4DoF

The equation of motion are:

$$
\begin{cases}
(m + 2v)\ddot{x} + (c_{x1} + c_{x2})\dot{x} + (k_{x1} + k_{x2})x + (ac_{x1} - bc_{x2})\dot{\beta} + (ak_{x1} - bk_{x2})\beta = 0 \\
(m + 2v)\ddot{y} + (c_{y1} + c_{y2})\dot{y} + (k_{y1} + k_{y2})y + (-ac_{y2} + bc_{y1})\dot{\alpha} + (-ak_{y2} + bk_{y1})\alpha = 0 \\
(a^2 v_{y2} + b^2 v_{y1} + I_d)\ddot{\alpha} + (a^2 c_{y2} + b^2 c_{y1})\dot{\alpha} + I_p \Omega \dot{\beta} + (-ac_{y2} + bc_{y1})\dot{y} + \\
\quad + (a^2 k_{y2} + b^2 k_{y1})\alpha + (-ak_{y2} + bk_{y1})y = 0 \\
(a^2 v_{x2} + b^2 v_{x1} + I_d)\ddot{\beta} + (a^2 c_{x2} + b^2 c_{x1})\dot{\beta} - I_p \Omega \dot{\beta} + (ac_{x2} - bc_{x1})\dot{x} + \\
\quad + (a^2 k_{x2} + b^2 k_{x1})\beta + (ak_{x2} - bk_{x1})x = 0
\end{cases}
$$

$$(6.17)$$

in this case it has simmetric rotor and the bearing supports are isotropic; the inertance (constant of proportianality) is equal in vertical and horizontal directions; the equation of motion becomes:

$$\begin{cases} (m + 2v)\ddot{x} + c_{xT}\dot{x} + k_{xT}x = 0 \\ (m + 2v)\ddot{y} + c_{yT}\dot{y} + k_{yT}y = 0 \\ (a^2v_{y2} + b^2v_{y1} + I_d)\ddot{\alpha} + c_R\dot{\alpha} + I_p\Omega\dot{\beta} + k_R\alpha = 0 \\ (a^2v_{x2} + b^2v_{x1} + I_d)\ddot{\beta} + c_R\dot{\beta} - I_p\Omega\dot{\alpha} + k_R\beta = 0 \end{cases} \tag{6.18}$$

Letting:

$$\begin{cases} k_{xT} = k_{x1} + k_{x2} \\ k_{yT} = k_{y1} + k_{y2} \\ k_{xC} = -ak_{x1} + bk_{x2} \\ k_{yC} = -ak_{y1} + bk_{y2} \\ k_{xR} = a^2k_{x1} + b^2k_{x2} \\ k_{yR} = a^2k_{y1} + b^2k_{y2} \end{cases} \tag{6.19}$$

and

$$\begin{cases} c_{xT} = c_{x1} + c_{x2} \\ c_{yT} = c_{y1} + c_{y2} \\ c_{xC} = -ac_{x1} + bc_{x2} \\ c_{yC} = -ac_{y1} + bc_{y2} \\ c_{xR} = a^2c_{x1} + b^2c_{x2} \\ c_{yR} = a^2c_{y1} + b^2c_{y2} \end{cases} \tag{6.20}$$

Consider of a rigid rotor on isotropic supports, the support stiffness and damping are the same in the both x and y directions. Thus:

$$\begin{cases} k_{xT} = k_{yT} = k_T \\ c_{xT} = c_{yT} = c_T \end{cases} \tag{6.21}$$

Then the equation of motion can be written more concisely as:

$$\begin{cases} (m + 2v)\ddot{x} + c_T\dot{x} + k_Tx = 0 \\ (m + 2v)\ddot{y} + c_T\dot{y} + k_Ty = 0 \\ (a^2v_{y2} + b^2v_{y1} + I_d)\ddot{\alpha} + c_R\dot{\alpha} + I_p\Omega\dot{\beta} + k_R\alpha = 0 \\ (a^2v_{x2} + b^2v_{x1} + I_d)\ddot{\beta} + c_R\dot{\beta} - I_p\Omega\dot{\alpha} + k_R\beta = 0 \end{cases} \tag{6.22}$$

It is helpful to express these equations in matrix form as:

$$M\ddot{q} + (C + \Omega G)\,\dot{q} + Kq = 0 \tag{6.23}$$

where:

$$M = \begin{bmatrix} m + v_{x1} + v_{x2} & 0 & 0 & av_{x2} - bv_{x1} \\ 0 & m + v_{y1} + v_{y2} & -av_{y2} + bv_{y1} & 0 \\ 0 & -av_{y2} + bv_{y1} & a^2 v_{y2} + b^2 v_{y1} + I_d & 0 \\ av_{x2} - bv_{x1} & 0 & 0 & a^2 v_{x2} + b^2 v_{x1} + I_d \end{bmatrix} \tag{6.24}$$

$$K = \begin{bmatrix} k_{x1} + k_{x2} & 0 & 0 & ak_{x2} - bk_{x1} \\ 0 & k_{y1} + k_{y2} & -ak_{y2} + bk_{y1} & 0 \\ 0 & -ak_{y2} + bk_{y1} & a^2 k_{y2} + b^2 k_{y1} & 0 \\ ak_{x2} - bk_{x1} & 0 & 0 & a^2 k_{x2} + b^2 k_{x1} \end{bmatrix} \tag{6.25}$$

$$C = \begin{bmatrix} 2c_{x1} + 2c_{x2} & 0 & 0 & 2ac_{x2} - 2bc_{x1} \\ 0 & 2c_{y1} + 2c_{y2} & -2ac_{y2} + 2bc_{y1} & 0 \\ 0 & -2ac_{y2} + 2bc_{y1} & 2a^2 c_{y2} + 2b^2 c_{y1} & 0 \\ 2ac_{x2} - 2bc_{x1} & 0 & 0 & 2a^2 c_{x2} + 2b^2 c_{x1} \end{bmatrix} \tag{6.26}$$

$$G = \begin{bmatrix} 0 & 0 & 0 & 0 \\ 0 & 0 & 0 & 0 \\ 0 & 0 & 0 & I_P \\ 0 & 0 & -I_P & 0 \end{bmatrix} \tag{6.27}$$

and,

$$q = \begin{bmatrix} x & y & \beta & \alpha \end{bmatrix}^T \tag{6.28}$$

The mass, damping and the stiffness matrices, M, C and K are symmetric and positive definite matrices. In contrast, the gyroscopic matrix G is skew-symmetric. To determine the roots of Equations [6.23], it must rearrange the equation in the followig form:

$$\begin{bmatrix} C + \Omega G & M \\ M & 0 \end{bmatrix} \frac{d}{dt} \begin{Bmatrix} q \\ \dot{q} \end{Bmatrix} + \begin{bmatrix} K & 0 \\ 0 & -M \end{bmatrix} \begin{Bmatrix} q \\ \dot{q} \end{Bmatrix} = \begin{Bmatrix} 0 \\ 0 \end{Bmatrix}$$

This is an 8x8 eigenvalue problem was formed and solved numerically. The Eigenvalue problem using Matlab has the following Mass, Stiffness and Gyroscopic matrices obtained used the following data:

$$
\begin{cases}
m = 122.68 \, kg \, mass \, of \, rotor \\
a = b = 0.25m \, distance \, of \, the \, bearing \, from \, the \, center \, of \, rotor \\
k_{x1} = k_{y1} = k_{x2} = k_{y2} = 1 \cdot 10^6 \, MN/m \, Stiffness \\
c_{x1} = c_{y1} = 10 \, Ns/m \, Damping \\
c_{x2} = c_{y2} = 10 \, Ns/m \, Damping \\
v_{x1} = v_{y1} = v_{x2} = v_{y2} = 60 \, kg \, Inertance \\
I_P = 0.6134 \, kgm^2 \, Polar \, inertia \\
I_d = 2.8625 \, kgm^2 \, Diametral \, inertia \\
\Omega = 4000 \, rev/min \, rotor \, speed
\end{cases}
\tag{6.29}
$$

Mass, Stiffness and gyroscopic matrices are:

$$
M = \begin{bmatrix}
242.68 & 0 & 0 & 0 \\
0 & 242.68 & 0 & 0 \\
0 & 0 & 10.36 & 0 \\
0 & 0 & 0 & 10.36
\end{bmatrix}
\tag{6.30}
$$

$$
K = \begin{bmatrix}
2.3 \cdot 10^6 & 0 & 0 & 75 \cdot 10^3 \\
0 & 2.3 \cdot 10^6 & 75 \cdot 10^3 & 0 \\
0 & -75 \cdot 10^3 & 1.44 \cdot 10^5 & 0 \\
75 \cdot 10^3 & 0 & 0 & 1.44 \cdot 10^5
\end{bmatrix}
\tag{6.31}
$$

$$
C = \begin{bmatrix}
23 & 0 & 0 & 0.75 \\
0 & 23 & -0.75 & 0 \\
0 & -0.75 & 1.44 & 0 \\
0.75 & 0 & 0 & 1.44
\end{bmatrix}
\tag{6.32}
$$

$$
G = \begin{bmatrix}
0 & 0 & 0 & 0 \\
0 & 0 & 0 & 0 \\
0 & 0 & 0 & 0.61 \\
0 & 0 & -0.61 & 0
\end{bmatrix}
\tag{6.33}
$$

Solving the Eigenvalue problem using Matlab the natural frequencies that depends of value of inertance can be obtained. In the Figure (6.6) it is reported the influence of inertance on natural frequencies of vibration system that behave similary as in Chapter [6.3], using the same matlab code:
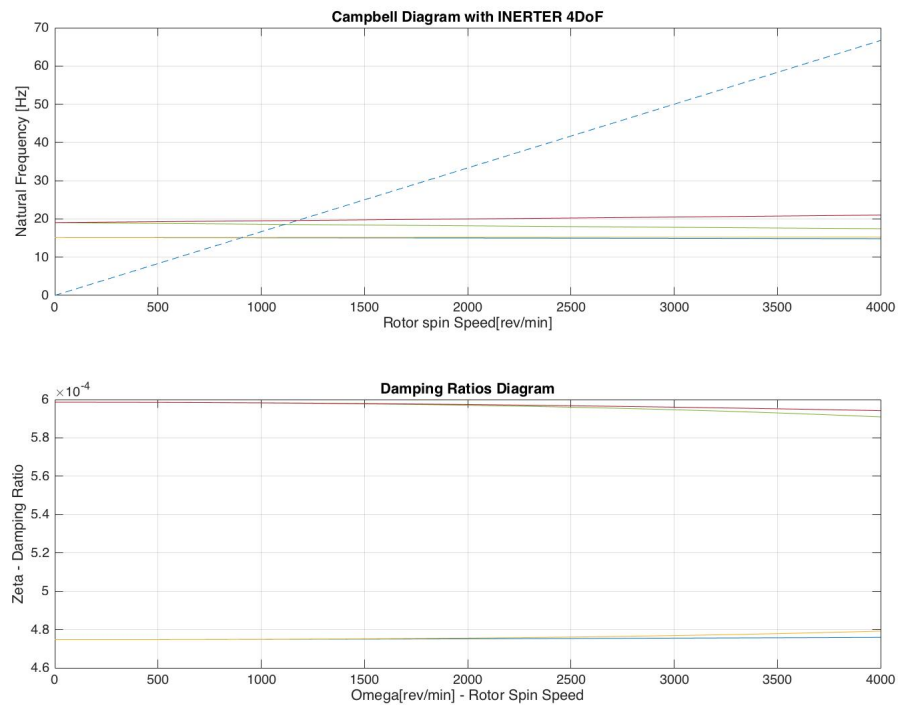

Figure 6.5: Campbell Diagram - 4DoF with Inerter

Preposition 3:

The natural frequency ω_n of an 4DoF Rotor System with four inerter are deacreasing function of the inertance v. Thus, inerter can reduce the natural frequency of an 4DoF Rotor System as dimonstrated in the figure (6.6). However, we can obtain the same result by increasing the total mass of the rotor without the introduction of four inerter. Thus, we conclude that this case is not very interesting for the purpose of our studies.
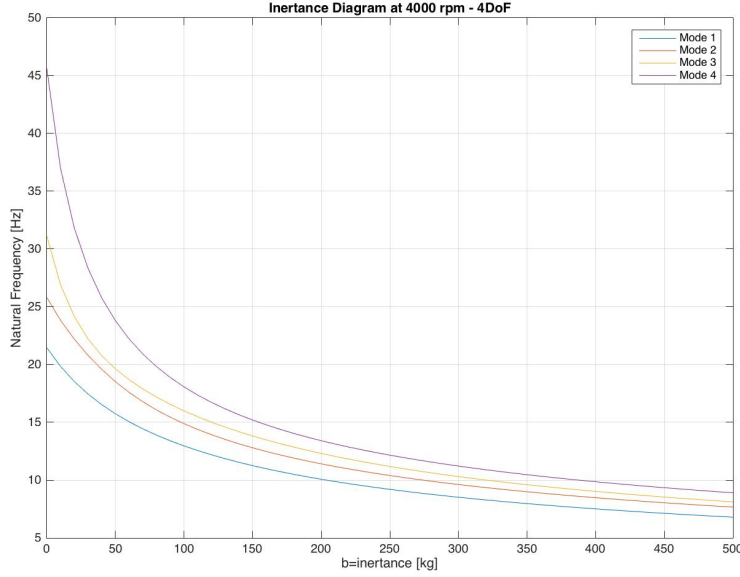
Figure 6.6: Inertance Diagram - 4DoF with Inerter

Forced Response

Like in Example [3.4] it has only one unbalance and it can calculated the response relative to that unbalance. In Matrix notation, the Equation [6.23] can be written as :

$$M\ddot{q} + (C + \Omega G)\,\dot{q} + Kq = F \tag{6.34}$$

where:

$$F = \begin{Bmatrix} m\epsilon\Omega^2 cos\Omega t \\ m\epsilon\Omega^2 sin\Omega t \\ 0 \\ 0 \end{Bmatrix} = \Re \begin{Bmatrix} m\epsilon \\ -jm\epsilon \\ 0 \\ 0 \end{Bmatrix} \Omega^2 e^{j\Omega t} \quad \epsilon = 0.1 \cdot 10^{-3} \; [m] \tag{6.35}$$

The steady-state solution is found by assuming a response of the form $q(t) = \Re\left(q_0 e^{j\Omega t}\right)$. Thus the equation become:

$$\left[-\Omega^2[M] + j\Omega(\Omega[G] + [C] + [K])\right] q_0 e^{j\Omega t} = \Omega^2 b_0 e^{j\Omega t} \tag{6.36}$$

where:

$$b_0 = \begin{Bmatrix} m\epsilon \\ -jm\epsilon \\ 0 \\ 0 \end{Bmatrix} \tag{6.37}$$

and, hence:

$$q_0 = \left[-\Omega^2[M] + j\Omega(\Omega[G] + [C] + [K])\right]^{-1}\Omega^2 b_0 \tag{6.38}$$

where:

$$FRF = \frac{1}{\left[-\Omega^2[M] + j\Omega(\Omega[G] + [C]) + [K]\right]} \tag{6.39}$$

The response can be obtained as a funcion of rotational speed which is shown in Figure (6.7). This response is similar at the response shown in Figure (3.3). Also in this case it has two peaks in the response, thus two critical speeds because it is examined the Isotropic case. It can be concluded that the inerter in parallel configuration with stiffness and damping dont effect to reduce the peak of resonance. The only effect is that the second peak of the reasonance occurs earlier than the case without Inerter. The same result it can get going to increare the mass of rigid rotor without introduce an inerter.
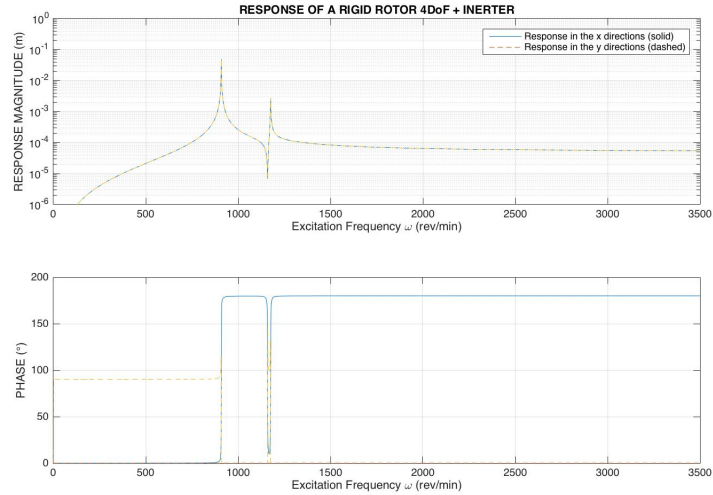

Figure 6.7: Response of Rigid Rotor - 4DoF with Inerter

6.5   System of 5DoF with Inerter

This system is different from previus cases because it has 5DoF as shown in Figure (6.8). Firstly, the equation of the motion for this system are introduced using Maple. This rotor has five degree of freedom because it can translate in the directions Ox and Oy and it can also rotate about these axes. The fifth degree of fredoom is given by the introduction of the *inerter*.

The partial code of Maple that it is used for delevop the equation of the motion in reported in the following script:
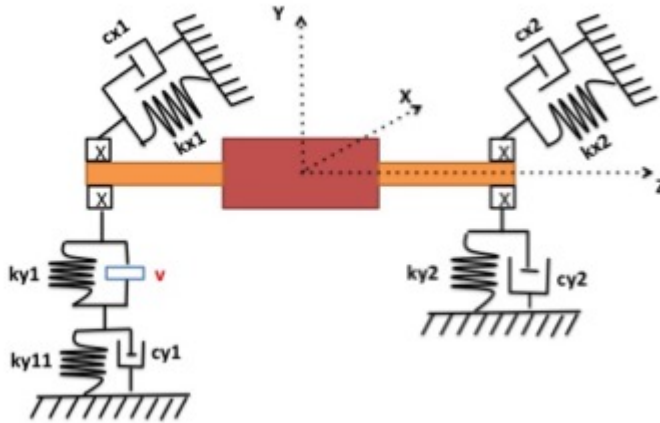

Figure 6.8: Rigid Rotor - 5DoF with Inerter

```
1   %1st define the body frame
2   >linear_modeling({x(t),y(t),alpha(t), beta(t)}); ...
       %rotations due to bearings elastiticy
3
4   >BF := translate(......... * rotate ...
       ('Y',beta(t))*.....set_frame_name(BF,'BF'):
5
6   %Definition of rotor mass properties
7   >rotor := make_BODY(..........); show(rotor);
8
9   %Right Bearing
10  >GR := make_POINT(ground, 0, 0, a); show(GR);
11  >PR := make_POINT(BF, 0, 0, a); show(PR);
12  >Δ := comp_Y(PR, ground)-comp_Y(GR, ground);
```

```
13 >eta := comp_X(PR, ground)-comp_X(GR, ground);
14
15 >FY_R := -kY2*Δ-cY2*(diff(Δ, t));
16 >FX_R := -kX2*eta-cX2*(diff(eta, t));
17
18 %bearing force
19 >bearing_PR := make_FORCE(..........): show(bearing_PR);
20
21 %Left Bearing
22 >............
23
24 %Newton Equations
25 eqnsN := newton_equations({rotor,bearing_PR,bearing_PL}): ...
       show(%);
26 eqnNL := kY11*yL(t)+cY1*(diff(yL(t), t)) = ...
       kY1*Δ1+vL*(diff(Δ1, t, t));
27
28 %Euler Equations
29 >eqnsE := ...
       euler_equations({rotor,bearing_PR,bearing_PL},CoM(rotor)):
30 >show(eqnsE);
31 .....................
32 %text
33 .....................
34 %State space formulation:
35 >interface(rtablesize = 20);
36 >xx,xeqns := first_order(qeqns,q,t);
37 <xx>,<xeqns>;
38 >implicit_state_space(...........);
39 end
```

The equations of the motion for this system using the script are:

$$
\begin{cases}
m\ddot{x} + (c_{x1} + c_{x2})\,\dot{x} + (k_{x1} + k_{x2})\,x + (ac_{x2} - bc_{x1})\,\dot{\beta} + (ak_{x2} - bk_{x1})\,\beta = 0 \\
(m + vL)\,\ddot{y} - vL\ddot{y}_L + c_{y2}\dot{y} - k_{y1}y_L + (k_{y1} + k_{y2})\,y + (-ak_{y2} + bk_{y1})\alpha + \\
-ac_{y2}\dot{\alpha} + v_L b\ddot{\alpha} = 0 \\
(b^2 v_L + I_d)\,\ddot{\alpha} + c_{y2}a^2\dot{\alpha} + (a^2 k_{y2} + b^2 k_{y1})\,\alpha - b\,(k_{y1}y_L + v_L\ddot{y}_L) + \dot{\beta}I_p\Omega + \\
+v_L b\ddot{y} - ac_{y2}\dot{y} + (-ak_{x2} - b_{x1}) = 0 \\
I_d\ddot{\beta} - \dot{\alpha}I_p\Omega + (a^2 k_{x2} + b^2 k_{x1})\,\beta + (a^2 c_{x2} + b^2 c_{x1})\,\dot{\beta} + (ac_{x2} - bc_{x1})\,\dot{x} + \\
+ (ak_{x2} - bk_{x1})\,x = 0 \\
k_{y11}y_L + c_{y1}\dot{y}_L = k_{y1}\,(\alpha b + y - y_L) + v_L(\ddot{\alpha}b + \ddot{y} - \ddot{y}_L)
\end{cases}
$$

$$(6.40)$$

The procedure to determine the Campbell Diagramm and Forced Lateral Response is very similar to the previus case. This case has a system of 5DoF, thus it has 5 natural frequencies and 5 critical speeds. The data for this system are the same used in [6.29]. In this case *mass*, *stiffness* and *gyroscopic* matrices are:

$$M = \begin{bmatrix} 122.68 & 0 & 0 & 0 & 0 \\ 0 & 182.68 & 15.00 & 0 & -60.00 \\ 0 & 15.00 & 6.61 & 0 & -15.00 \\ 0 & 0 & 0 & 2.86 & 0 \\ 0 & -60.00 & -15.00 & 0 & 60.00 \end{bmatrix} \tag{6.41}$$

$$K = \begin{bmatrix} 2.3 \cdot 10^6 & 0 & 0 & 75 \cdot 10^3 & 0 \\ 0 & 2.3 \cdot 10^6 & -75 \cdot 10^3 & 0 & -1.0 \cdot 10^6 \\ 0 & -75 \cdot 10^3 & 1.44 \cdot 10^5 & 0 & -2.5 \cdot 10^5 \\ 75 \cdot 10^3 & 0 & 0 & 1.44 \cdot 10^5 & 0 \\ 0 & -1.0 \cdot 10^6 & -2.5 \cdot 10^5 & 0 & 2.0 \cdot 10^6 \end{bmatrix} \tag{6.42}$$

$$C = \begin{bmatrix} 46 & 0 & 0 & 1.50 & 0 \\ 0 & 26.00 & -6.50 & 0 & 0 \\ 0 & -6.50 & 1.63 & 0 & 0 \\ 1.50 & 0 & 0 & 2.88 & 0 \\ 0 & 0 & 0 & 0 & 20.00 \end{bmatrix} \tag{6.43}$$

$$G = \begin{bmatrix} 0 & 0 & 0 & 0 & 0 \\ 0 & 0 & 0 & 0 & 0 \\ 0 & 0 & 0 & 0.61 & 0 \\ 0 & 0 & -0.61 & 0 & 0 \\ 0 & 0 & 0 & 0 & 0 \end{bmatrix} \tag{6.44}$$

Solving the Eigenvalue problem in Matlab, is found that the natural frequencies depends of value of inertance. To determine these frequencies it is used an inertance v=60kg and it has been obtanined the Campbell Diagram shown in Figure (6.9); In the Figure (6.10) it is reported the influence of inertance on natural frequencies of 5DoF vibration system. It can be observed that also in this case, by increasing the value of inertance, the natural frequencies decreases up to a value of 100kg.
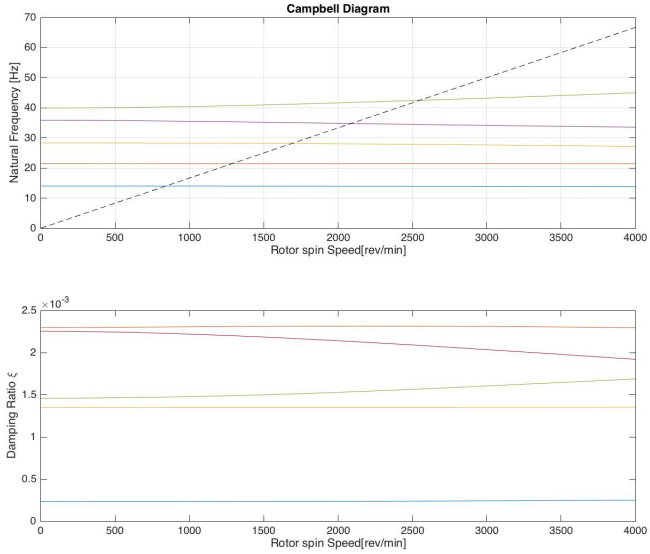
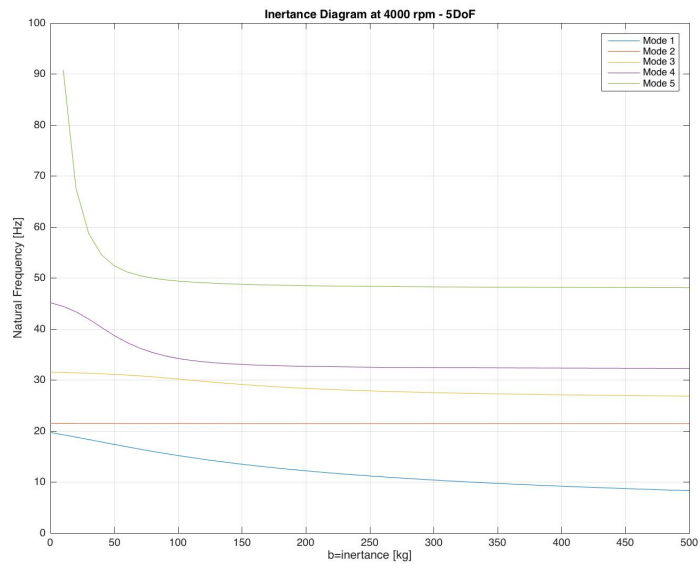Figure 6.9: Campbell Diagram - 5DoF with Inerter

Figure 6.10: Inertance Diagram - 5DoF with Inerter

Subsequently the first frequency continues to decrease with increasing of the inertance while the others remain almost constant. Then, is calculated the Forced Lateral Response as in previous case using the same equations:

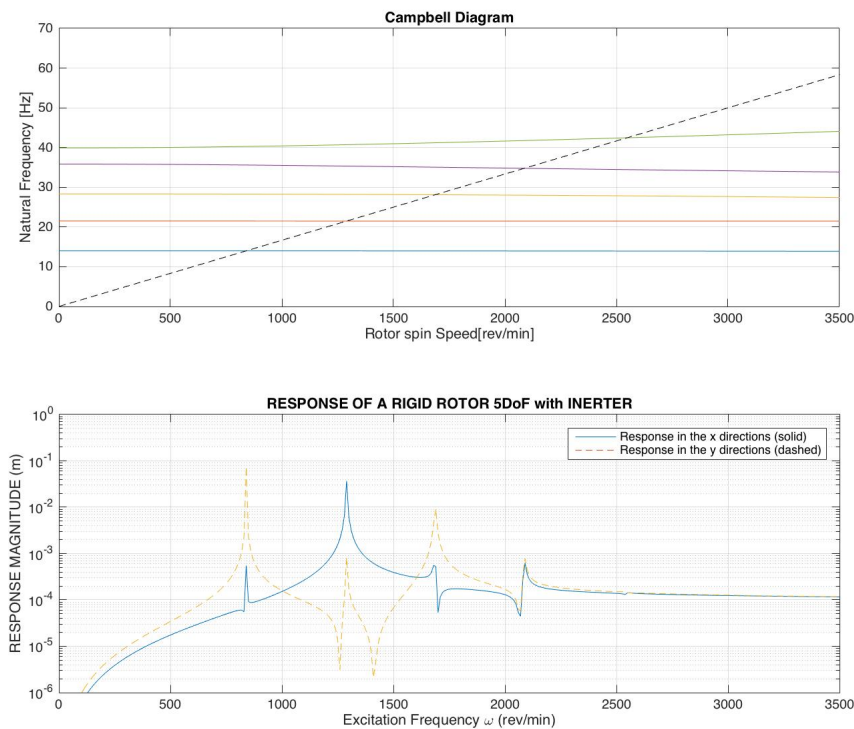$$FRF = \frac{1}{[-\Omega^2[M] + j\Omega(\Omega[G] + [C]) + [K]]} \tag{6.45}$$

Figure 6.11: Response of a Rigid Rotor - 5DoF with Inerter

The response can be obtained as a funcion of the rotational speed which is shown in Figure (6.11). This response is similar to the response shown in Figure (3.5). Also in this case there are five peaks in the response as our system, has five Degree of freedom, thus five critical speeds. Looking at the diagram it can also say that the magnitude of the first frequency response, with the introduction of the inerter, is reduced along the x-axis.

Equation of motion

The equations of motion for this system of 5DOF were obtained, as mentioned earlier, using Maple. To confirm of what has been achieved is correct in terms of equations and formulas the stiffness and inertance are given the following values:

$k_{y1} = 1 \cdot 10^{12} \, N/m \, (to \, infinity)$
$v = 0.001 \, kg \, (to \, zero)$

Then, using the data [6.29] are obatained the results of the 4dof system. This allowed us to confirm that the equations developed by Maple for the system to 5DOF are fair and the results obtained are reliable.

6.6 System of 6DoF with Inerter

To develop the equations of motion for this system, the Maple script is used as for 5DoF system. This case has two inerters, one for each bearing. They are positioned both along the y-axis. This rotor has *six* degree of freedom because it can translate in the directions Ox and Oy and it also can rotate about these axes. The *fifth* and *sixth* degree of fredoom are given by the introduction of the *inerter*.
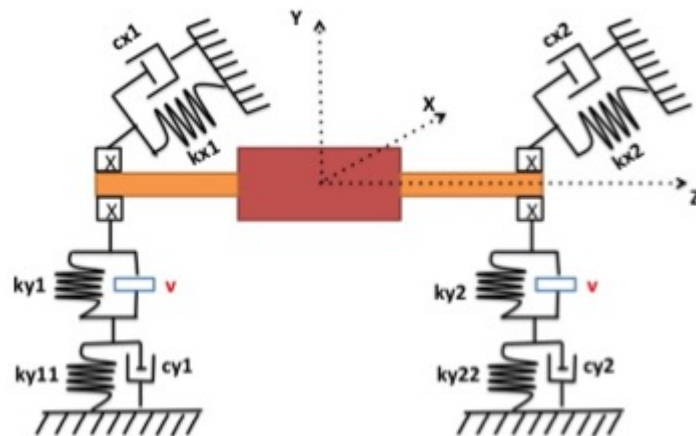

Figure 6.12: Rigid Rotor - 6DoF with Inerter

The Equations of the motion obtained using Maple for this system are:

$$
\begin{cases}
m\ddot{x} + (c_{x1} + c_{x2})\dot{x} + (k_{x1} + k_{x2})x + (ac_{x2} - bc_{x1})\dot{\beta} + (ak_{x2} - bk_{x1})\beta = 0 \\
(m + vL + vR)\ddot{y} - vL\ddot{y}_L - vR\ddot{y}_R - k_{y2}y_R - k_{y1}y_L + (k_{y1} + k_{y2})y + \\
+(-ak_{y2} + bk_{y1})\alpha + (-av_R + bv_L)\ddot{\alpha} = 0 \\
(a^2v_R + b^2v_L + I_d)\ddot{\alpha} + (-av_R + bv_L)\ddot{y} + (a^2k_{y2} + b^2k_{y1})\alpha - b(k_{y1}y_L + v_L\ddot{y}_L) + \\
+(-ak_{y2} + k_{y1})y + I_p\Omega\dot{\beta} + a(k_{y2}y_R + v_R\ddot{y}_R) = 0 \\
I_d\ddot{\beta} - \dot{\alpha}I_p\Omega + (a^2c_{x2} + b^2c_{x1})\dot{\beta} + (ac_{x2} - bc_{x1})\dot{x} + (ak_{x2} - bk_{x1})x + \\
+(a^2k_{x2} + b^2k_{x1})\beta = 0 \\
k_{y11}y_L + c_{y1}\dot{y}_L = k_{y1}(ab + y - y_L) + v_L(\ddot{a}b + \ddot{y} - \ddot{y}_L) \\
k_{y22}y_R + c_{y2}\dot{y}_R = k_{y2}(-\alpha a + y - y_R) + v_R(-\ddot{a}a + \ddot{y} - \ddot{y}_R)
\end{cases}
$$

$$(6.46)$$

where $vL =$ is the left inerter and $vR =$ is the right inerter.

The procedure to determine the Campbell Diagramm and Forced Lateral Response is very similar to the previus case. In this case it has a system with 6DoF, thus it has six natural frequencies and six critical speeds. The data for this system are:

$$
\begin{cases}
m = 122.68\,kg \\
a = b = 0.25\,m \\
k_{x1} = k_{y1} = 1 \cdot 10^6\,MN/m \\
k_{x2} = k_{y2} = 1 \cdot 10^6\,MN/m \\
c_{x1} = c_{y1} = 10\,Ns/m \\
c_{x2} = c_{y2} = 13\,Ns/m \\
v = 60\,kg\,Inertance \\
I_P = 0.6134\,kgm^2 \\
I_d = 2.8625\,kgm^2 \\
\Omega = 4000\,rev/min\,rotor\,speed
\end{cases}
$$

$$(6.47)$$

In this case for 6DoF Rigid Rotor system with inerter *mass*, *stiffness* and *gyroscopic* matrices are:

$$M = \begin{bmatrix} 122.68 & 0 & 0 & 0 & 0 & 0 \\ 0 & 242.68 & 0 & 0 & -60.00 & -60.00 \\ 0 & 0 & 10.36 & 0 & 15.00 & -15.00 \\ 0 & 0 & 0 & 2.86 & 0 & 0 \\ 0 & -60.00 & 15.00 & 0 & 60.00 & 0 \\ 0 & -60.00 & -15.00 & 0 & 0 & 60.00 \end{bmatrix} \tag{6.48}$$

$$K = \begin{bmatrix} 2.3 \cdot 10^6 & 0 & 0 & 75 \cdot 10^3 & 0 & 0 \\ 0 & 2.3 \cdot 10^6 & -75 \cdot 10^3 & 0 & -1.3 \cdot 10^6 & -1.0 \cdot 10^6 \\ 0 & -75 \cdot 10^3 & 1.44 \cdot 10^5 & 0 & 3.25 \cdot 10^5 & -2.5 \cdot 10^5 \\ 75 \cdot 10^3 & 0 & 0 & 1.44 \cdot 10^5 & 0 & 0 \\ 0 & -1.3 \cdot 10^6 & 3.25 \cdot 10^5 & 0 & 2.6 \cdot 10^6 & 0 \\ 0 & -1.0 \cdot 10^6 & -2.5 \cdot 10^5 & 0 & 0 & 2.0 \cdot 10^6 \end{bmatrix} \tag{6.49}$$

$$C = \begin{bmatrix} 46 & 0 & 0 & 1.50 & 0 & 0 \\ 0 & 0 & 0 & 0 & 0 & 0 \\ 0 & 0 & 0 & 0 & 0 & 0 \\ 1.50 & 0 & 0 & 2.88 & 0 & 0 \\ 0 & 0 & 0 & 0 & 26.00 & 0 \\ 0 & 0 & 0 & 0 & 0 & 20.00 \end{bmatrix} \tag{6.50}$$

$$G = \begin{bmatrix} 0 & 0 & 0 & 0 & 0 & 0 \\ 0 & 0 & 0 & 0 & 0 & 0 \\ 0 & 0 & 0 & 0.61 & 0 & 0 \\ 0 & 0 & -0.61 & 0 & 0 & 0 \\ 0 & 0 & 0 & 0 & 0 & 0 \\ 0 & 0 & 0 & 0 & 0 & 0 \end{bmatrix} \tag{6.51}$$

Solving the Eigenvalue problem using Matlab the natural frequencies depend on value of the inertance. To determine these frequencies it is used an inertance v=60kg and it is obtanined the following Campbell Diagram reported in Figure(6.13):

As for the case in 5DOF also for this system with 6DoF it is seen the trend of the frequencies with the inertance. It is noted immediately that in this case the frequencies continue to decrease with the increase of the inertance.
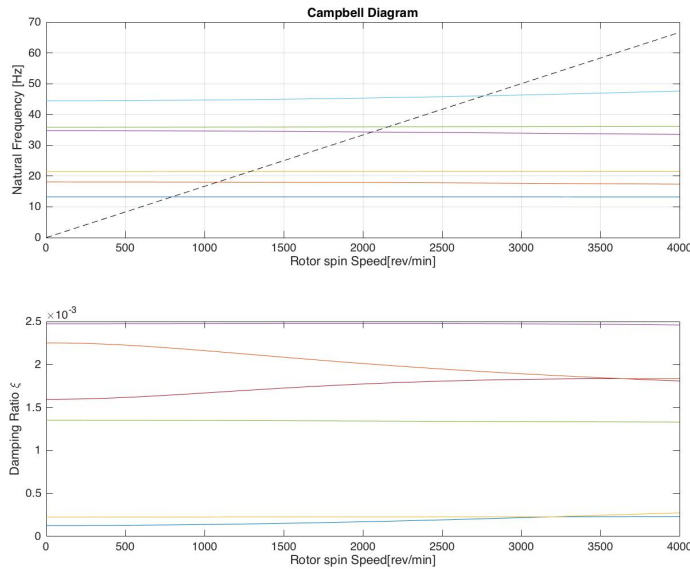
Figure 6.13: Campbell Diagram - 6DoF with Inerter

Preposition 4: *The natural frequency ω_n of an 6DoF Rotor System with two inerter are deacreasing function of the inertance v_{x1} and v_{x2}. Thus, inerter can reduce the natural frequency of an 6DoF Rotor System like dimostred in the figure (6.14).*

Forced Response

As in previous case it can calculated the Forced Lateral Response. The response can be obtained as a funcion of rotational speed which is shown in Figure (6.14). This response is similar at the response shown in Figure (3.5). Also in this case it has six peaks in the response because our system, has six Degree of freedom, thus six critical speeds. Looking at the diagram it can be also infered that the magnitude of the first and second frequency response, with the introduction of the inerter, is reduced along the x-axis.

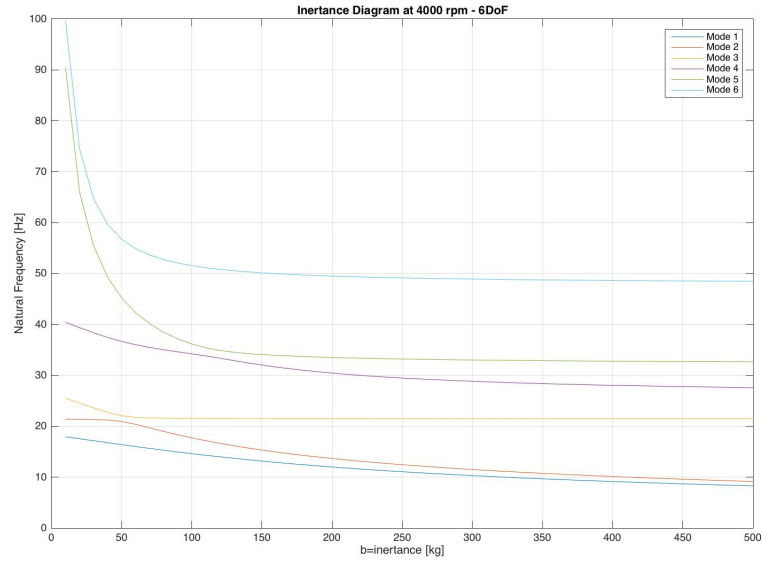$$FRF = \frac{1}{\left[-\Omega^2[M] + j\Omega(\Omega[G] + [C]) + [K]\right]} \tag{6.52}$$

Figure 6.14: Inertance Diagram - 6DoF with Inerter

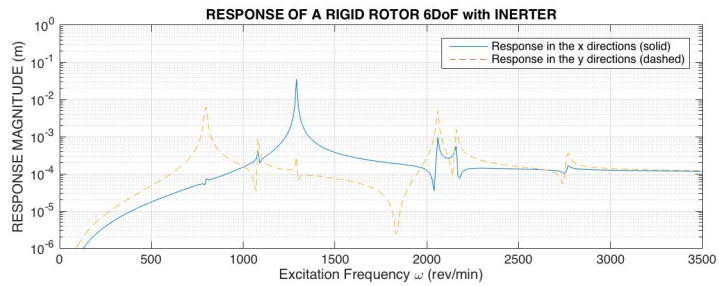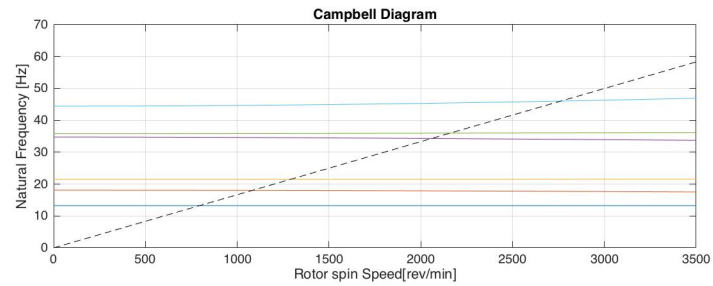
Figure 6.15: Response of a Rigid Rotor - 6DoF with Inerter

Equation of motion

The equations of motion for this system of 6DOF were obtained, as mentioned earlier, using Maple. To confirm of what has been achieved is correct in terms of equations and formulas the stiffness and inertance are given the following values:

$$k_{y1} = 1 \cdot 10^{12} \, N/m \, (to \, infinity)$$
$$k_{y2} = 1 \cdot 10^{12} \, N/m \, (to \, infinity)$$
$$v = 0.001 \, kg \, (to \, zero)$$

Then, using the data [6.29] are obatained the results of the 4dof system. This allowed us to confirm that the equations developed by Maple for the system to 6DOF are fair and the results obtained are reliable.

Chapter 7

Design of Fluid Inerter

7.1   Introduction

This chapter presents the mechanical design and implementation of a fluid inerter realized in Dynamics Laboratory at Institute of Sound Vibration (ISVR) at University of Southampton.

7.2   Fluid Inerter Modelling

Consider a piston and cylinder driving fluid through a helical tube surroinding the cylinder, as shown in Figure (7.1)
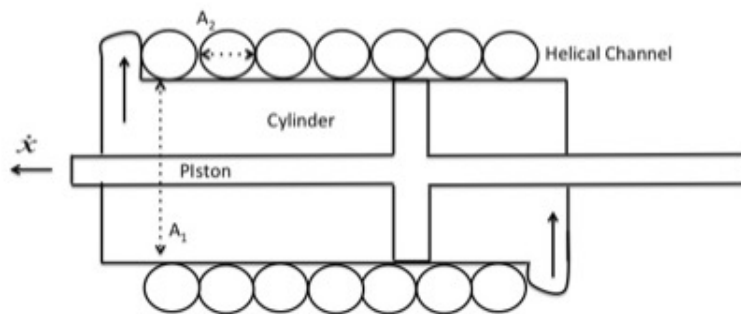

Figure 7.1: Piston and Cylinder fluid inerter

Let F be the equal and opposite force applied to the terminals and x be

the relative displacement between them. An ideal inerter is described by the following equation:

$$F = b\ddot{x} \tag{7.1}$$

where b is the *inertance* (costant of proportionality) in the unit of kg. The inertance of ideal inerter [13] for a fluid inerter device is:

$$b = \rho l \frac{A_1^2}{A_2} \tag{7.2}$$

where A_1 is annular area of the main cylinder, A_2 is channel cross sectional area, ρ is fluid density and l is channel length.

Large value of *inertance* are depends by:

- ρ density of the fluid inerter: the value of inertance depends on the fluid: with low density (i.e air) the inertance will be low while with high density (i.e oil or water) the value of the inertance will be higher compared to the first case.

- l channel length: the value of inertance depends on l, increasing l increases the inertance of the system and deacreasing l deacreases the inertance b.

- $\frac{A_1}{A_2}$ ratio of the piston area to the channel area: increasing A_1 increases also the inertance of the system and increasing A_2 reduces the inertance.

To build the fluid inerter the following cylinder double acting both double ended was used. The cylinder has the following characteristics:

- Piston area $A_1 = 1.1 \cdot 10^{-3}\, m^2$

- Channel area $A_2 = 28.2 \cdot 10^{-6}\, m^2$

- Channel length: $1.68\, m$

- Cylinder Type: Double Acting Double Ended Rod

During the experiment the copper pipe was replaced by a rubber tube to have less losses in the curved parts. Once built, the inerter was placed on a test bench for testing.
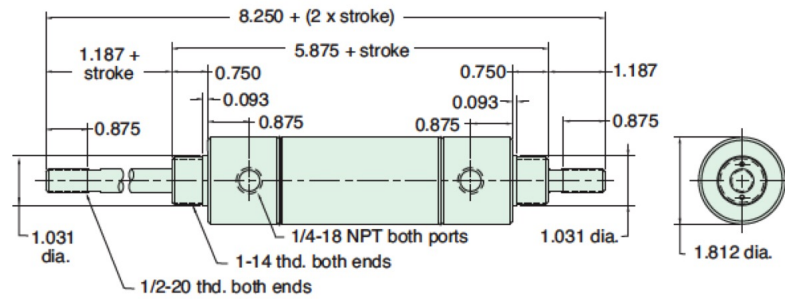
Figure 7.2: Cylinder fluid inerter

Figure 7.3: Caracteristics of Cylinder fluid inerter
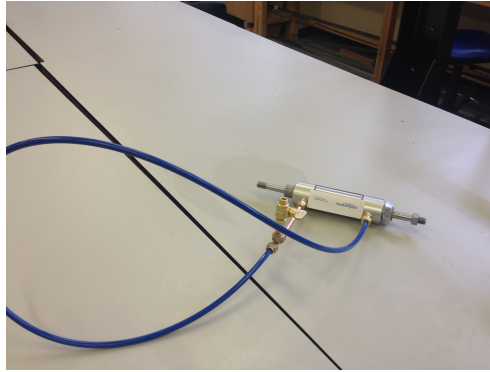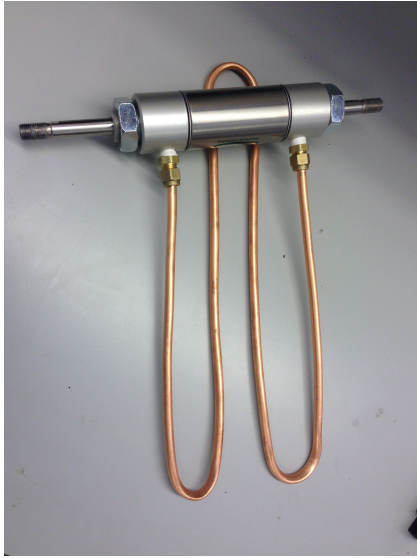

Figure 7.4: Copper pipe and Rubber tube
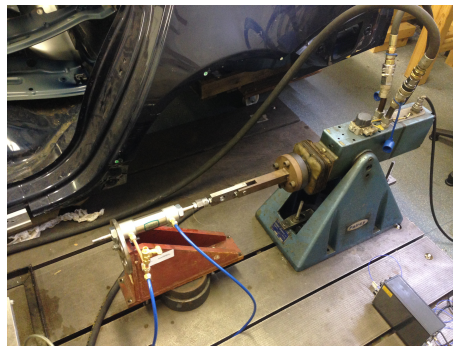
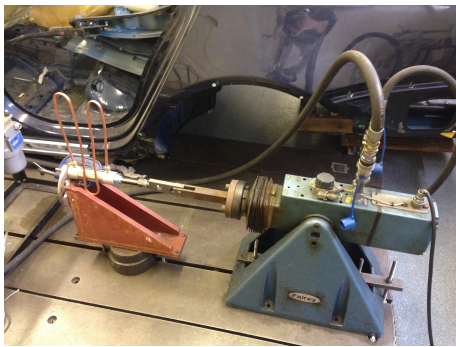Figure 7.5: Cylinder with copper pipe and rubber tube

Figure 7.6: Fluid Inerter - Test Bench

7.3 Test Bench

The schematic of the test bench realised at the University of Southampton is the following:
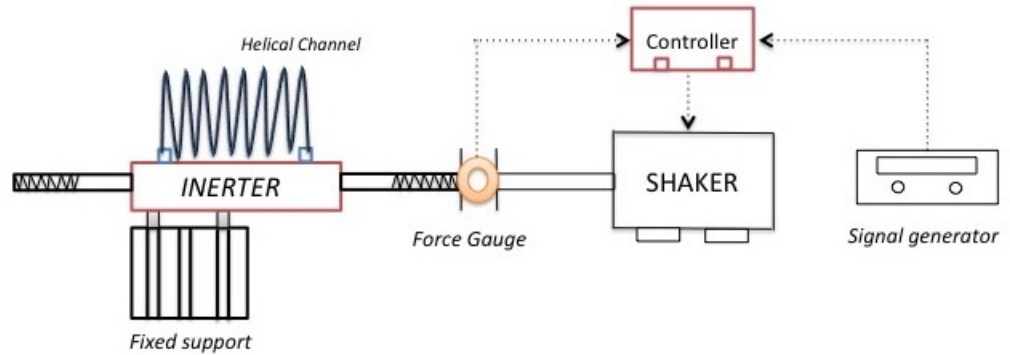

Figure 7.7: Schematic of experiment with fluid inerter

where the characteristics of the individual components of the scheme are:

Hydraulic shaker of Fairey Industry

Figure 7.8: Hydraulic Shaker

Equipment:

The hydraulic shaker assembly is comprised of:

- 1 shaker unit

- 1 hydraulic pump

- 1 servo controller

It should be noted that it is difficult to determine exactly which specification of shaker is being used, the situation being further complicated by the hydraulic pump producing 800 psi (pump is specified max 1000 psi) rather than the 3000 psi stated in the documentation.

Force:

From the available documentation on the low thrust vibration the maximum force (adjusted for pressure difference) is between 890 to 2850N.

Stroke:

The absolute maximum movement that can be obtained by the shaker is 100 mm, though this reduces with frequency. At 5 V peak to peak at a gain of 5, which was the input limit for smooth motion during testing, stroke was seen to be 40mm at 1Hz reducing with frequency to approximately 20mm at 10Hz.

Hydraulic Cylinder:

The Hydraulic cylinder (Double Acting Double Ended Rod-28-2) used to realize the inerter has the dimensions shown in Figure (7.10).

- BORE: $1 + 3/4 \, [inch]$

- ROD: $1/2 \, [inch]$

- PORT: $1/4 \, [inch]$

To calculate the inertance of the "Fluid Inerter" the following Matlab Code was used:
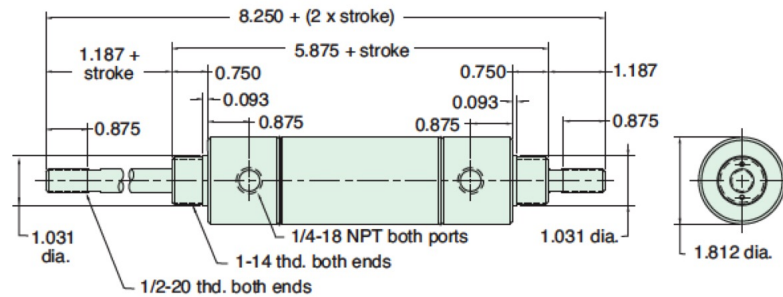
Figure 7.9: Hydraulic Cylinder

```
1   %Inertance:
2
3   BORE=1+3/4;
4   ROD=1/2;
5   PORT=1/4;
6
7   Db=(BORE/0.039370)*(10^-3);
8   Dr=(ROD/0.039370)*(10^-3);
9   D2=(PORT/0.039370)*(10^-3);
10
11  rho=950 density of particolar oil;
12  l=1.42; % in meter
13
14  A1=(Db^2-Dr^2)*(pi/4) % Piston Area
15
16  A2=(pi/4)*D2^2 %Channel Area
17
18  b=rho*l*(A1^2/A2)  %valore in kg
19  %b = 86.5119kg
```

Kistler Gauge Force:

The Kistler Gauge Force is a component force sensor for measuring dynamic and quasi-static forces in z direction. Measuring range 0-90000N, Temperature -196-200C.

- Very compact

- Extremely high rigidity

- Threshold $< 0,01N$, indipendent of measuring range.

Figure 7.10: Gauge Force

Mounting:

The load washers must be installed between two plane-parallel, rigid and fine-machined (preferably ground) faces. This is necessary to achieve a good load distribution on one hand and a wide frequency response on the other hand. The load washers should always be installed under preload. The reasons are:
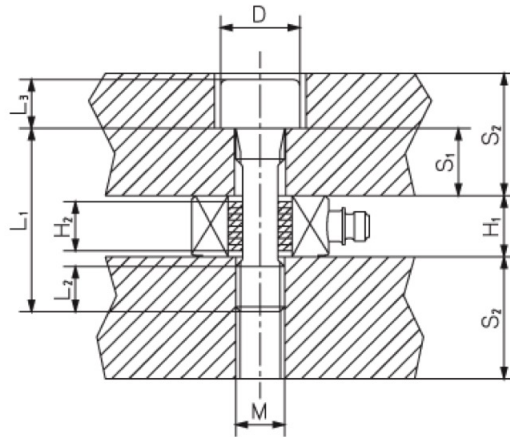

Figure 7.11: Mounting Sensor Type 9031A

- the sensor is fixed in this way

- measuring compression and tension

- the faces are pressed together which allows to benefit fully

- of the rigidity of the sensor

Other Components:

Signal Generator:

Signal Generator. Hewlett Packard. 15 Mhz Function / Arbitrary wave form generator

Figure 7.12: Signal Generator - Hewlett Packard

Oscilloscope:
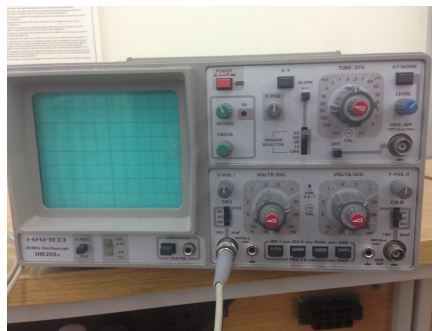
Oscilloscope. HM 203-s. 20Mhz

Figure 7.13: Oscilloscope

Preliminary operation:

- The hydraulic cylinder was fixed to the support with the help of a Clevis Bracket designed for our inerter.

- The Kistel Gauge Force was mounted between the inerter and the shaker with the help of two aluminum plates.

- The accelerometer PCB Piezotronics was insert in the inerter.

- The signal generator for position control of the shaker and the oscilloscope were used to observe the change of sinusoidal signal over time.

Matching between Shaker and Signal Generator:

The matching between volt and shaker position is measured positioning a graduate scale in centimetre (from -10 cm to 10 cm) under the shaker as shown in Figure (7.16)
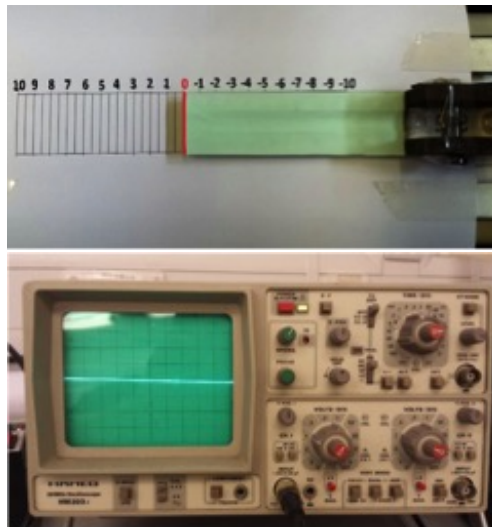

Figure 7.14: Matching the displacement value on the graduate scale and voltage value on the oscilloscope

The start position is 0 cm and the signal of transducer visualized on the oscilloscope is 0 V. By moving the shaker using the Signal Generator (Hewlett Packard), the transducer response in volt changes visualizing the

corresponding voltage value on the oscilloscope. The measure matching in centimetres is obtained reading the displacement on the graduate scale.

The matching scale from volt to cm was found to be $2V = 1cm$ and is represented with a graph in the Figure (7.17):
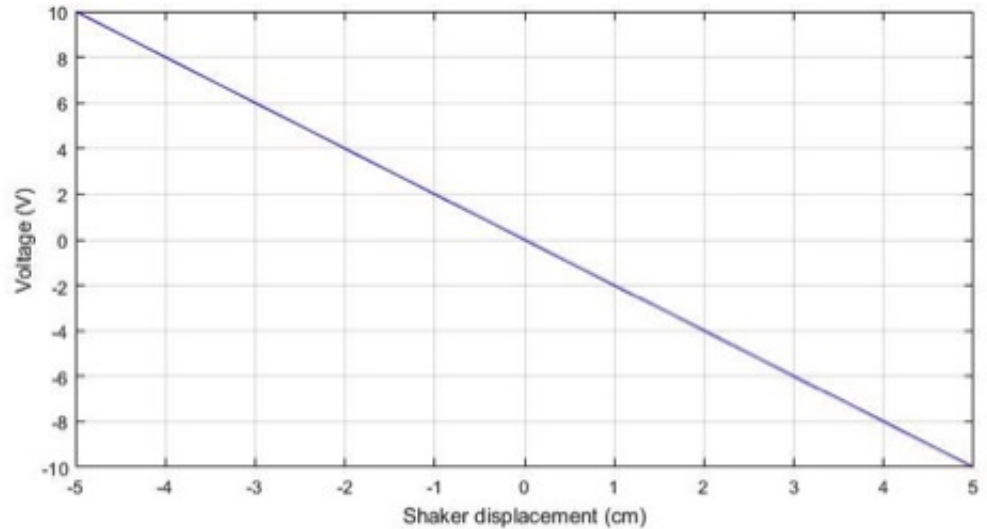

Figure 7.15: Matching Volt-cm

Test Bench Complete:

In the following figure is reported the complete Test Bench realized for the experiments in dynamics laboratory at University of Southampton.

7.4 Test and results

This part of the chapter presents the testing of the Fluid Inerter properties under different loads, amplitutes and frequencies. The Hydraulic Shaker was employed to obtain under different load and dimensions the data mentioned above. The load range for this experiment is from 0 to 2850N and the frequency range is from 0 to 5Hz. The Force Gauge 208/C01 and the Accelerometer are used to obtain the Force and Inerter displacement under this condition. The aim is to demostrate that a fluid inerter was realized.
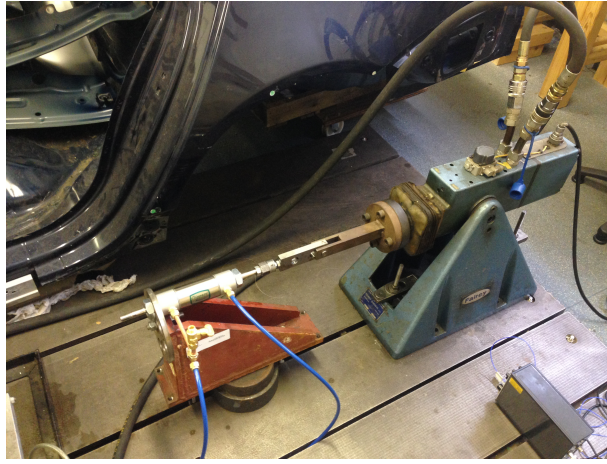
Figure 7.16: Test Bench configuration when completed

For this experiment, the parasitic damping caused by frictional losses in the fluid can be considered to act in parallel to the device inertance as shown in Figure (7.17).
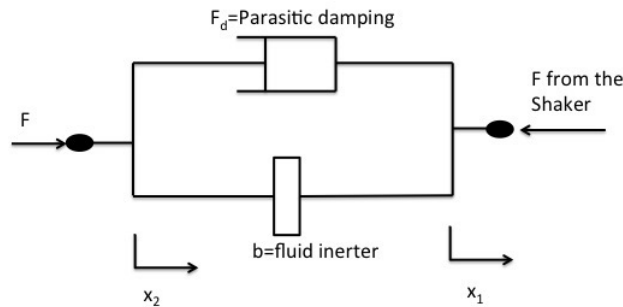

Figure 7.17: Model of fluid inerter with parasitic damping

The force F_d due to parasitic damping is taken to be a function of the strut velocity, and the force due to inertance is considered ideal and a linear function of the acceleration:

$$F = F_d \left(\dot{x}_2 - \dot{x}_1 \right) + b \left(\ddot{x}_2 - \ddot{x}_1 \right) \tag{7.3}$$

where x_1 and x_2 are the position of the device terminals and b is the inertance of fluid inerter given by Equation [4.27] reported here for convenience.

$$b = \rho l \frac{A_1^2}{A_2} \tag{7.4}$$

During the experiments different values of inertance are obtained by varying the channel length l. The density ρ of the oil (Engine oil SAE-30) used is $950\,kg/m^3$. Engine oils are generally formulated oils. The characteristics of the oil used in the experiments in terms of kinematic viscosity and density over temperature are shown in Figure (7.20).
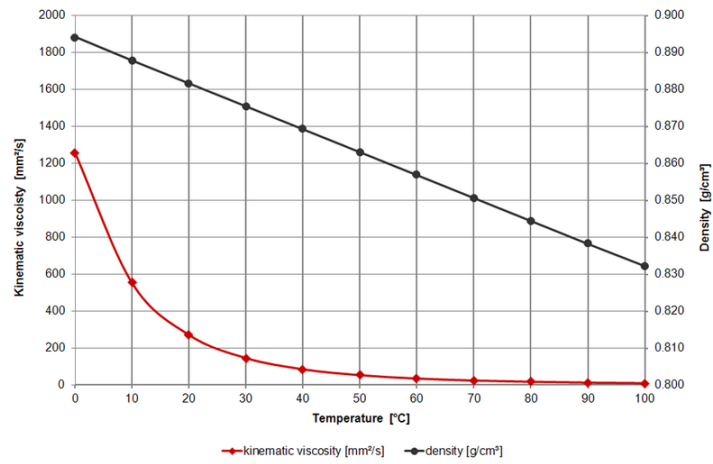

Figure 7.18: Kinematic viscosity and Density over temperature

Force due to inertance

The force due to inertance can be obtained by solving the caratteristic equation of ideal inerter [4.19] repeated here for convenience:

$$F = b\ddot{x} \tag{7.5}$$

Letting:

$$x = Acos(\omega t) \tag{7.6}$$

and differentiating this equation twice with respect to time gives:

$$\ddot{x} = -\omega^2 Acos(\omega t) = -\omega^2 x \tag{7.7}$$

where A depends by the matching map shown in Figure (7.17) and ω depends by frequency.

Example   For Voltage=10V the shaker dispalcement is $|5|\ cm$, thus $A = 0.05\ m$. If the frequency is 5Hz, $\omega = 5 \cdot 2\pi = 31.42\ rad/sec$. Hence, the acceleration is: $\ddot{x} = \omega^2 \cdot A = 49.35\ m/s^2$. Now, if $b = 60\ kg$, using the equation [7.5] is possible to calculate the force due to inertance:

$F = b\ddot{x} \rightarrow F = 60 \cdot 49.35 = 2961\ N$

Experimental results of the fluid inerter

In the Dymanics Laboratory, a test bench for experiments was realised (Figure 7.7 and 7.8) and the results for testing the fluid inerter proprieties under different load, amplitude and frequency are presented in this Section. From the behaviour showed in the experimental results, in particular in test 1 to 5, it can be concluded that the device built is a fluid inerter.

Test 1:

The data used for this experiment are:

- Voltage=1.5 volt

- Frequency=1Hz

Sinusoidal responses from the testing of the external-helix inerter with Engine oil SAE-30 are reported in the Figure (7.19).

Is possible to calculate the Equation [7.3] for each case. The force damping is calculated from the area of diagram Force-Displacement using the following Equation:

$$F_d = c = \frac{Area}{\pi \cdot \omega \cdot maxdisp^2} \tag{7.8}$$

Where the area is calculated using Matlab. For this Test 1 the force damping and the force due to inertance are reported following:

$$F1 = F_{damping} + F_{inerter} \tag{7.9}$$

$$F_{damping} = F_d \left(\dot{x}_2 - \dot{x}_1 \right) \tag{7.10}$$

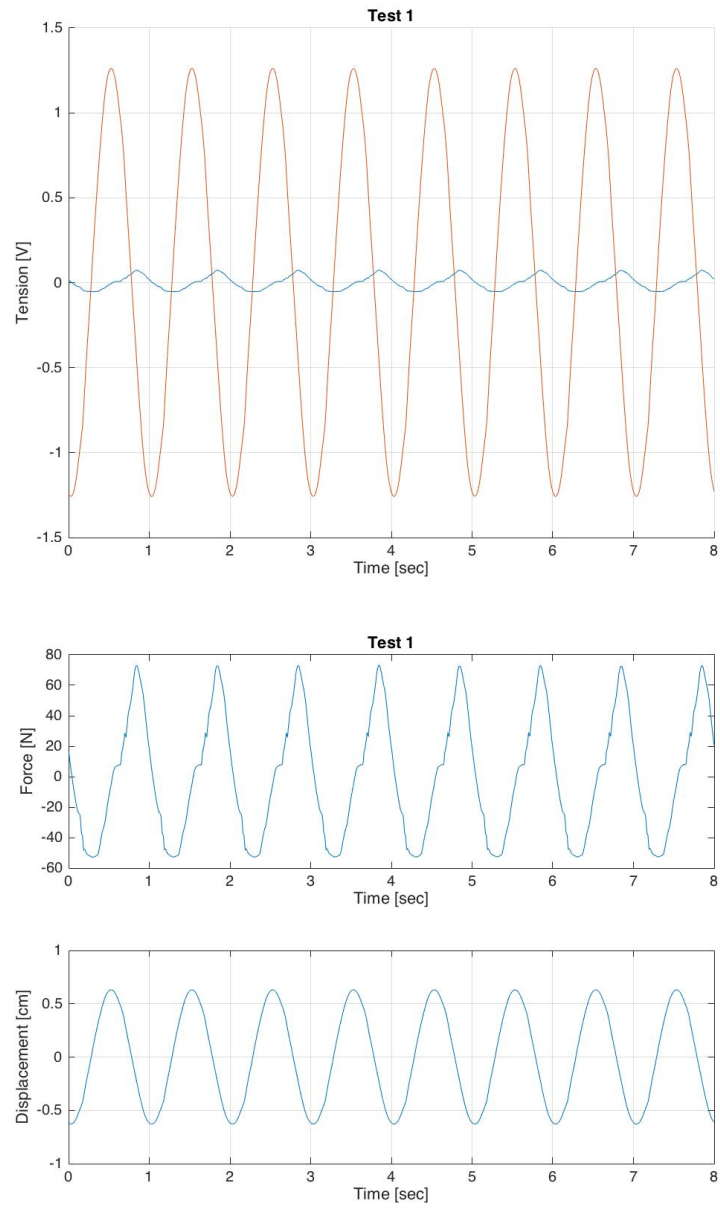$$F_{inerter} = b \left(\ddot{x}_2 - \ddot{x}_1 \right) \tag{7.11}$$
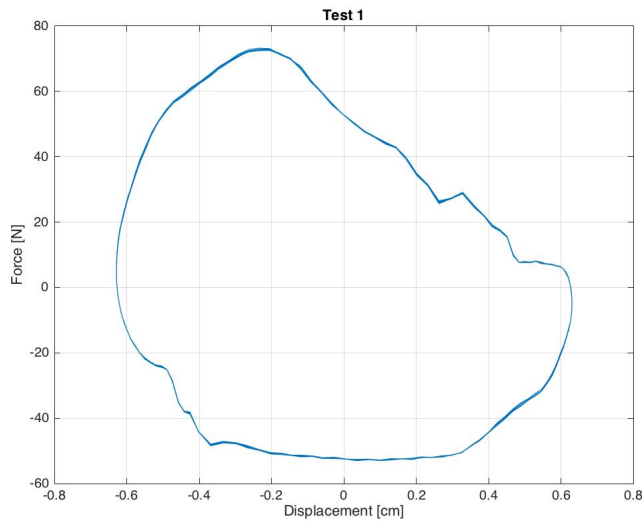
Figure 7.19: Test 1

Figure 7.20: Force-Displacement diagram

Test 2:

The data used for this experiment are:

- Voltage=1.5 volt

- Frequency=2Hz

Sinusoidal responses and the diagram Force-Displacement from the testing of the external-helix inerter with Engine oil SAE-30 are reported in the Figure (7.23 and 7.22).

Test 3:

The data used for this experiment are:

- Voltage=1 volt

- Frequency=3Hz

Sinusoidal responses and the diagram Force-Displacement from the testing of the external-helix inerter with Engine oil SAE-30 are reported in the Figure (7.23 and 7.22).

Figure 7.21: Test 2

Figure 7.22: Test 2 and 3

Figure 7.23: Test 3

Figure 7.24: Test 4 and 5

Test 4:

The data used for this experiment are:

- Voltage=2volt

- Frequency=2Hz

Sinusoidal responses and the diagram Force-Displacement from the testing of the external-helix inerter with Engine oil SAE-30 are reported in the Figure (7.25 and 7.24).

Test 5:

The data used for this experiment are:

- Voltage=4volt

- Frequency=5Hz

Sinusoidal responses and the diagram Force-Displacement from the testing of the external-helix inerter with Engine oil SAE-30 are reported in the Figure (7.24 and 7.26).
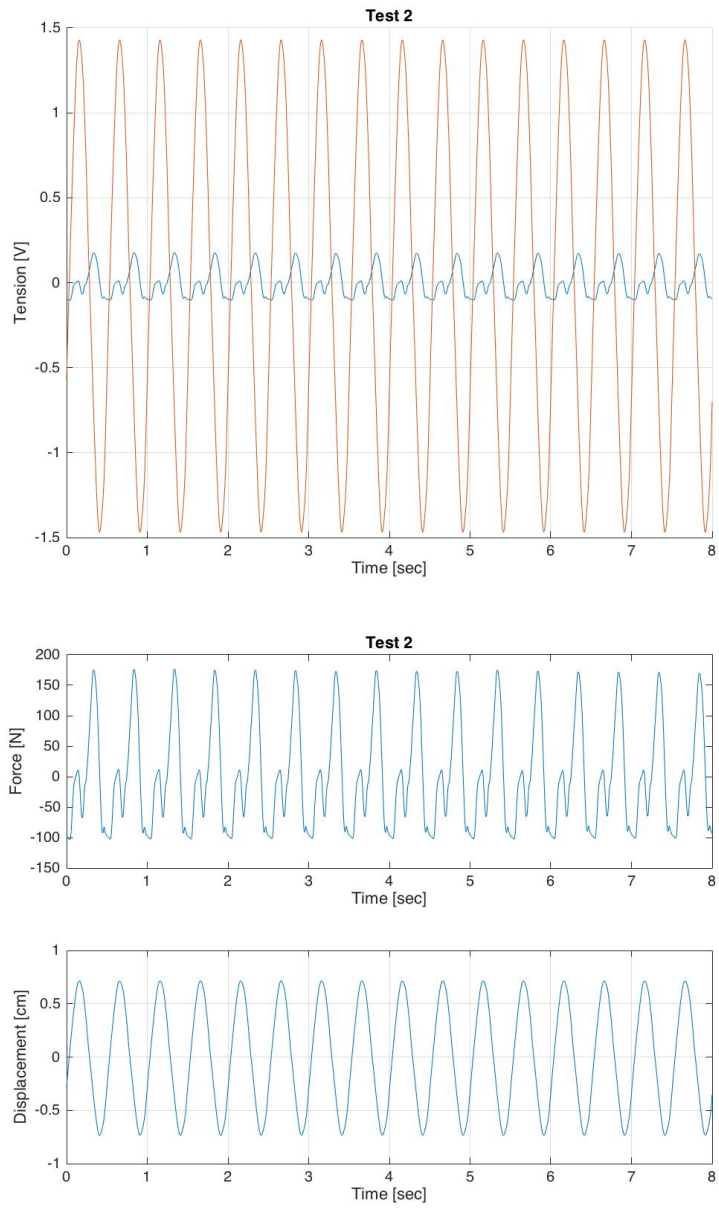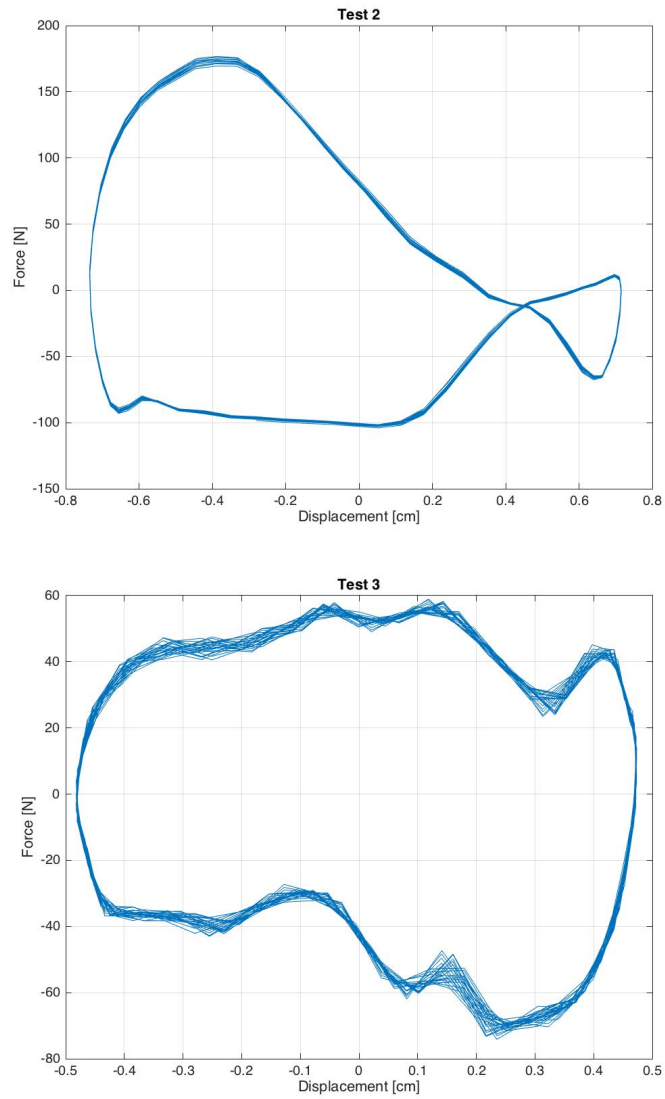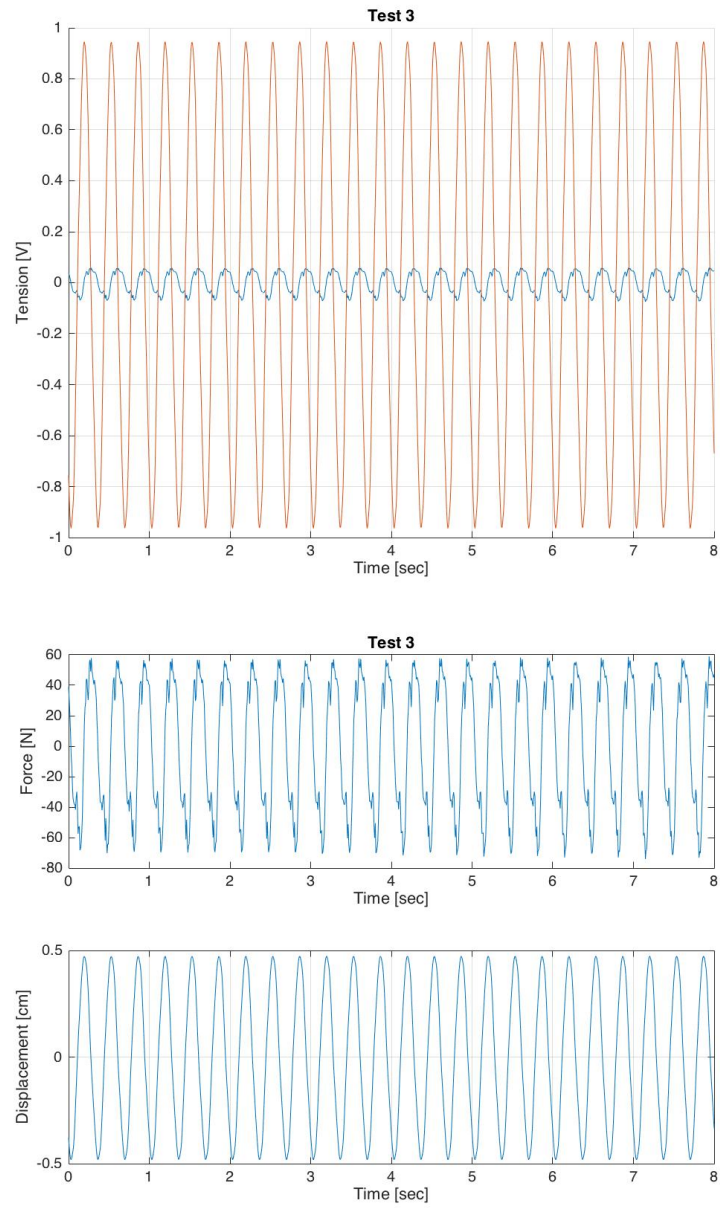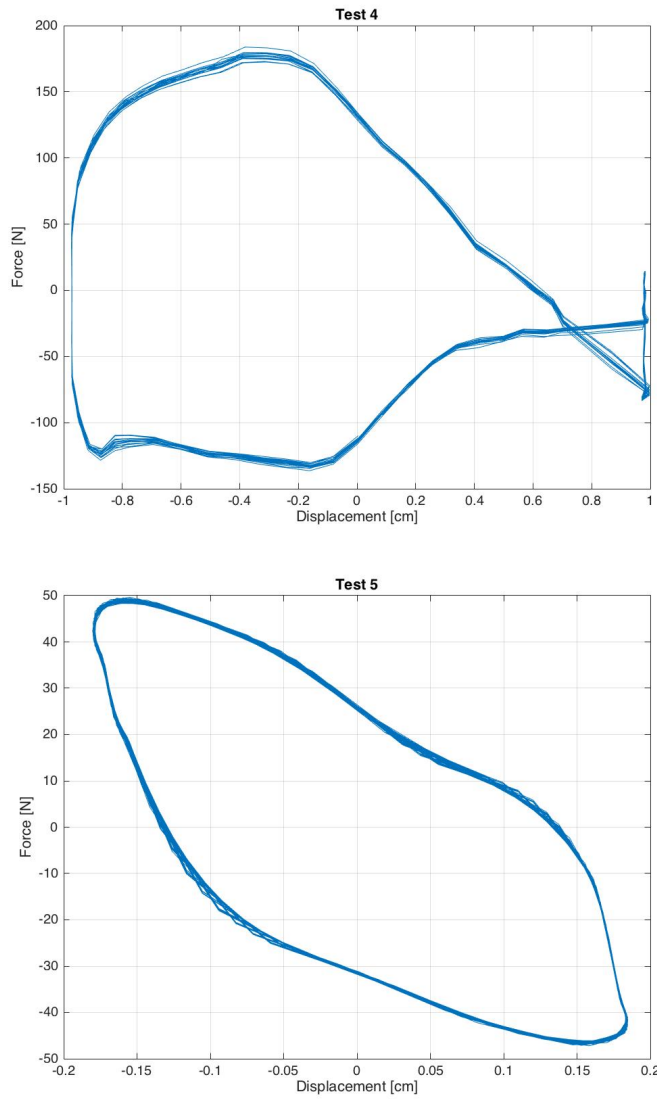
Test 6:

The data used for this experiment are:

- Voltage=7volt

- Frequency=3Hz

Sinusoidal responses and the diagram Force-Displacement from the testing of the external-helix inerter with Engine oil SAE-30 are reported in the Figure (7.27 and 7.28).
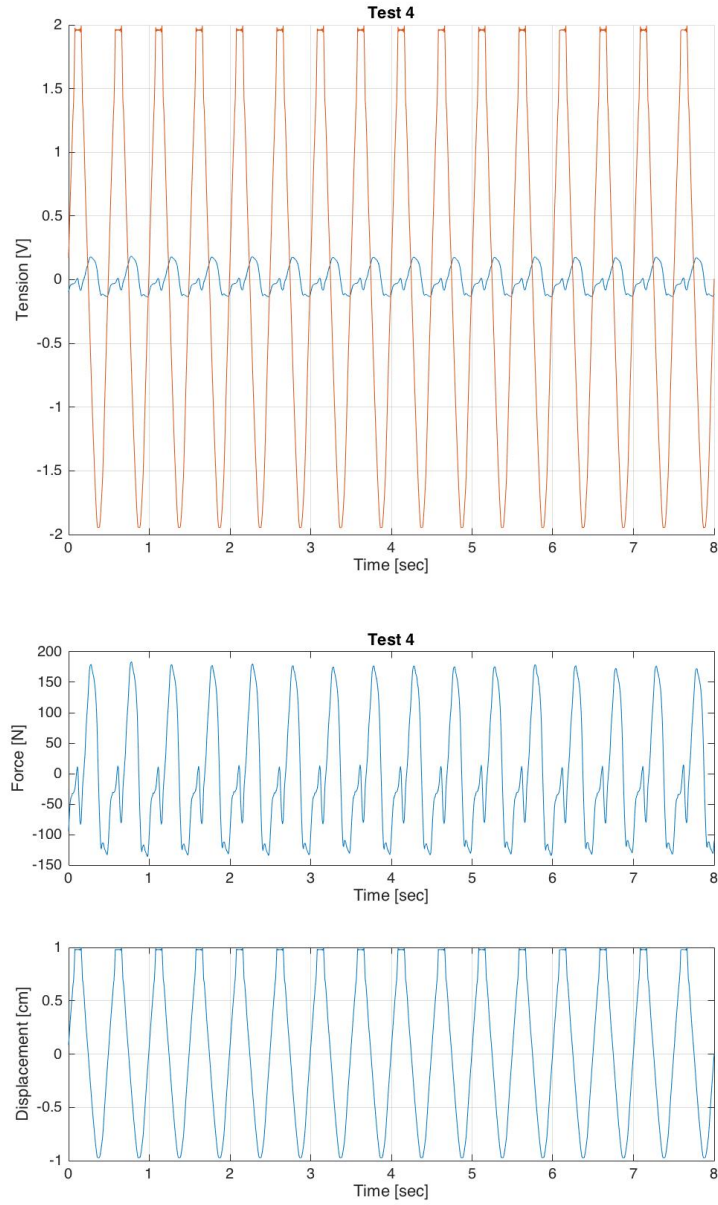
Figure 7.25: Test 4
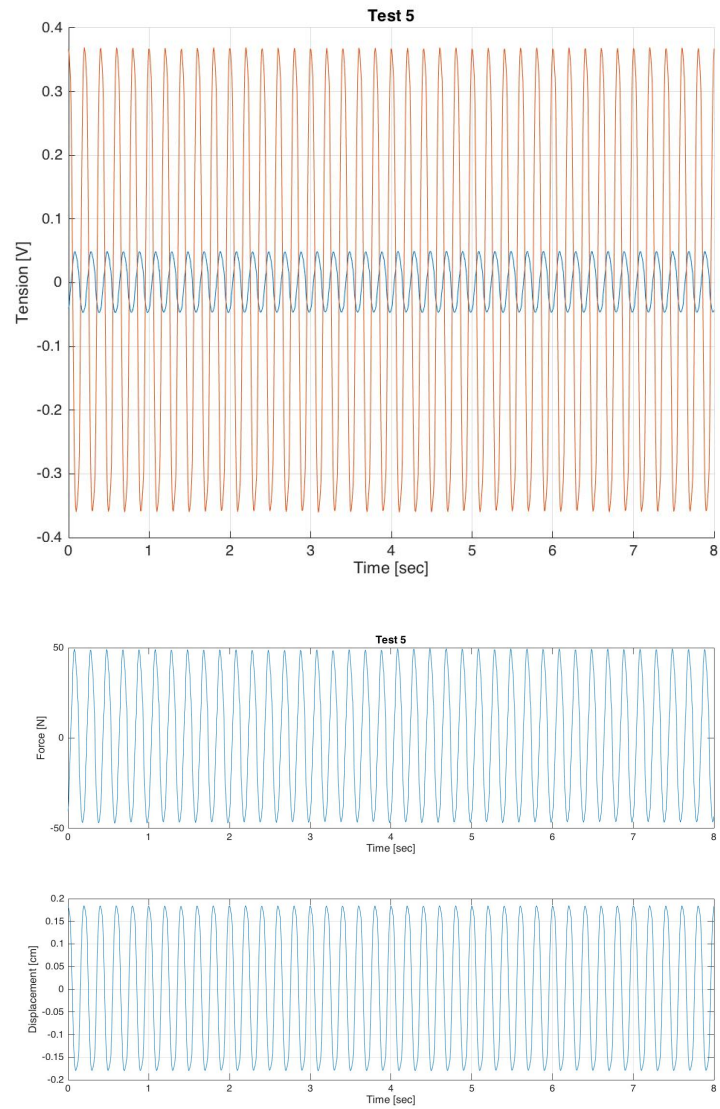
Figure 7.26: Test 5
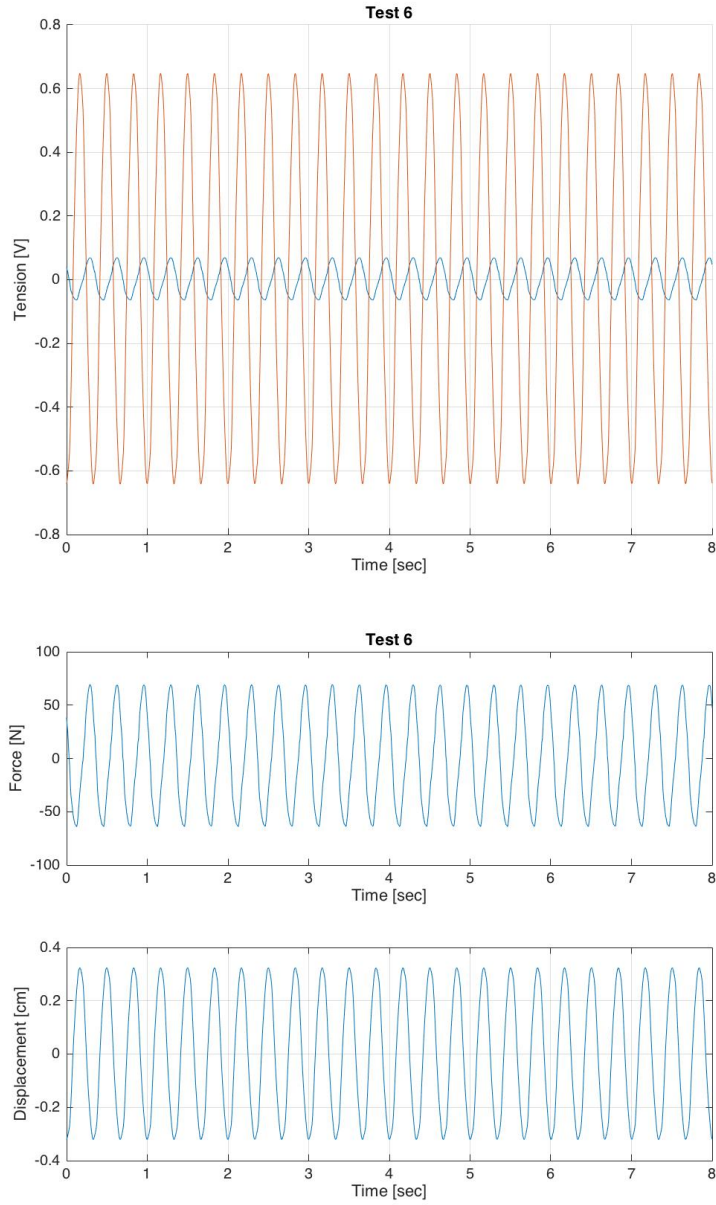
Figure 7.27: Test 6
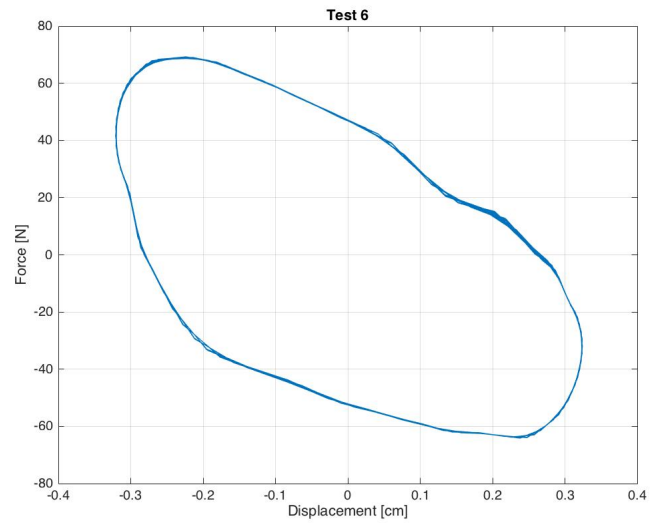
Figure 7.28: Force-Displacement diagram

Conclusion Esperiment

From the behaviour showed in the experimental results, in particular in test 1 to 6, it can be concluded that the device built is a fluid inerter because the Displacements and Forces are in opposite phase.

This script is shows the Matlab Cod that I use to obtain the Force and Displacment diagram reported in the Figure (7.21, 7.22, 7.23, 7.24, 7.25 and 7.26).

```matlab
load file from nomefile.txt
num=dlmread('07v3hz.txt');
t=linspace (0,8,1024)';
y=num(:,1);
y1=num(:,2);

%Plot Force and displacement
figure(1); hold on;
plot(t,y); plot(t,y1);
xlabel ('Time [sec]')
ylabel ('Tension [V]')
title('Test 1: ')
grid on;

%Plot Force and displacement
figure(2);
subplot(2,1,1), plot(t,y);
xlabel ('Time [sec]')
ylabel ('Displacement [cm]')
title('Test 1: ')
subplot(2,1,2), plot(t,y1);
xlabel ('Time [sec]')
ylabel ('Force [kN]')
grid on;
```

Chapter 8

Conclusion

Since their for appearance reported in [1], Inerters have become a hot topic in recent years, spreading to a variety of applications especially in vehicle [2], train [3], building suspension system [4], etc. Automotive suspensions are design to provide many functions ranging from vibration isolation of the passenger compartment to control of road inputs and vertical tire loads to optimize braking, acceleration and handling. The interest in improving and optimizing suspensions has become of great importance in the academic community and automotive manufactures. In Chapter 5 is reported a preliminary optimisation study of the possible benefits of the application of an inerter to an automotive suspension. For some relatively simple struts it was shown that improvements could be obtained in a quarter-car vehicle model across a wide range of static suspensions stiffnesses. Improvements of about 10% or greater were shown for measures of ride, tyre normal load and handling. Furthermore in case of rotors (i.e turbines, electric motors) no existing applications is reported. It was hence very interesting to understand the potentiality of inerter applications to rotordynamics systems. In this thesis, mathematical and numerical simulations are used to investigate the performance and stability of a rigid rotor on flexible supports with different configurations of inerter. The experimental results conducted on a manufactured inerter are also reported.

Firstly, the first part of this thesis (Chapter 2 and 3) developed the equations of the motion for a rigid rotor on flexible support using Maple code. The Equations [2.6] represent the dynamics of the rotors for Isotropic Flexible Support and the Equations [2.14] represent the dynamics of the rotors for

Anisotropic Flexible Support. In Chapter 2.5 the effect of viscous damping in the bearing (Figure 2.3) was taken into consideration in order to obtain the Equations [2.29].Then, Chapter 3 examined how the rotor bearings systems respond to force and found the response to a mass eccentricity of $0.1\,mm$. The results is reported in the Figure 3.3 for Isotropic Supports and Figure 3.5 for Anisotropic Supports. It was then possible to define the critical speed for the rotor system. It is clear from the Campbell Diagram, shown in Figure (3.4), that there are four critical speeds in four degrees of freedom model of a system.

The objective of the second part of this thesis (Chapter 6) is to study fundamental influence of inerter on the natural frequencies of vibrations system. The fact that inerter can reduce the natural frequencies of vibration system is theoretically demostrated in this chapter and the question that how to efficiently use inerter to reduce the natural frequencies is also adressed. The traditional methods to reduce the natural frequencies of an elastic system are either deacreasing the elastic stiffness or increasing the mass of vibration system. It is shown in the Chapter 6 that a parallel-connected inerter can also effectively reduce natural frequencies. From the Chapter 6 we can conclude that:

Single DoF System with Inerter

For a S-DoF Rotor system with inerter shown in Figure (6.1), the equation of motion of free vibration system is Equation [6.1]. The natural frequency ω_n of an SDoF Rotor System is deacreasing function of the inertance v. Thus, inerter can reduce the natural frequency of an SDoF Rotor System.

Two DoF System with Inerter

For a 2-DoF Rotor system with inerter shown in Figure (6.2), the equation of motion of free vibration system is Equation [6.7].The natural frequency ω_n of an TDoF Rotor System with two inerter are deacreasing function of the inertance v_{x1} and v_{x2}. Thus, inerter can reduce the natural frequency of an TDoF Rotor System like dimostred in the Figure (6.3).

4-DoF System with Inerter

For a 4 DoF Rotor system with inerter shown in Figure (6.4), the equation of motion of free vibration system is Equation [6.17].The natural frequency ω_n of an 4DoF Rotor System with four inerter are deacreasing function of the inertance v. Thus, inerter can reduce the natural frequency of an 4DoF Rotor System like dimostred in the figure (6.6). However, the same result can be obtained by increasing the total mass of the rotor without the introduction of four inerter. Thus, it is concluded that the inerter increase the mass of the rotor system.

5-DoF System with Inerter

For a 5-DoF Rotor system with inerter shown in Figure (6.8), the equation of motion of free vibration system is Equation [6.40]. The natural frequency ω_n of an 5DoF Rotor System with one inerter in the y-direction are deacreasing function of the inertance v. Thus, inerter can reduce the natural frequency of an 5DoF Rotor System as proved in figure (6.10).

6-DoF System with Inerter

For a 6-DoF Rotor system with inerter shown in Figure (6.12), the equation of motion of free vibration system is Equation [6.46].The natural frequency ω_n of an 6DoF Rotor System with two inerter are deacreasing function of the inertance v_{x1} and v_{x2}. Thus, Figure (6.14) shoes that the inerter can reduce the natural frequency of a 6 DoF Rotor System.

The objective of the third and last part of this thesis (Chapter 7) it is built in the Dynamics Laboratory of ISVR a Fluid Inerter (Figure 7.5 and 7.6). The fluid inerter implementation introduced in the Chapter [4] and [5] is robust and durable due to its simple design. The device size is comparable to ball screw implementations [2]. It is shown that the device can be modelled as an ideal inerter in parallel with a parasitic damping component. The inertance of the fluid inerter is estimated from the Equation [7.2] and depends on the density of a fluid, on the channel length and on the ratio of the piston area over the channel area. Changing these parameters also change the value of the inertance. However, the value of annular area and channel cross sectional area for the experiment are fixed. For this reason the value of inertance depends only by the fluid density and channel length.

In the Dymanics Laboratory, a test bench for experiments was realised (Figure 7.7) and the results for testing the fluid inerter proprieties under different load, amplitude and frequency are presented in Chapter 7 of this thesis. From the behaviour showed in the experimental results, in particular in test 1 to 6, it can be concluded that the device built is a fluid inerter.

Future Work

This thesis has investigated the influence of an inerter on the natural frequencies of a rotor systems with singe to multiple degrees of freedom, the fact that inerter can reduce the natural frequencies of these system was clearly demonstrated. Future work could consist in testing the inerter device built in ISVR at high frequencies and to prove that even for these high frequencies it behave like an Inerter. Furthermore, this thesis investigated only numerically the application of an inerter to rotor dynamic systems. A natural prosecution of the work is the installation of such a device in a rotor (for example in a turbine). Experimental data should prove that the application of the device increases the overall mass of the system and decreases its natural frequencies in the case of a rotor too.

Bibliography

[1] M.Z.Q Chen, C.Papageorgiou, F. Scheibe, F. Wand and M. C. Smith, "IEEE Circuit and System Magazine", Volume 9, Number 1, First Quarter 2009.

[2] M.C. Smith, Fu-Cheng Wang, "Performance Benefits in Passive Vehicle Suspensions Employing Inerters", Conference Paper in Proceedings of the IEEE Conference on Decision and Control - January 2004.

[3] F.C. Wang, C.H. Yu, M.L. Chang and M.S. Hsu, "The performance improvements of train suspension systems with inerters", 45th IEEE Conference on Decision and Control, San Diego, Usa, 2006.

[4] F.C. Wang, C.W. Chen, M.K. Liao and M.F. Hong, "Performance Analyses of Building Suspension Control with Inerters", 46th IEEE Conference on Decision and Control, New Orleans,LA, Usa, 2007.

[5] M.I. Friswell, J.E.T. Penny, S.D. Garvey and A.W. Lees, "Dynamics f Rotating Machines", Cambridge University Press, 2010.

[6] S.Y. Yoon et al., "Control of Surge in Centrifugal Compressors by Active Magnetic Bearings", Spinger-Verlag London 2013.

[7] E.Swanson, C.D. Powell, S. Weissman, "A Pratical Review of Rotating Machinery Critical Speeds and Modes", Sound and Vibration - May 2005.

[8] V. Fedak, P. Zaskalicky and Z. Gelvanic, "Analysis of Balancing of Unbalanced Rotors and Long Shaft usign GUI Matlab", Department of Electrical Engineering and Mechatronics, FEEaI, Technical University of Koice, Slovakia.

[9] M.C. Smith, "Synthesis of mechanical networks: the inerter", IEEE Transactions on Automatic Control, 47, 1648-1662,2002.

[10] M.C. Smith, "Society of Instrument and Control Engineers (SICE)", Annual Conference, Fukui-Japan, August 2003.

[11] Xin-Jie Zhang, M. Ahmadian, K. Hui Guo, "On the benefits of semi-active suspensions with inerter", Center for Vehicle System and safty, Virginia Tech, VA, USA.

[12] Chen, MZQ; Hu,Y; Huang, L.; Chen, G., "Influence of inerter on natural frequencies of vibration systems", Journal of Sound and Vibration, 2014, v.333 n.7, p.1874-1887.

[13] S.J. Swift, M.C. Smith, A.R. Glover, C. Papageorgiou, B.Gartner and N.E. Houghton, "Design and Modelling of a Fluid Inerter", International Journal of Control, 2013.

[14] Y. Hu, M.Z.Q. Chen, "Performance evaluation for inerter-based dynamic vibration absorbers", International Journal of Mechanical Sciences, 2014.

[15] A. Agrawal, "Performance Improvement of Automotive Suspension System using Inerters and an Adaptive Controller", Master Thesis, University of Waterloo - Master of Applied Science in Mechanical and Mechatronics Engineering, 2013.

[16] O. Gerger, "Design, Control and Optimization of Vehicle Suspensions with Inerters", Master Thesis, School of Natural and Applied Sciences of Middle East Technical University, 2013.

[17] M. C. Smith, "Synthesis of Mechanical Networks: The Inerter", IEEE Transactions on Automatic Control, Vol.47, NO.10, October 2002.

[18] C. Papageorgiou, O.G. Lockwood, N.E. Houghton and M.C. Smith, "Experimental Testing and Modelling of a Passive Mechanical Steering Compensator for High-Perfomance Motorcycles", European Control Conference Kos, Greece, 2007.

[19] F.C. Wang, M.F. Hong and T.C. Lin, "Designing and testing a hydraulic inerter", Department of Mechanical Engineering, National Taiwan University, Tapei, Taiwan, China, 2010.

[20] Malcolm C. Smith, "Inerters and Formula One", University of Cambridge Department of Engineering, International Centre for Mathematical Sciences, 15 South College Street, Edinburgh ,22 July 2014

[21] X.Q. Sun, L. Chen, S.H. Wang, X.L. Zhang and X.F. Yang, "performance investigation of vehicle suspension system with nonlinear ball-screw inerter", School of Automotive and Traffic Engineering, Jiangsu University, Zhenjiang, China, October 2015.
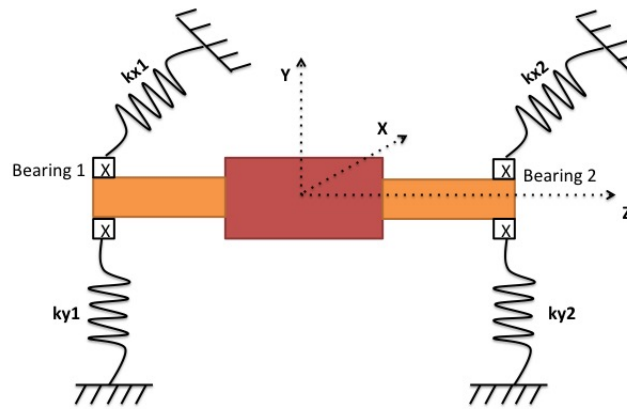
Appendix A

Mode Shape - Isotropic Case

Figure A.1: Rigid Rotor on Elastic Support

In Appendix A are presented the Mode Shape of the 4DoF rotor system which is described in Chapter [2]. The Mode Shape are obtained used the following data:

- $m = 122.68\,kg$ (mass of the rotor)

- $a = b = 0.25\,m$ (distance bearing)

- $k_{x1} = k_{y1} 1 \cdot 10^6 \, MN/m$ (stiffness)

- $k_{x2} = k_{y2} = 1.3 \cdot 10^6 \, MN/m$ (stiffness)

- $I_P = 0.6134 \, kgm^2$ (polar inertia)

- $I_d = 2.8625 \, kgm^2$ (diametral inertia)

- $\Omega = 4000 \, rev/min \, rotor \, speed$

For this System the Undamped Frequencies are: Undamp.1=21.3270Hz, Undamp.2=21.5794Hz, Undamp.3=29.5823Hz, Undamp.4=43.6158Hz. The Natural Frequency Map for 4-DoF rotor system is shown in Figure (A.2)
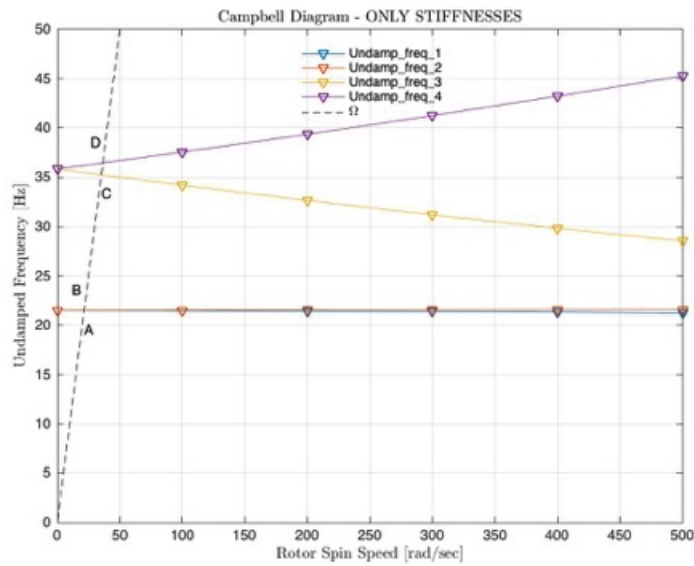

Figure A.2: Campbell Diagram

where the critical speed are:

- Point A = 134.8402 rad/sec 21.4927 Hz

- Point B = 135.2749 rad/sec 21.5042 Hz
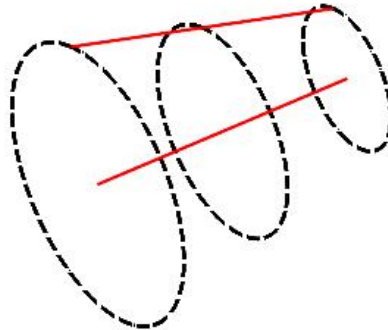
- Point C = 204.7548 rad/sec 35.2565 Hz

- Point D = 253.6948 rad/sec 36.4615 Hz

The Eigenvectors of the system are reported in the following table:

|	Mode 1	Mode 2	Mode 3	Mode 4
x(t)	1.00	0.77	0.04	0.01
y(t)	1.00	0.77	0.04	0.01
$\alpha(t)$	0.60	1.00	1.00	1.00
$\beta(t)$	0.60	1.00	1.00	1.00

The Mode Shape are:

Nat_freq_1=21.32Hz

Mode 1 (BW)

Figure A.3: Mode Shape: Mode 1

In the Figure (A.3), (A.4), (A.5) and (A.6) BW indicated the "Backward Mode" and the FW indicated the "Foward Mode". In the plane (α, β), the orbit is a circle. The mode rotates in a clockwise direction and because the positive rotor spin has been defined to be counterclockwise, is called a backward mode, otherwise the mode rotates in the counterclockwise direction and is called a foward mode.

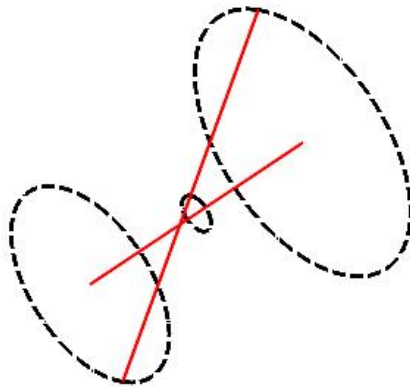The following script reports the partial Maple code used to obtain the Mode Shape.

Nat_freq_2=21.57Hz
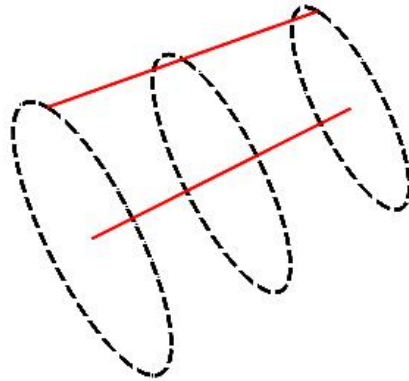
Mode 2 (FW)

Figure A.4: Mode Shape: Mode 2

Nat_freq_3=29.58Hz

Mode 3 (BW)

Figure A.5: Mode Shape: Mode 3

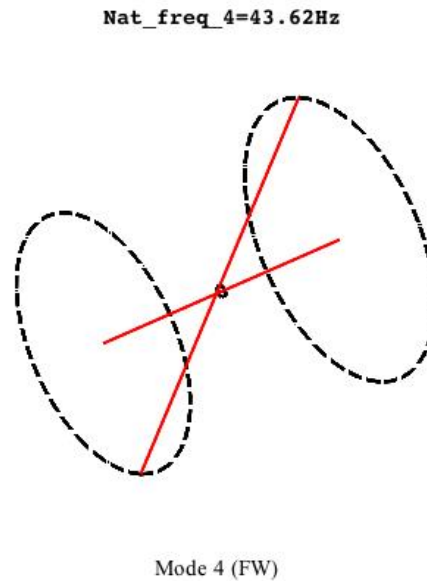**Nat_freq_4=43.62Hz**

Mode 4 (FW)

Figure A.6: Mode Shape: Mode 4

```
1  %PLOTTING Mode Shapes
2  %Mode1:
3  %Right Bearing
4  >xR := proc (theta); Re((.25*U[4, ix]+U[1, ix])*exp(I*theta));
5  >yR := proc (theta); Re(((-1)*.25*U[3, ix]+U[2, ...
       ix])*exp(I*theta));
6  %Left Bearing
7  >xL := proc (theta); Re(((-1)*.25*U[4, ix]+U[1, ...
       ix])*exp(I*theta));
8  >yL := proc (theta); Re((.25*U[3, ix]+U[2, ix])*exp(I*theta));
9  %Center of Gravity:
10 >xG := proc (theta); Re(U[1, ix]*exp(I*theta));
11 >yG := proc (theta); Re(U[2, ix]*exp(I*theta));
12 %ORBIT SHAPE:
13 >L := plot3d([xL(theta), yL(theta), -.25], theta = 0 .. 2*Pi);
14 >R := plot3d([xR(theta), yR(theta), .25], theta = 0 .. 2*Pi);
15 >G := plot3d([xG(theta), yG(theta), 0], theta = 0 .. 2*Pi, ...
       linestyle = dash);
16 Mod1 := plots[display](L, G, R, title = "Mode 1 in 3D", ...
       titlefont = [COURIER, BOLD, 12], axes = NORMAL, ...
       linestyle = dash);
17 %SHAFT SHAPE:
```

```
18 >axis_f := PLOT3D(CURVES(subs(data, [[0, 0, -b], [0, 0, ...
      a]])));
19 >t1 := cat("Nat_freq_1=", nat_freq1, "Hz");
20 >axis_m := PLOT3D(CURVES(subs(data, [[xL(0), yL(0), -b], ...
      [xR(0), yR(0), a]])));
21 >M1 := plots[display](Mod1, axis_f, axis_m, axes = none, ...
      title = t1, color = red, thickness = 2, caption = ...
      typeset("Mode 1"));
22 %ORBIT SHAPE:
23 >L := plot3d([xL(theta), yL(theta), -.25], theta = 0 .. 2*Pi);
24 >R := plot3d([xR(theta), yR(theta), .25], theta = 0 .. 2*Pi);
25 >G := plot3d([xG(theta), yG(theta), 0], theta = 0 .. 2*Pi, ...
      linestyle = dash);
26 Mod1 := plots[display](L, G, R, title = "Mode 1 in 3D", ...
      titlefont = [COURIER, BOLD, 12], axes = NORMAL, ...
      linestyle = dash);
27 %SHAFT SHAPE:
28 >axis_f := PLOT3D(CURVES(subs(data, [[0, 0, -b], [0, 0, ...
      a]])));
29 >t1 := cat("Nat_freq_1=", nat_freq1, "Hz");
30 >axis_m := PLOT3D(CURVES(subs(data, [[xL(0), yL(0), -b], ...
      [xR(0), yR(0), a]])));
31 >M1 := plots[display](Mod1, axis_f, axis_m, axes = none, ...
      title = t1, color = red, thickness = 2, caption = ...
      typeset("Mode 1"));
32
33 %Mode 2
34 mode2; ix := 7; q;
35 .................
36
37 %Mode 3
38 mode3; ix := 3; q;
39 .................
40
41 %Mode 4
42 mode4; ix := 1; q;
43 Right Bearing
44
45 plots[display](matrix(2, 2, [[M1, M2], [M3, M4]]));
```

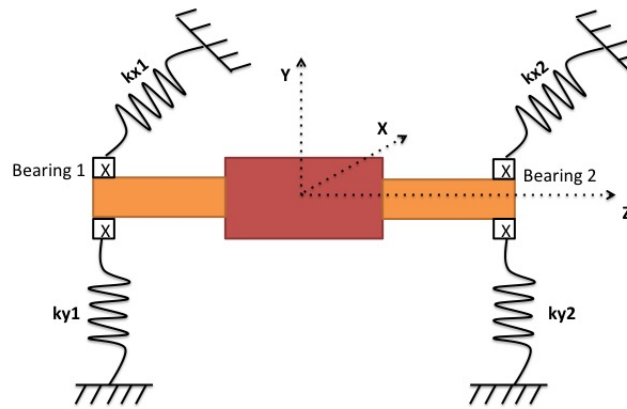# Appendix B

Mode Shape - Anisotropic Case

Figure B.1: Rigid Rotor on Elastic Support

In Appendix A are presented the Mode Shape of the 4DoF rotor system which is described in Chapter [2]. The Mode Shape are obtained used the following data:
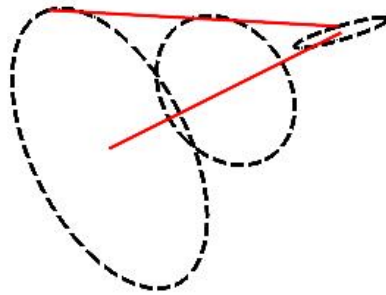
- $k_{x1} = 1 \cdot 10^6 \, MN/m$ (stiffness)

- $k_{y1} = 1.5 \cdot 10^6 \, MN/m$ (stiffness)

- $k_{x2} = 1.3 \cdot 10^6 \, MN/m$ (stiffness)

- $k_{y2} = 1.8 \cdot 10^6 \, MN/m$ (stiffness)

The Undamped Frequencies are: Undamp.1=21.44Hz, Undamp.2=22.43Hz, Undamp.3=30.26Hz, Undamp.4=44.40Hz.

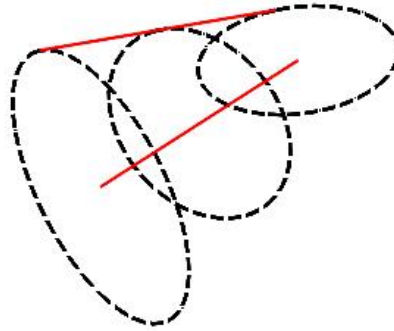The Mode shape are:

Nat_freq_1=21.44Hz

Mode 1 (BW)

Figure B.2: Mode Shape: Mode 1

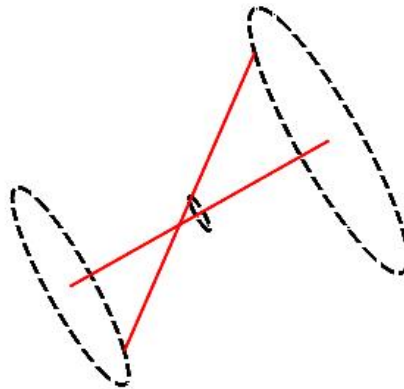The Mode Shape of Anisotropic Case are obtained using the same Maple Code of Isotropic Case (Appendix A)

Nat_freq_2=22.43Hz

Mode 2 (FW)

Figure B.3: Mode Shape: Mode 2

Nat_freq_3=30.26Hz

Mode 3 (BW)

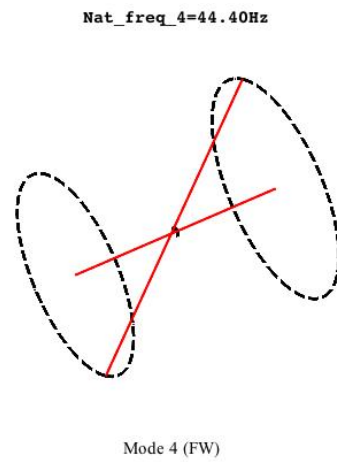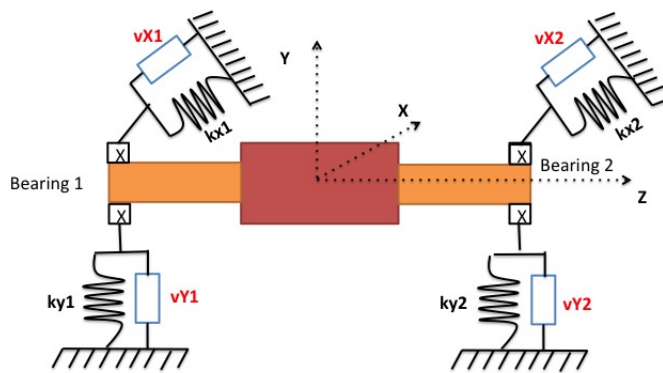Figure B.4: Mode Shape: Mode 3

Nat_freq_4=44.40Hz

Mode 4 (FW)

Figure B.5: Mode Shape: Mode 4

Appendix C

Mode Shape - 4DoF with Inerter



5.jpg

Figure C.1: Rotor System with Inerter

Using the data reported in Appendix A the Mode Shape of the 4DoF rotor system with inerter are Shown in Figure (C.2, C.3, C.4 and C.5). As demonstrated in Chapter [6]. The natural frequency ω_n of an 4DoF Rotor System with four inerter are deacreasing function of the inertance v.

Thus, inerter can reduce the natural frequency of an 4DoF Rotor System as dimonstrated in the figure (6.6). The natural frequencies of the system are reported in the following table where $v_{x1} = v_{x2} = v_{y1} = v_{y2} = v = 60kg$:

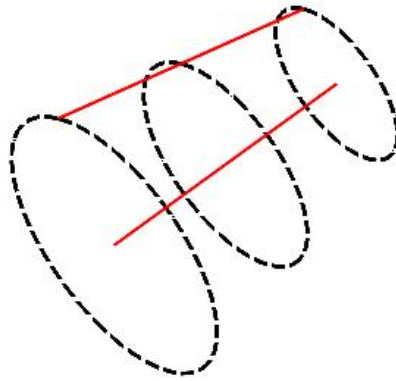|	Without Inerter	With Inerter ($v = 60kg$)
Mode 1	21.32 Hz	14.84 Hz
Mode 2	21.57 Hz	15.23 Hz
Mode 3	29.58 Hz	17.46 Hz
Mode 4	43.63 Hz	21.01 Hz

The Mode Shape of this system are:

Undamped_freq_1=14.84Hz
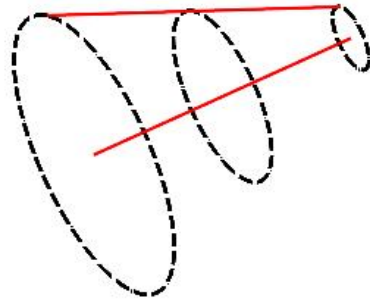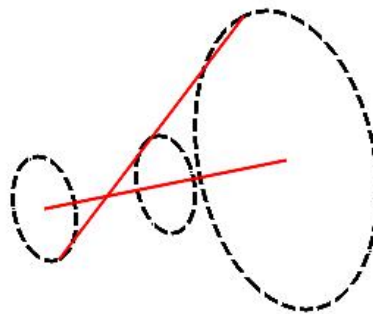

Mode 1 (BW)

Figure C.2: Mode Shape: Mode 1

Undamped_freq_2=15.23Hz

Mode 2 (FW)

Figure C.3: Mode Shape: Mode 2

Undamped_freq_3=17.46Hz

Mode 3 (BW)

Figure C.4: Mode Shape: Mode 3

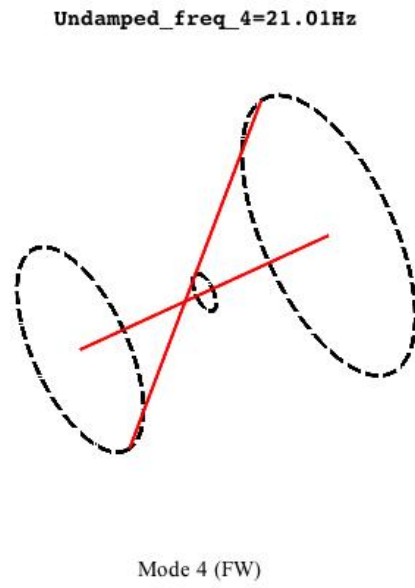Undamped_freq_4=21.01Hz

Mode 4 (FW)

Figure C.5: Mode Shape: Mode 4

Appendix D

Equation of motion

This Appendix presents the accurancy of the Equations [6.40] and [6.46] obtained using Maple for $5DoF$ and $6DoF$ rotor dynamic system. The Equations of the motion for $4DoF$ free vibration system, including damping at the supports and gyroscopic effects, are given in Equation [2.29] and are repeated here for convenience:
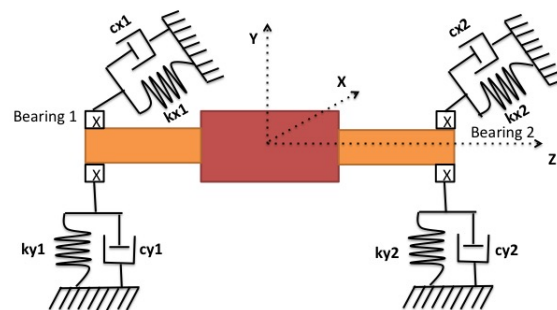

Figure D.1: 4DoF Rotor System

$$\begin{cases} m\ddot{x} + c_{xT}\dot{x} + c_{xC}\dot{\alpha} + k_{xT}x + k_{xC}\alpha = 0 \\ m\ddot{y} + c_{yT}\dot{y} - c_{yC}\dot{\beta} + k_{yT}y - k_{yC}\beta = 0 \\ I_d\ddot{\alpha} - I_p\Omega\dot{\beta} + c_{xC}\dot{x} + c_{xR}\dot{\alpha} + k_{xC}x + k_{xR}\alpha = 0 \\ I_d\ddot{\beta} + I_p\Omega\dot{\alpha} - c_{yC}\dot{y} + c_{yR}\dot{\beta} - k_{yC}y + k_{yR}\beta = 0 \end{cases} \tag{D.1}$$

It is helpful to express these equations in matrix form as:

$$M\ddot{q} + (C + \Omega G)\,\dot{q} + Kq = 0 \tag{D.2}$$

The mass, damping and the stiffness matrices, M, C and K are symmetric and positive definite matrices. In contrast, the gyroscopic matrix G is skew-symmetric. To determine the roots of Equations [2.29], it must rearrange the equation in the followig form:

$$\begin{bmatrix} C + \Omega G & M \\ M & 0 \end{bmatrix} \frac{d}{dt} \begin{Bmatrix} q \\ \dot{q} \end{Bmatrix} + \begin{bmatrix} K & 0 \\ 0 & -M \end{bmatrix} \begin{Bmatrix} q \\ \dot{q} \end{Bmatrix} = \begin{Bmatrix} 0 \\ 0 \end{Bmatrix}$$

This is an Eigenvalue Problem was formed and solved numerically. The four Natural Frequencies obtained used the following data are:

$$\begin{cases} m = 122.68\,kg\,mass\,of\,rotor \\ a = b = 0.25m\,distance\,of\,the\,bearing\,from\,the\,center\,of\,rotor \\ k_{x1} = k_{y1} = 1 \cdot 10^6\,MN/m\,Stiffness \\ k_{x2} = k_{y2} = 1.3 \cdot 10^6\,MN/m\,Stiffness \\ c_{x1} = k_{y1} = 10\,Ns/m\,Damping \\ c_{x2} = k_{y2} = 13\,Ns/m\,Damping \\ I_P = 0.6134\,kgm^2\,Polar\,inertia \\ I_d = 2.8625\,kgm^2\,Diametral\,inertia \\ \Omega = 4000\,rev/min\,rotor\,speed \end{cases} \tag{D.3}$$

- First Natural Frequency: ω_{n1}= 21.340 [Hz]

- Second Natural Frequency: ω_{n2}= 21.570 [Hz]

- Third Natural Frequency: ω_{n3}= 29.580 [Hz]

- Fourth Natural Frequency: ω_{n4}= 43.620 [Hz]

5DoF Rotor Dynamic System

This system is different from previus cases because it has 5DoF as shown in Figure
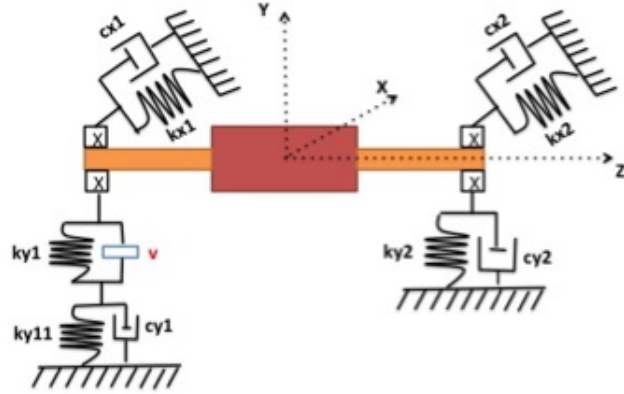

Figure D.2: Rigid Rotor - 5DoF with Inerter

The equation of the motion for this system are introduced using Maple and are repeated here for convenience:

$$
\begin{cases}
m\ddot{x} + (c_{x1} + c_{x2})\,\dot{x} + (k_{x1} + k_{x2})\,x + (ac_{x2} - bc_{x1})\,\dot{\beta} + (ak_{x2} - bk_{x1})\,\beta = 0 \\
(m + vL)\,\ddot{y} - vL\ddot{y}_L + c_{y2}\dot{y} - k_{y1}y_L + (k_{y1} + k_{y2})\,y + (-ak_{y2} + bk_{y1})\alpha + \\
\quad -ac_{y2}\dot{\alpha} + v_L b\ddot{\alpha} = 0 \\
(b^2 v_L + I_d)\,\ddot{\alpha} + c_{y2}a^2\dot{\alpha} + (a^2 k_{y2} + b^2 k_{y1})\,\alpha - b\,(k_{y1}y_L + v_L\ddot{y}_L) + \dot{\beta}I_p\Omega + \\
\quad + v_L b\ddot{y} - ac_{y2}\dot{y} + (-ak_{x2} - b_{x1}) = 0 \\
I_d\ddot{\beta} - \dot{\alpha}I_p\Omega + (a^2 k_{x2} + b^2 k_{x1})\,\beta + (a^2 c_{x2} + b^2 c_{x1})\,\dot{\beta} + (ac_{x2} - bc_{x1})\,\dot{x} + \\
\quad + (ak_{x2} - bk_{x1})\,x = 0 \\
k_{y11}y_L + c_{y1}\dot{y}_L = k_{y1}\,(\alpha b + y - y_L) + v_L(\ddot{\alpha}b + \ddot{y} - \ddot{y}_L)
\end{cases}
$$

$$\text{(D.4)}$$

To confirm of what has been achieved is correct in terms of equations and formulas the stiffness and inertance are given the following values:

$k_{y1} = 1 \cdot 10^{12}\, N/m\, (to\, infinity)$

$v = 0.001\, kg\, (to\, zero)$

Then, using the data [D.3] are obatained the same results of the 4dof system.

- First Natural Frequency: ω_{n1}= 21.280 [Hz]

- Second Natural Frequency: ω_{n2}= 21.560 [Hz]

- Third Natural Frequency: ω_{n3}= 29.480 [Hz]

- Fourth Natural Frequency: ω_{n4}= 43.520 [Hz]

- Fifth Natural Frequency: ω_{n4}= 16000 [Hz]

This allowed us to confirm that the equations developed by Maple for the system to 5DOF are fair and the results obtained are reliable.

6DoF Rotor Dynamic System

To develop the equations of motion for this system, the Maple script is used as for 5DoF system. This case has two inerters, one for each bearing. They are positioned both along the y-axis. This rotor has *six* degree of freedom because it can translate in the directions Ox and Oy and it also can rotate about these axes. The *fifth* and *sixth* degree of fredoom are given by the *inerter*.
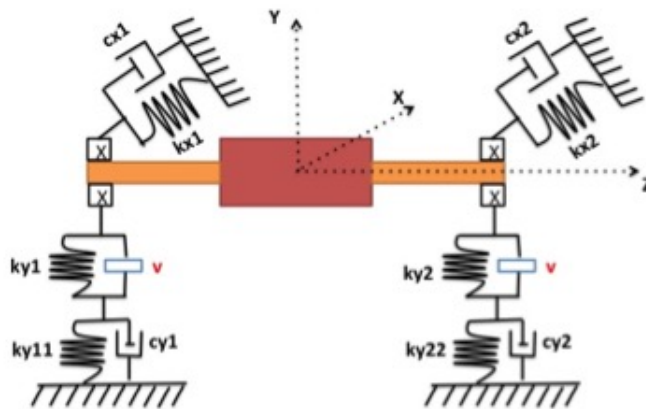

Figure D.3: Rigid Rotor - 6DoF with Inerter

The Equations are repeated here for convenience:

$$
\begin{cases}
m\ddot{x} + (c_{x1} + c_{x2})\,\dot{x} + (k_{x1} + k_{x2})\,x + (ac_{x2} - bc_{x1})\,\dot{\beta} + (ak_{x2} - bk_{x1})\,\beta = 0 \\
(m + vL + vR)\,\ddot{y} - vL\ddot{y}_L - vR\ddot{y}_R - k_{y2}y_R - k_{y1}y_L + (k_{y1} + k_{y2})\,y + \\
\quad + (-ak_{y2} + bk_{y1})\alpha + (-av_R + bv_L)\ddot{\alpha} = 0 \\
(a^2 v_R + b^2 v_L + I_d)\,\ddot{\alpha} + (-av_R + bv_L)\ddot{y} + (a^2 k_{y2} + b^2 k_{y1})\,\alpha - b\,(k_{y1}y_L + v_L\ddot{y}_L) + \\
\quad + (-ak_{y2} + k_{y1})\,y + I_p\Omega\dot{\beta} + a\,(k_{y2}y_R + v_R\ddot{y}_R) = 0 \\
I_d\ddot{\beta} - \dot{\alpha}I_p\Omega + (a^2 c_{x2} + b^2 c_{x1})\,\dot{\beta} + (ac_{x2} - bc_{x1})\,\dot{x} + (ak_{x2} - bk_{x1})\,x + \\
\quad + (a^2 k_{x2} + b^2 k_{x1})\,\beta = 0 \\
k_{y11}y_L + c_{y1}\dot{y}_L = k_{y1}\,(\alpha b + y - y_L) + v_L(\ddot{\alpha}b + \ddot{y} - \ddot{y}_L) \\
k_{y22}y_R + c_{y2}\dot{y}_R = k_{y2}\,(-\alpha a + y - y_R) + v_R(-\ddot{\alpha}a + \ddot{y} - \ddot{y}_R)
\end{cases}
$$

$$(\text{D.5})$$

To confirm of what has been achieved is correct in terms of equations and formulas the stiffness and inertance are given the following values:

$k_{y1} = 1 \cdot 10^8\ N/m\,(to\,infinity)$
$k_{y2} = 1 \cdot 10^8\ N/m\,(to\,infinity)$
$v = 0.001\ kg\,(to\,zero)$

Then, using the data [D.3] are obatained the same results of the 4dof system.

- First Natural Frequency: $\omega_{n1} = 21.260$ [Hz]

- Second Natural Frequency: $\omega_{n2} = 21.540$ [Hz]

- Third Natural Frequency: $\omega_{n3} = 29.380$ [Hz]

- Fourth Natural Frequency: $\omega_{n4} = 43.380$ [Hz]

- Fifth Natural Frequency: $\omega_{n4} = 16000$ [Hz]

- Sixth Natural Frequency: $\omega_{n4} = 16000$ [Hz]

This allowed us to confirm that the equations developed by Maple for the system to 6DOF are fair and the results obtained are reliable.